5-2015

Elucidating the role of Rumi and O-glucosylation in the Drosophila eye

Amanda Haltom

ELUCIDATING THE

ROLE OF RUMI AND *O*-GLUCOSYLATION IN THE *DROSOPHILA* EYE

by

Amanda Rae Haltom, B.S.

APPROVED:

_____
Hamed Jafar-Nejad, M.D.

_____
William Mattox, Ph.D.

_____
Michael Galko, Ph.D.

_____
Kartik Venkatachalam, Ph.D.

_____
Sheng Zhang, Ph.D.

_____
Hugo Bellen, D.V.M, Ph.D.

APPROVED:

_____
Dean, The University of Texas
Graduate School of Biomedical Sciences at Houston

ELUCIDATING THE

ROLE OF RUMI AND *O*-GLUCOSYLATION IN THE *DROSOPHILA* EYE

A

DISSERTATION

Presented to the Faculty of
The University of Texas
Health Science Center at Houston
and
The University of Texas
MD Anderson Cancer Center
Graduate School of Biomedical Sciences
in Partial Fulfillment

of the Requirements

for the Degree of

DOCTOR OF PHILOSOPHY

by
Amanda Rae Haltom, B.S.
Houston, Texas

March 2015

Acknowledgements

First, I would like to thank my mentor Dr. Hamed Jafar-Nejad for patiently taking me in as a baby scientist and teaching more than I thought I could learn. He has molded the lab to be a very supportive, encouraging environment that allowed me to grow personally and professionally. I appreciate the time he took talking to me about my science and helping me improve my critical thinking skills, writing skills and technical skills. I also appreciate the time he took to guide me through my PhD through committee meetings. I know that I have become a much better scientist under his teachings.

I would also like to thank all of my committee members, Drs. William Mattox, Michael Galko, Sheng Zhang, Kartik Venkatachalam, and Hugo Bellen for taking their time to attend my meetings and providing me with invaluable scientific support and advice. I am especially grateful to Dr. Mattox for serving as my on-site mentor and guiding me through administrative and, on a couple occasions, emotional problems throughout my PhD. I always appreciated knowing that I could go to Dr. Mattox for problems and he would be on my side, and I knew that if he wasn't on my side, I was wrong.

I would next like to thank the current lab members Dr. Tom Lee, Seung-Yeop Han, Dr. Antonio Galeone, Dr. Shakeel Thakurdas, Mario Lopez, and former lab members Dr. Jessica Leonardi and Yi-Dong Li for their support, kindness and encouragement throughout my doctoral studies. They have greatly contributed to the lab environment that I came to appreciate after hearing horror stories from some of my classmates. We always got along with each other and tried to help out one another whenever we could, and I will always be grateful for this. I don't think I could've had better coworkers and I don't think any of my future labs will have such a kind and supporting environment as this one.

My classmates in the Genes and Development program, along with coordinator Elisabeth Lindheim, have provided an incredible amount of emotional support throughout my time at GSBS. I loved getting to know everyone and sharing stories, and they are much of the

reason I am able to say I had a positive experience in graduate school. I am sad to be leaving the Genes and Development program but very happy I won't be far away. I would especially like to thank my classmate and friend Niza Nemkul for helping me get through the PhD. I met her at the beginning of my first semester and my experience here would not have been the same without her. We shared the difficult, the celebratory, the depressing, the stressful, and the enjoyable times of graduate school together. I don't know if I would have survived without her emotional support. I would also like to thank Alejandro Villar-Prados, my friend and future husband, for his emotional support during my last couple years as a graduate student. I met him late in my education but it's difficult to imagine there was a time before him. He has been able to handle me in my worst times and support me in my stressful times and I will always be grateful for that.

Lastly, I would like to thank my family, for I am sure I would not have gotten through this experience without them. I want to thank my dad for his financial support and career advice, and it was his pestering that pushed me to apply to graduate school and that guided my entire career path. My mom was very crucial to my success as well for her emotional support. Talking things through with her is the only reason I get through the tough times of life and I will never stop appreciating that.

ELUCIDATING THE

ROLE OF RUMI AND *O*-GLUCOSYLATION IN THE *DROSOPHILA* EYE

Amanda Rae Haltom, B.S.

Advisory Professor: Hamed Jafar-Nejad, M.D.

Rumi is a protein *O*-glucosyltransferase that adds the sugar *O*-glucose onto the serine in the target sequence C-S-X-S-(P/A)-C found within properly folded EGF repeats. It was first discovered to modify the *Drosophila* Notch extracellular domain and to be required for Notch signaling in a temperature dependent manner, but other targets of Rumi remained unknown. Several other proteins in the *Drosophila* proteome harbor multiple consensus sequence highly predictive of *O*-glucose, including the transmembrane protein Crumbs and the secreted protein Eyes shut (Eys). Both of these proteins are required for proper eye development and mutations in their human homologs cause a blindness disorder named retinitis pigmentosa. Therefore, we sought to determine whether Rumi plays a role in photoreceptor development. We found that *rumi*$^{-/-}$ animals have defects in photoreceptor spacing in which many neighboring rhabdomeres are attached. This phenotype cannot be explained by the loss of *O*-glucose on Notch or Crumbs. However, *eys* genetically interacts with *rumi*, and in *rumi*$^{-/-}$ animals at the start of rhabdomere separation, Eys accumulates intracellularly and decreased levels of Eys reach the extracellular space. Overexpressing a mutant Eys transgene which contains no intact *O*-glucosylation sites also results in intracellular accumulation of Eys, suggesting that loss of *O*-glucose from Eys is the cause. Additionally, both the intracellular accumulation and the rhabdomere attachment defect grow more severe at higher temperatures, and Eys degrades at higher temperatures in *rumi*$^{-/-}$. In addition, removing one copy of the chaperone *Hsc70-3* enhances the *rumi*$^{-/-}$ phenotype. Together, these data suggest that loss of *O*-glucose from Eys

causes a defect in its proper folding, which leads to decreased Eys reaching the extracellular space and therefore a failure in full separation of the rhabdomeres. In addition to the rhabdomere separation defect, *rumi*$^{-/-}$ photoreceptors degenerate when placed in constant light. However, this defect seems to be independent of the enzymatic function of Rumi, suggesting Rumi may play a chaperone role as well.

Table of Contents

List of Illustrations

List of Tables

Abbreviations

Act: Actin

arRP: autosomal recessive Retinitis Pigmentosa

B4galt1*:* UDP-Gal:betaGlcNAc beta 1,4- galactosyltransferase, polypeptide 1

Chp: chaoptin

Crb: Crumbs

DLL: Delta-like

EGF: Epidermal Growth Factor-like repeat

Eogt: EGF-domain specific *O*-linked *N*-acetylglucosamine transferase

ep-CAM: epithelial cell adhesion molecule

ER: endoplasmic reticulum

Eys: Eyes shut

Fng: Fringe

GlcNAc: *N*-acetylglucosamine

GMD: GDP-D-mannose dehydratase

GPI: glycophosphatidylinositol

GXYLT: glucoside xylosyltransferase

ICD: intracellular domain

IRS: interrhabdomeral space

LDL: low density lipoprotein

LFng: Lunatic Fringe

MFng: Manic Fringe

Ofut: *O*-fucosyltransferase

PD: pupal development

Pofut: Protein *O*-fucosyltransferase

PRC: photoreceptor cell

Prom: prominin

SOP: sensory organ precursor

TEM: transmission electron microscopy

XXYLT: xyloside xylosyltransferase

CHAPTER I

INTRODUCTION:

O-LINKED GLYCOSYLATION ON EGF REPEATS

Glycosylation

Glycosylation is defined as the covalent attachment of a sugar to lipids or proteins, added post- or co-translationally. This type of modification is the most common post-translational modification of proteins and plays a many of roles in protein structure and function. The two major types of glycans are N-linked and *O*-linked glycans; an N-linked glycan is a sugar attached to an asparagine residue and an *O*-linked glycan is attached to a serine and/or threonine residue. Some of these enzymes only add their respective sugar onto a known target sequence of amino acids; some have no defined consensus sequence yet, such as *O*-mannosylation and *O*-GalNAcylation (Bennett et al. 2012; Breloy et al. 2008). Some types of *O*-linked glycans are found on Epidermal Growth Factor-like (EGF) repeats, which is a 30-40 amino acid protein domain found in the extracellular domain of some transmembrane proteins and secreted proteins (discussed below). Although *O*-linked glycans are relatively rare, our knowledge of their function has grown within the last several years, especially regarding *O*-linked glycans on EGF repeats. This review will discuss the *O*-linked glycans found on EGF repeats: *O*-glucose, *O*-fucose, and *O*-GlcNAc (Figure 1-1).

EGF repeats

Epidermal Growth Factor (EGF) is a small growth factor of 53 amino acids and is important for cell motility (Segall et al. 1996), proliferation (Kato et al. 1998), differentiation (Traverse et al. 1994), and survival (Arteaga 2001; Zaczek et al. 2005). It is characterized by 6 conserved cysteine residues which form 3 disulfide bonds (Savage et al. 1973; Winkler et al. 1986). Many larger proteins contain a 30 to 40-amino acid sequence similar to EGF, which is frequently repeated and found only extracellularly on secreted or transmembrane proteins. These are typically referred to as EGF-like repeats, or EGF repeats. The repeat number can vary on different proteins from one in several coagulation factors and other proteins to more than 300 in *Drosophila* cell adhesion protein Dumpy. Moreover, a subset of EGF repeats can bind calcium, which plays important roles in protein folding and proper protein-protein

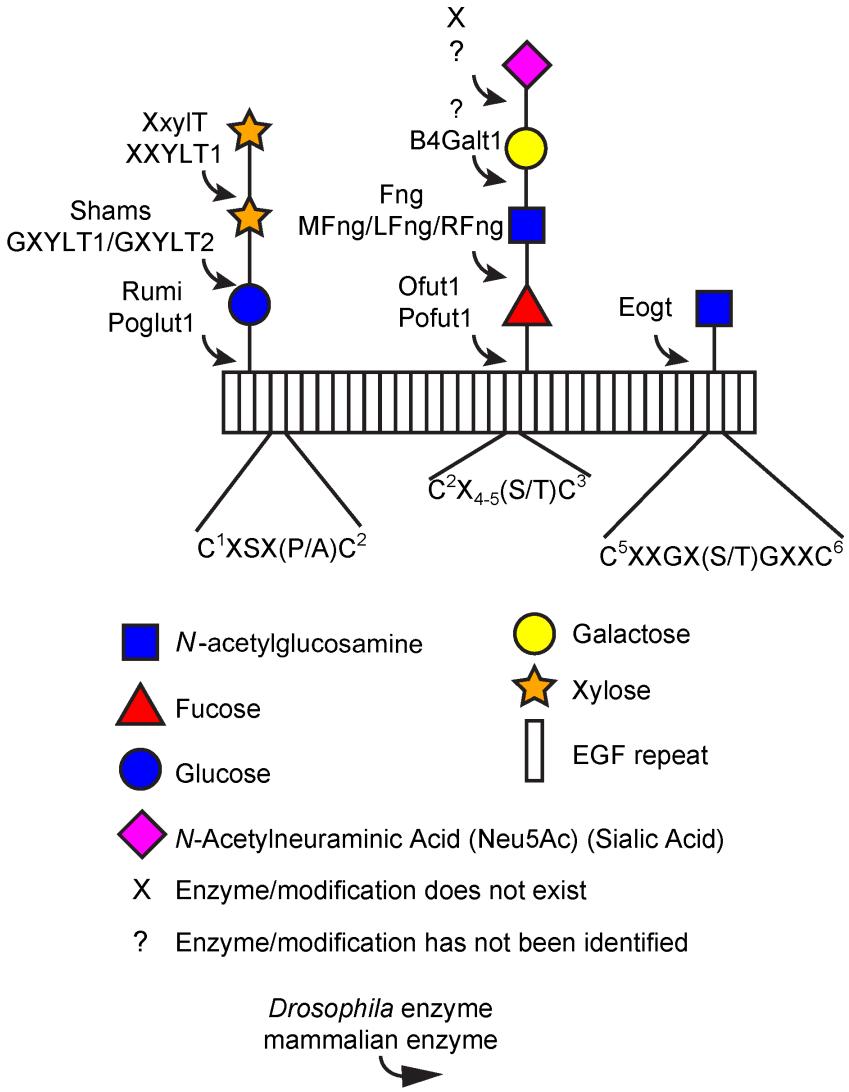

Figure 1-1. O-linked glycans found on EGF repeats in *Drosophila* and mammals. Each modification is shown with the corresponding enzyme that adds the sugar. The consensus sequence for each glycan is listed below, although the sequence for *O*-GlcNAc is based on a small number of data points. Note that a single EGF repeat can possess all 3 modifications (Matsuura et al. 2008). Fng: Fringe, MFng: Manic Fringe, LFng: Lunatic Fringe, RFng: Radical Fringe

interactions (Downing et al. 1996; Fehon et al. 1990; Rand et al. 1997; Rebay et al. 1991). Additionally, EGF repeats tend to be heavily glycosylated, and these glycan modifications are the focus of this review.

EGF repeats are found on functionally diverse proteins; for example, many growth factors, cell adhesion receptors, cell adhesion molecules, plasma proteins, and extracellular matrix components contain EGF repeats (Appella et al. 1988). Most of the functions of these EGF repeats involve mediating protein-protein interactions and trafficking. Growth factors that compete with EGF for binding to the EGF receptor family, such as heregulin, contain EGF repeats. These are required for the affinity of heregulin to its receptor (Barbacci et al. 1995). Similarly, the EGF repeats in the epithelial cell adhesion molecule (ep-CAM) are required for its adhesive properties between neighboring cells (Balzar et al. 2001). Additionally, coagulation factors contain EGF repeats. A cofactor involved in preventing coagulation, thrombomodulin, requires its EGF repeats to perform its cofactor activities so that the downstream targets can be activated and blood clotting can occur (Esmon et al. 1982; Kurosawa et al. 1988; Suzuki et al. 1989; Wang et al. 2000). Furthermore, EGF repeats are involved in protein trafficking. In low density lipoprotein (LDL), small deletions that include loss of a cysteine residue impair LDL trafficking to the cell membrane (Yamamoto et al. 1986).

Notch signaling

The *O*-glycans found on EGF repeats play important roles in the function of Notch receptors and have been well studied in this context. Notch signaling is a cell-cell signaling pathway that is critical for the development and adult homeostasis of animals (Artavanis-Tsakonas and Muskavitch 2010; Kopan and Ilagan 2009). For signaling to occur, the transmembrane ligands from one cell bind the transmembrane Notch receptor in a neighboring cell, causing the Notch intracellular domain (ICD) to be cleaved and released into the cell, where it can translocate to the nucleus and promote expression of its target genes. *Drosophila* is frequently used to study Notch signaling since they have only one Notch receptor, but mammals have 4 Notch receptors

(Notch1-4) and 5 canonical ligands: Jagged1, Jagged2, Delta-like (DLL) 1, DLL3 and DLL4. In *Drosophila*, the only two ligands are the Jagged homolog Serrate and Delta. The *Drosophila* Notch receptor and the mammalian receptors have up to 36 EGF repeats. The EGF repeats of the receptors contain all three types of *O*-glycans found on EGF repeats, and two (*O*-glucose and *O*-fucose) are critical for Notch function (Acar et al. 2008; Bruckner et al. 2000; Fernandez-Valdivia et al. 2011; Lee et al. 2013; Matsuura et al. 2008; Moloney et al. 2000b; Okajima and Irvine 2002; Sasamura et al. 2003; Shi and Stanley 2003; Takeuchi et al. 2011; Zhou et al. 2008) (summarized in Table 1-1), so Notch will be discussed at length below.

O-linked glycans on EGF repeats

O-glucose

The *O*-glucose modification is added to serine residues and was discovered nearly 3 decades ago on the EGF repeats of bovine blood coagulation factors VII and IX (Hase et al. 1988). The *O*-glucose was found as a disaccharide, extended by a xylose to form glucose-xylose, or a trisaccharide to form glucose-xylose-xylose. Generating a serine to alanine mutation to prevent the addition of *O*-glucose resulted in a decrease in the clotting activity of factor VII in vitro (Bjoern et al. 1991). This was the first evidence that the *O*-glucose glycan could be biologically relevant. To determine the consensus sequence for *O*-glucose, the sequences for the *O*-glucosylation sites in human and bovine factor VII, factor IX, protein Z, and human thrombospondin were compared, which revealed the consensus sequence to be C^1-X-S-X-P-C^2 (Nishimura et al. 1989), later modified to C^1-X-S-X-P/A-C^2 (Rana et al. 2011). Additionally, mouse Notch1, Notch2 and *Drosophila* Notch were found to be modified with *O*-glucose (Acar et al. 2008; Fernandez-Valdivia et al. 2011; Moloney et al. 2000b; Rana et al. 2011; Whitworth et al. 2010). In *Drosophila* Notch, 18 out of 36 EGF repeats contain the consensus sequence for *O*-glucose, more predicted sites than any other protein. Additionally, every consensus sequence identified in mass spectrometry analysis in *Drosophila* Notch and mammalian Notch1 contains the sugar modification

	Rumi	Ofut1
Non-enzymatic	?	Chaperone for Notch
Enzymatic	Folding: redundant	Folding: redundant
	Substrate for xylose	Substrate for GlcNAc
	S2 cleavage	Trafficking

Table 1-1. Summary of the roles of Rumi and Ofut1 on Notch.

(Acar et al. 2008; Lee et al. 2013; Rana et al. 2011), indicating that the consensus sequence is highly predictive for the addition of *O*-glucose. Close to 50 proteins are predicted to contain the *O*-glucose modification in mammals and 14 in *Drosophila* (Fernandez-Valdivia et al. 2011; Haltom et al. 2014), and it is possible that *O*-glucose plays a role on other targets besides Notch.

In 2008, the corresponding *O*-glucosyltransferase, named Rumi, was discovered in a screen for modulators of Notch signaling in *Drosophila* (Acar et al. 2008). The group found that Rumi, which contains a KDEL ER-retention domain and is a soluble ER protein, is required to prevent temperature-dependent loss of Notch signaling in flies. Further characterization revealed that Rumi is the sole protein *O*-glucosyltransferase able to modify Notch in both flies and mice (Fernandez-Valdivia et al. 2011; Takeuchi et al. 2011). *O*-glucose is not required for *Drosophila* Notch and mammalian Notch to bind to ligands, but it is required for Drosophila Notch to undergo S2 cleavage (Acar et al. 2008; Fernandez-Valdivia et al. 2011). Additionally, although some Notch ligands harbor Rumi consensus sequences (Jafar-Nejad et al. 2010), Rumi is not required in the signal sending cell in flies (Acar et al. 2008; Fernandez-Valdivia et al. 2011). It has been proposed that the presence of the glucose residues allows Notch to undergo the conformational changes necessary to reveal the S2 cleavage site upon ligand binding (Jafar-Nejad et al. 2010; Leonardi et al. 2011), which will provide access to ADAM/TACE/Kuzbanian proteases responsible for cleaving the protein upon ligand binding (Brou et al. 2000; Lieber et al. 2002). In *Drosophila*, all *O*-glucose sites seem to contribute to Notch function in a redundant and/or additive fashion, although mutations in single sites do not significantly affect Notch signaling with some exceptions (Leonardi et al. 2011). The *O*-glucose sites in EGF10-15 are more important than others, and these surround the site of ligand binding, EGF12, although ligand binding is not affected upon loss of Rumi (Acar et al. 2008). *O*-glucose is also required for mammalian Notch1 in an additive and/or redundant fashion with one exception. A serine-to-alanine mutation in EGF28 significantly decreases the ability of mouse Notch1 to respond to Delta-like 1, without affecting Jagged1-induced signaling (Rana et

al. 2011). This site is not present in *Drosophila* Notch and in mammalian Notch receptors other than Notch1 (Fernandez-Valdivia et al. 2011; Jafar-Nejad et al. 2010), and it is not clear whether the observed effect on DLL1 signaling is due to the loss of sugar or a conformational change in EGF28.

As mentioned earlier, *O*-glucose in flies and mammals can be extended by one or two xylose residues to form a xylose-glucose disaccharide or a xylose-xylose-glucose trisaccharide. In humans, the addition of the xylose residue to glucose is mediated by two enzymes, glucoside xylosyltransferase (GXYLT) 1 and GXYLT2, and the extension to a trisaccharide is mediated by xyloside xylosyltransferase (XXYLT1) (Sethi et al. 2012; Sethi et al. 2010). GXYLT1 and GXYLT2 add xylose specifically to an *O*-glucosylated substrate, and although GXYLT1 appears more active than its counterpart, no distinct specificity for either is apparent. All three contain the domains of type II transmembrane proteins, although this has not been confirmed. All three xylosyltransferases are predicted to reside in the Golgi, however Sethi et al (2012) provides strong evidence that XXYLT1 resides in the ER (Sethi et al. 2012; Sethi et al. 2010). Additionally, XXYLT1 is highly specific for the Xylose-Glucose disaccharide, as it is unable to modify substrates with only an *O*-linked xylose. The predominant sugar in mouse Notch1 is the xylose-xylose-glucose trisaccharide, but interestingly *Drosophila* Notch only contains the trisaccharide on EGF16 and 18. The *Drosophila* gene that has the highest homology with human XXYLT1 is CG11388, but whether this gene actually encodes the XXYLT enzyme remains to be determined.

Recently, Lee et al identified and characterized the sole *Drosophila* GXYLT, which they named Shams (Lee et al. 2013). This enzyme adds xylose to a subset *O*-glucosylated EGF repeats of Notch, EGF repeats 14-20. In vivo mutational analysis of a *Notch* genomic transgene indicates that EGF16-20 contain the functionally important sites of xylosylation, which is only a subset of EGF repeats with the *O*-glucose modification. However, all EGF repeats in mouse Notch1 with *O*-glucose are extended to the trisaccharide (Rana et al. 2011). Although loss of *Drosophila* Rumi leads to a loss of Notch signaling in all contexts studied so

far (Acar et al. 2008; Leonardi et al. 2011; Perdigoto et al. 2011), loss of Shams leads to a gain of Notch signaling in certain development processes. Shams is expressed at a higher level in the pupal wing than the larval wing disc, and loss of Shams results in Notch accumulation inside and at the cell surface of pupal wing cells. These data indicate that addition of xylose fine tunes Notch signaling in *Drosophila* by negatively regulating Notch in specific contexts. Interestingly, overexpression of human GXYLT1 in *Drosophila* results in stronger *Notch* loss of function phenotypes than overexpression of Shams, suggesting that human GXYLT1 is a more efficient xylosyltransferase, which corresponds with the mass spectrometry data that all the glucosylated EGF repeats in mouse Notch are xylosylated. However, the increased xylosylation of mouse Notch may also be due, at least in part, to the fact that mammals have two GXYLT enzymes, which could lead to more efficient xylosylation.

A potential mechanism for the gain of Notch signaling upon loss of Shams is increased Notch availability at the cell surface, but it remains to be determined whether xylose also affects other steps in Notch signaling including ligand binding. Of note, EGF16-20 in Notch harbor the xylose modification, but the EGF repeats most important for ligand binding are EGF 11 and 12 (Rebay et al. 1991) and before this study, no specific functions have been assigned to EGF16-20 (Pei and Baker 2008; Yamamoto et al. 2012). The precise mechanisms underlying the regulation of *Drosophila* Notch signaling by xylose and the functional significance of GXYLT1/2 and XXYLT1 in mammalian Notch signaling remain to be determined.

O-fucose

O-fucose modifications were initially discovered in human urine in the 1970s (Hallgren et al. 1975) and were later identified on an EGF repeat on urinary-type plasminogen activator (Kentzer et al. 1990). The modification is also present on other proteins such as the EGF repeats of blood plasma factors and Notch (Harris and Spellman 1993; Kentzer et al. 1990;

Moloney et al. 2000b). The consensus sequence was identified as C^2-X-X-G-G-(S/T)-C^3 (Harris et al. 1992; Harris and Spellman 1993) but was later modified to C^2-X-X-X-X-(S/T)-C^3 (Haines and Irvine 2005). However, this sequence must be within a properly folded EGF repeat for *O*-fucose to be added (Wang and Spellman 1998). The mammalian protein *O*-fucosyltransferase (Pofut1) was discovered by protein isolation and molecular cloning (Wang et al. 2001) and the *Drosophila* homolog was discovered by the same group shortly after and named Ofut1 (Okajima and Irvine 2002). Like Rumi, Pofut1/Ofut1 is a soluble, ER localized enzyme (Luo and Haltiwanger 2005). Recently, human *POFUT1* was discovered to be mutated in patients with Dowling-Degos disease, a rare, autosomal dominant genodermatosis (Li et al. 2013). Mammalian agrin is a target of Pofut1 and contains one *O*-fucose modification on EGF4 that is required for agrin to regulate the amount of nicotinic acetylcholine receptors at the postsynaptic membrane of the mammalian neuromuscular junction (Kim et al. 2008). Interestingly, loss of Pofut1 results in a gain of agrin function, such that without *O*-fucose, agrin recruits more acetylcholine receptors to the postsynaptic membrane, resulting in higher acetylcholine receptor clustering.

Although only a few proteins have been identified to contain the *O*-fucose modifications, such as urokinase plasminogen activator (uPA), tissue type plasminogen activator, several blood coagulation factors, and Notch (Harris and Spellman 1993; Kentzer et al. 1990; Moloney et al. 2000b), over 100 proteins contain the consensus sequence for *O*-fucose and are predicted to be *O*-fucosylated (Rampal et al. 2007). The most studied target of Pofut1 is the Notch receptor, which has the most potential *O*-fucose target sites out of all other potential targets (Jafar-Nejad et al. 2010; Rampal et al. 2007). The first evidence that *O*-fucose is required for Notch signaling was the loss of Jagged1-induced Notch signaling in cells deficient in fucose (Chen et al. 2001; Moloney et al. 2000a). Moreover, both Notch and its ligands are modified with *O*-fucose in flies and mice (Moloney et al. 2000b; Panin et al. 2002). In *Drosophila*, Ofut1 is required for the activation of Notch signaling (Okajima and Irvine 2002; Okajima et al. 2003). RNAi-mediated knockdown of *ofut1* results in a loss of wing tissue and a

repression of Notch target genes, indicative of loss of Notch signaling (Okajima and Irvine 2002). Loss of *ofut1/Pofut1* in flies and mice is embryonic lethal and causes phenotypes resembling a global loss of Notch signaling (Okajima and Irvine 2002; Okajima et al. 2003; Sasamura et al. 2003; Shi and Stanley 2003). *Pofut1* null mice are embryonic lethal at E10 and heart-specific conditional Pofut1 mutant exhibit cardiovascular defects resembling heart-specific conditional RBP-Jk mutant mice (Okamura and Saga 2008). In *Pofut1* knockdown C2C12 cells, which are mouse myogenic cells, the cells differentiate prematurely due to attenuated Notch signaling. In *Drosophila*, Ofut1 does not seem to be required in signal-sending cells, i.e. the cells expressing Notch ligands (Okajima and Irvine 2002). Furthermore, mouse DLL1 with mutations in its *O*-fucosylation sites accumulates intracellularly but still localizes to the cell surface and can still activate Notch in neighboring cells. This observation suggests that *O*-fucose is not required for ligand function but is required for Notch receptor function. However, it remains unknown whether this is true for all Notch ligands.

Pofut1/Ofut1 is a soluble endoplasmic reticulum protein that can recognize misfolded EGF repeats and functions as a chaperone for Notch. Loss of Ofut1 in *Drosophila* S2 cells results in accumulation of Notch in the ER, and loss of Ofut1 in flies results in defects in the Notch endosomal trafficking. Both of these defects can be rescued by expression of a full length Ofut1 that lacks the catalytic domain, suggesting a chaperone function of Ofut1 (Okajima et al. 2005; Sasamura et al. 2007). In some contexts, Notch is reduced at the cell surface in Ofut1/Pofut1 deficient cells, which can be rescued by expression of a catalytically inactive Ofut1/Pofut1 (Okamura and Saga 2008; Stahl et al. 2008; Yao et al. 2011). Additionally, the full length Ofut1 lacking the enzymatic domain binds Notch and is sufficient for proper Notch folding (Okajima et al. 2005). A second chaperone function of Ofut1 is that it is required for the transport of Notch to the lysosome upon endocytosis. Loss of Ofut1 results in the retention of Notch in endosomes and the prevention of Notch degradation, and overexpression of Ofut1 causes decreased levels of Notch, perhaps due to impaired transport to the lysosome (Sasamura et al. 2007).

To determine the extent of the Ofut1 chaperone activity, a mutant genomic fragment of Ofut1 was generated containing a point mutation in the GDP-fucose binding domain (Okajima et al. 2005). This allele was introduced in *Drosophila* and used, along with mutations in other genes that prevent fucosylation without affecting Ofut1 levels such as a defective enzyme responsible for the generation of GDP-fucose called GDP-D-mannose dehydratase (GMD), to determine the contribution of the chaperone activity and enzymatic activity to Notch function (Okajima et al. 2008; Okajima et al. 2005). Surprisingly, the results were not as consistent as one would expect, and the ability of the Ofut1 enzymatic mutant transgene to rescue *ofut1* null mutations is dependent on the site of insertion into the fly genome. Therefore, the chaperone contribution of Ofut1 could be suggested but not proven from these studies.

One group recently sought to overcome this problem by generating a knock-in allele of the enzymatic null *ofut1* to more accurately separate the enzymatic and chaperone functions. They found that embryos homozygous for the mutant allele $ofut^{R245A\ knock\text{-}in}$, which lacks enzymatic function, exhibit a severe, temperature sensitive neurogenic phenotype in which more neural precursors develop than in wild type animals. However, animals homozygous for the *ofut1* null allele $ofut^{4R6}$ show a severe neurogenic phenotype at lower temperatures, indicating that the chaperone function is required to prevent the neurogenic phenotype at lower temperatures. Additionally, animals deficient in enzymes required in the GDP-fucose pathway show a temperature-sensitive neurogenic phenotype, further supporting the notion that the temperature-sensitive neurogenic phenotype observed in $ofut^{R245A\ knock\text{-}in}$ animals is due to the loss of Ofut1 enzymatic function. Furthermore, additional sensory organ precursors (SOPs) develop at higher temperatures in *ofut1* mutants, suggesting defects in Notch signaling. Additionally, loss of *O*-fucose causes Notch to accumulate intracellularly at higher temperatures, which also occurs upon loss of *O*-glucose from Notch. However, in animals double mutant for *rumi* and $ofut^{R245A\ knock\text{-}in}$, SOP number increased even at lower temperatures. In all contexts tested, double mutant *rumi* and *ofut1* animals resulted in the same defects as $ofut^{R245A\ knock\text{-}in}$, but at a lower temperature. These data indicate that *O*-glucose and *O*-fucose

play a partially redundant role in regulating Notch signaling, likely through promoting proper Notch folding.

The *O*-fucose on Notch can be extended to form a disaccharide, trisaccharide, or tetrasaccharide. Fringe (Fng) proteins are a group of enzymes that extend the *O*-fucose modification to GlcNAcβ1-3Fuc to generate the disaccharide. Fng was first discovered to be required for dorsal-ventral boundary specification in the *Drosophila* wing, and loss of *fng* results in a loss of wing tissue, leading to the descriptive name of the gene (Irvine and Wieschaus 1994; Kim et al. 1995). Null mutations in *Drosophila fng* result in larval lethality (Irvine and Wieschaus 1994). Fng was later shown to modulate Notch signaling (Bruckner et al. 2000; Fleming et al. 1997; Klein and Arias 1998; Moloney et al. 2000a; Panin et al. 1997). Addition of GlcNAc to *O*-fucose by Fng results in a sensitization of Notch to Delta signaling and the inhibition of Notch-Serrate signaling at the level of ligand binding (Bruckner et al. 2000; Fleming et al. 1997; Moloney et al. 2000a; Okajima et al. 2003; Panin et al. 1997).

The same basic mechanism applies to mammalian systems, however with more complexity. Mammals have four Notch receptors, five Notch ligands and three Fng homologs: Manic Fringe (MFng), Lunatic Fringe (LFng), and Radical Fringe (RFng). Although biochemically, all 3 Fng homologs have the same enzymatic function, *in vivo* the story is rather different. The Fng homologs can affect Notch signaling differently depending on which ligand binds Notch. Shown by co-culture and luciferase assays, LFng promotes Delta-like 1 (DLL1) Notch1 signaling and suppresses Jagged1 induced Notch1 signaling (Hicks et al. 2000; Yang et al. 2004). Additionally, MFng inhibits Jagged1 induced Notch1 signaling (Chen et al. 2001; Hicks et al. 2000; Moloney et al. 2000a; Yang et al. 2004) and promotes DLL1 induced Notch1 signaling more weakly than LFng (Yang et al. 2005). RFng promotes DLL1 induced Notch1 signaling strongly, and interestingly also promotes signaling by Jagged1 (Yang et al. 2005). Moreover, although the mammalian Fng glycosyltransferases modulate Notch signaling, they do not alter ligand-Notch binding (Yang et al. 2005).

The above-mentioned functions of Fng are in the context of trans signaling of Notch, meaning that the ligand from a neighboring cell binds to Notch, but until recently it remained unknown whether this function was the same in the context of cis inhibition. Cis inhibition is the binding of Notch to its ligand in the same cell, resulting in the sequestration of the Notch receptor and making it unavailable to receive the signal from neighboring cells. Lebon et al sought to determine whether Fng played a role on Notch in the context of cis inhibition (LeBon et al. 2014). They used a co-culture system in which a fluorescent based Notch reporter and the fluorescent tagged Dll1 and Jagged1were utilized to monitor expression (Sprinzak et al. 2010). They showed that, when any of the 3 Fng homologs are expressed, cis interactions between Notch1 and Dll1 are stronger. However, expression of MFng or LFng in cells expressing Notch1 and Jagged1 decreases the level of cis inhibition. In contrast, expression of RFng enhances cis inhibition between Notch1 and Jagged1, similar to its role in Notch1 and Dll1 cis inhibition. These observations are supported by *in vivo* fly genetic experiments.

The mechanism of the different response of Notch to different ligands when modified by GlcNAc has just begun to be elucidated. Taylor et al performed *in vitro* experiments to determine whether the structure of Notch changes and/or if the affinity of Notch to its ligands changes in response to GlcNAc. These experiments were designed to determine whether the effects of Fng on Notch-ligand signaling are due to structural changes in response to the sugar or due to a difference in ligand affinity. This group generated a human Notch1 fragment (EGF11-13), which contains the ligand-binding domain, and assessed the effect of different glycosylation states on the fragment's ability to bind to Jagged1 and DLL ligands (Taylor et al. 2014). They determined that the addition of *O*-fucose, which adds only to EGF12 in the fragment, partially enhances binding of the fragment to Jagged1, but this binding is significantly enhanced when GlcNAc is added by LFng. These glycan modifications do not affect binding between the Notch fragment and DLL4. However, Notch binding to DLL1 is slightly and significantly enhanced by *O*-fucose and GlcNAc, respectively, on the Notch fragment. Based on crystal structure analysis, the authors propose that the addition of the sugars to EGF12 does

not induce a conformational change of Notch, but rather may be directly involved in the ligand binding. Howver, the results presented by the group are surprising given that *in vivo*, the presence of LFng enhances Notch1-DLL1 signaling but inhibits Notch1-Jagged1 signaling. The authors propose that GlcNAc modifications on other EGF repeats function to inhibit Notch1-Jagged1 signaling, and as a result, the GlcNAc on the only EGF repeat tested did not fully recapitulate the *in vivo* phenotypes.

Although extensive work has been done to elucidate the effect of each mammalian Fng homolog on Notch function, only LFng seems to be important for mouse development. LFng is expressed in the presomitic mesoderm, rhombomeres 3 and 5, developing ear, retina and spinal cord, and is required for proper skeletal development (Cohen et al. 1997; Evrard et al. 1998; Johnston et al. 1997). Animals mutant for LFng show reduced viability and fertility, although some survive to adulthood (Evrard et al. 1998; Zhang and Gridley 1998). MFng is expressed in the neural tube, head, cranial nerves, dorsal root ganglia, and otic vesicle (Cohen et al. 1997; Johnston et al. 1997). RFng is expressed in the developing limb bud, head, anterior neural tube, branchial arches (Cohen et al. 1997; Johnston et al. 1997). However, neither MFng nor RFng appear to be required for viability and fertility in mice (Moran et al. 1999; Moran et al. 2009; Zhang et al. 2002). Moreover, mutations in human LFng cause spondylocostal dysostosis (Sparrow et al. 2006), but no diseases have been associated with mutations in MFng or RFng. It is unlikely that MFng and RFng have no role in the homeostasis of organisms given that they are so highly conserved, but more studies are required to determine exactly what those roles might be.

Although only LFng is important for mouse development, MFng and RFng play roles in the immune system. Notch1 signaling is required in the thymus to suppress B cell development and promote T cell development (Radtke et al. 1999; Stanley and Guidos 2009). Loss of LFng results in increased B cell development, and LFng is required to enhance Notch signaling during B/T cell fate decision (Stanley and Guidos 2009; Visan et al. 2006). Loss of MFng alone does not show any defects in B/T cell fate. However, loss of both MFng and LFng results in a

greater decrease in Notch activation and a greater impairment of T cell fate than loss of LFng alone, suggesting that MFng can at least partially compensate for loss of LFng (Stanley and Guidos 2009).

In mammals, the extension of GlcNAc-fucose disaccharide to a trisaccharide results in Galactose-GlcNAc-Fuc which is present on mammalian Notch1 (Moloney et al. 2000a; Moloney et al. 2000b). This trisaccharide can further be extended to the tetrasaccharide, Sialic acid-Galactose-GlcNAc-Fuc, which was first observed on human clotting factor IX (Harris et al. 1993; Nishimura et al. 1992). The trisaccharide was found in *Drosophila* embryos, but it remains unknown whether this exists on *Drosophila* Notch (Aoki et al. 2008). The gene encoding the enzyme responsible for the addition of Galactose is *B4galt1* in mice. Loss of the *B4galt1* gene in mice is semi-lethal, and homozygous mice exhibit growth retardation, skeletal defects, impaired wound healing, defects due to endocrine deficiency, abnormal differentiation of intestinal villi, and increased proliferation of skin cells and cells of the small intestine (Asano et al. 1997; Chen et al. 2006; Lu et al. 1997; Mori et al. 2004). Additionally, the mutant mice have an extra lumbar vertebra (Chen et al. 2006). Moreover, a number of Notch components are misexpressed in the *B4galt1* mutant mice, which are also misexpressed in LFng mutant mice (Chen et al. 2006; Evrard et al. 1998; Zhang and Gridley 1998; Zhang et al. 2002). Few *B4galt1* null mice survive past 16 weeks. Therefore, *B4galt1* is not required for early embryonic development, but is required for late embryonic development and survival after birth.

Evidence suggests that the terminal Galactose is important for Notch signaling, but the sialic acid appears to be dispensable. In Chinese Hamster Ovary (CHO) cells deficient in the transporter required for sialic acid to be sent to the Golgi, loss of the sialic acid does not affect the usual inhibition of Jagged1-Notch signaling or the enhancement of Notch1-Dll1 signaling by LFng (Chen et al. 2001; Hou et al. 2012). However, in CHO cells deficient in Galactose, neither LFng nor MFng are able to inhibit Jagged1-induced Notch signaling, and LFng is unable to enhance Dll1-induced Notch signaling. MFng is still able to enhance Dll1-induced Notch signaling in the absence of Galactose (Hou et al. 2012). Additionally, although the presence of

O-fucose enhances the binding of Notch to Jagged1 and Dll1, addition of Galactose has no further effect on binding (Taylor et al. 2014). Collectively, these results suggest that Galactose is required for the function of Fng on Notch outside of ligand binding in some contexts.

O-GlcNAc

While searching for *O*-linked glycans on the extracellular domain of *Drosophila* Notch, the Okajima group unexpectedly discovered *O*-GlcNAc modification on EGF20 (Matsuura et al. 2008). They performed western blots on fragments of Notch with an *O*-GlcNAc antibody (CTD110.6) to search for other EGF repeats that may have the modification and found that the EGF1-10 and 22-31, but not EGF6-10, contain the O-GlcNAc modification. The signal is nearly eliminated in these fragments when they are treated with β-N-acetylhexosaminidase, which cleaves *O*-GlcNAc. This modification was later found on the EGF repeats of other proteins such as *Drosophila* Delta, Serrate, and Dumpy (Matsuura et al. 2008; Muller et al. 2013; Sakaidani et al. 2011), the latter of which is a large 2.5 MDa extracellular matrix protein with 308 EGF repeats without a clear mammalian homolog (Wilkin et al. 2000). Comparison of sites with a confirmed *O*-GlcNAc has suggested the putative consensus sequence $C^5XXGX(S/T)GXXC^6$ (Alfaro et al. 2012). As more target sites are analyzed, it is possible that this sequence will be refined, like those of *O*-glucose and *O*-fucose.

In 2011, the enzyme responsible for the addition of *O*-GlcNAc on EGF repeats was identified in *Drosophila* as EGF domain-specific *O*-GlcNAc transferase, or Eogt (Sakaidani et al. 2011). Eogt resides in the ER and is conserved in mice (Sakaidani et al. 2012). The maternal contribution of Eogt is required for embryonic development in a Notch-independent manner. *eogt* mutant flies that received the maternal component die between the second instar and early third instar larval stages. The mutant larvae display cuticle defects and defects in tracheal morphology similar to those observed in animals that lack *dumpy* (Prout et al. 1997; Sakaidani et al. 2011; Wilkin et al. 2000). Additionally, loss of Eogt or Dumpy in the wing results in wing blistering that is independent of integrin function. Moreover, Dumpy requires Eogt

enzymatic activity and the *O*-GlcNAc modification to function. These results highlight the importance of *O*-GlcNAc modification on Dumpy. However, mammals lack a Dumpy homolog, so the functional importance of *O*-GlcNAc in mammals remains to be determined.

Although *O*-GlcNAc is found on Notch, *eogt* mutants do not show Notch mutant phenotypes (Sakaidani et al. 2011). To determine whether other proteins are involved in the *eogt* null phenotype and may require *O*-GlcNAc to function, Muller et al performed genetic interaction experiments with genes that were likely to play a role in the wing adhesion phenotype of *eogt* mutants or with players that were predicted to be *O*-GlcNAcylated. Surprisingly, removal of one copy of an integrin in an *eogt* knock-down wing does not alter the phenotype, but removal of one copy of *wing blister*, which encodes laminin α chain, enhances the wing blistering phenotype. Additionally, the authors hypothesize that, although loss of *eogt* in any tissue does not recapitulate Notch mutant phenotypes, the effect of *O*-GlcNAc on Notch may be subtle. Therefore, the authors removed one copy of Notch or Notch pathway components in *eogt*-knockdown animals, which suppresses the wing blistering phenotype. This may be due to the loss of *O*-GlcNAc on Notch. However, *dumpy* alleles interact with the γ-secretase *Presenilin*, which is crucial for Notch pathway activation (Mahoney et al. 2006). Therefore, the genetic interaction may not be due to the loss of *O*-GlcNAc on Notch, but instead it is possible that Dumpy and Notch both contribute to wing adhesion.

Dumpy genetically interacts with components of the pyrimidine synthesis pathway, and feeding pyrimidine synthesis inhibitors to *dumpy* mutant flies reverses the defects in wing shape (Rizki and Rizki 1965); (Blass and Hunt 1980; Stroman 1974). Therefore, the authors sought to determine whether components of the pyrimidine synthesis pathway genetically interact with *eogt*. Reduction of genes that contribute to the synthesis of UMP/pyrimidine suppresses the wing blistering from *eogt* knock down. Consistent with this, the authors hypothesize that reducing the dosage of genes responsible for pyrimidine degradation should enhance the wing blistering phenotype, which proves to be correct, and such a genetic

interaction is lethal. Collectively, these data lead to the possibility that increased pyrimidine synthesis, such as increased Uracil, could cause the wing blistering phenotype in *eogt* mutants.

Less is known about the mammalian Eogt. Sakaidani et al identified and confirmed the biochemical function of mouse Eogt and found that the enzyme is expressed in all tissues examined (Sakaidani et al. 2012). Additionally, mammalian Eogt reaches optimal function when divalent cations, especially Mn^{2+}, are accessible, similar to the *Drosophila* enzyme (Sakaidani et al. 2012; Sakaidani et al. 2011). Transgenic expression of the human *EOGT* was able to rescue the wing blistering phenotypes in fly *eogt* knock-down wings, suggesting that the human Eogt has enzymatic activity and that the fly and human Eogt enzymes are functionally conserved (Muller et al. 2013). Moreover, mammalian Notch1 is modified by Eogt, and the O-GlcNAc sugar is extended by Galactose. However, the only evidence that Eogt is important for mammalian biology is the discovery of EOGT mutations in patients with autosomal recessive Adams-Oliver syndrome (Cohen et al. 2014; Shaheen et al. 2013). Adams-Oliver syndrome, or AOS, is a rare disorder characterized by aplasia cutis congenita (vertex scalp defects) and terminal transverse limb defects (Bonafede and Beighton 1979; Burton et al. 1976). Other mutations in Notch pathway components have been described in Adams-Oliver syndrome, such as mutations in *RBPJ*, which is the primary transcriptional regulator of Notch signaling, and mutations in *NOTCH1* (Hassed et al. 2012; Stittrich et al. 2014). These observations indicate that Eogt is important for mammalian biology and strongly suggest that *O*-GlcNAc is important for mammalian Notch signaling, although further studies are required to confirm these hypotheses.

CHAPTER II

INTRODUCTION:

DROSOPHILA PHOTORECEPTOR DEVELOPMENT

Drosophila eye organization

The *Drosophila* eye contains about 800 ommatidia, which are repetitive hexagonal units. Each ommatidium contains 20 cells, including 8 photoreceptors, which are highly polarized light-sensing cells. Each photoreceptor contains an apical organelle that is composed of ~10,000 stacks of microvilli called the rhabdomere (Figure 2-1). The photoreceptors are large cells and extend about 100 μm from distal to proximal. Each microvillus is 1.5 μm long and 50 nm wide (Kumar and Ready 1995; Leonard et al. 1992), is actin rich (Arikawa et al. 1990), and contains a protein complex that includes the photopigment rhodopsin. The tight packing of the microvilli allows a large surface area for the localization of rhodopsin so that the photoreceptor has the ability to be extremely sensitive to light. The outside photoreceptors, labeled R1-6, span the entire depth of the retina, about 85 μm. R7 is located in the distal half of the retina and R8 comprises the proximal half of the retina. R7/R8 mainly detect color, while the role of R1-6 is to detect motion (Gao et al. 2008; Morante and Desplan 2004; Wardill et al. 2012; Yamaguchi et al. 2008). The rhabdomeres are organized into a circular pattern so that every rhabdomere faces toward a centrally located "lumen," commonly referred to as the interrhabdomeral space (IRS) (Figure 2-1). Each photoreceptor targets its axon to one of about 800 units, called cartridges, located in the first optic brain region, the lamina. These form the first synapses for vision (Boschek 1971; Rister et al. 2007). The next synapses form in the medulla, then the lobula and finally the lobula plate.

This "open rhabdom" of *Drosophila* is different from most insects, which have "apposition" eyes in which all the rhabdomeres are fused at the center, typically called a fused rhabdom. This modification arose throughout evolution of insects to form a neural superposition eye (Braitenberg 1967; Kirschfeld 1967a). Neural superposition eye is a modified form of the apposition eye and comparatively can visualize the environment with the same resolution but with increased sensitivity. The advantages of this in the *Drosophila* eye biology are twofold. The separation of rhabdomeres in the open rhabdom allows each photoreceptor to "see" a

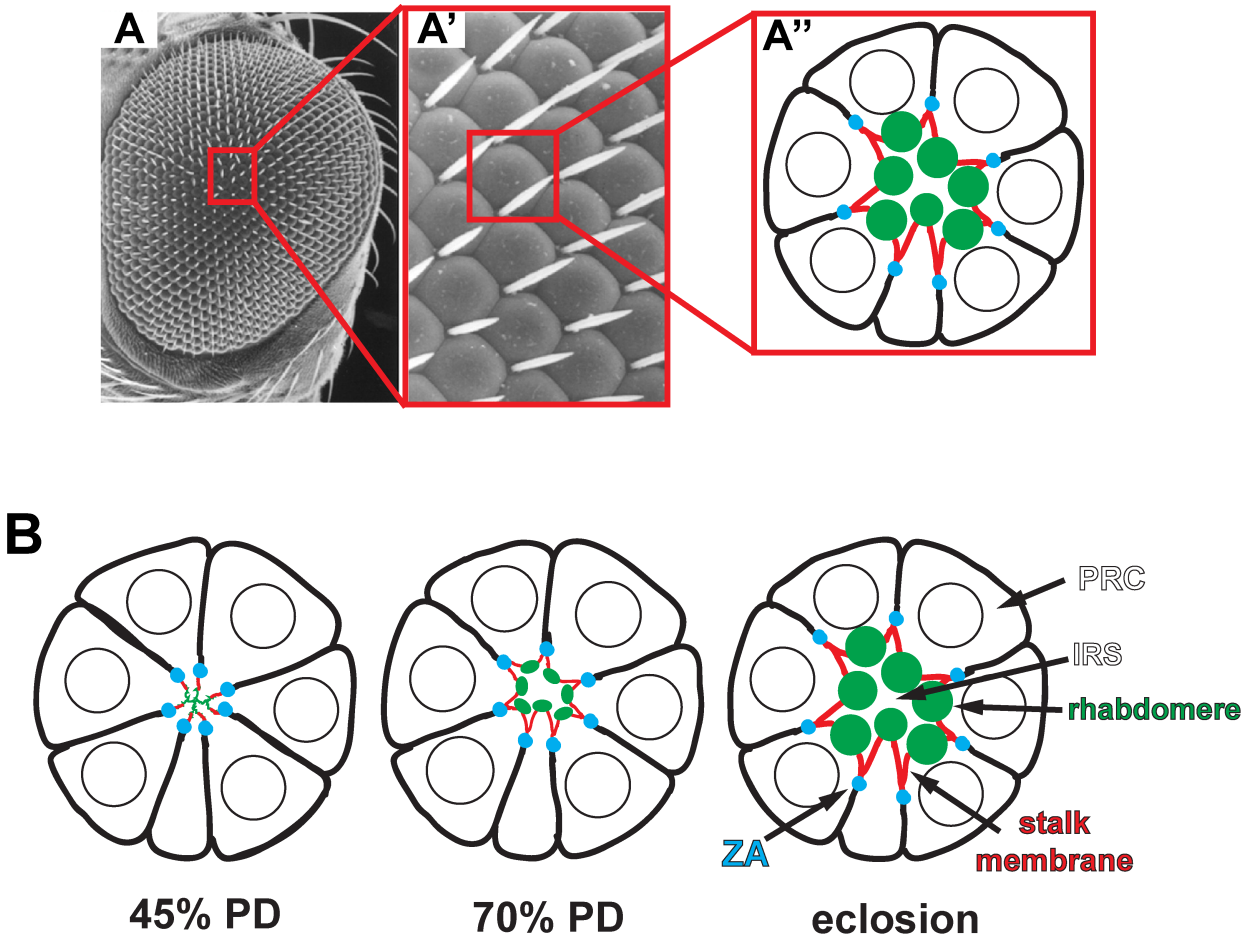

Adapted from Knust 2007

Figure 2-1. The structure and development of a *Drosophila* ommatidium. (A-A") Schematic showing the structure of one ommatidium in the context of an entire eye. (B) The development of the photoreceptors and the IRS. Starting at 45% pupal development, the rhabdomeres are fused at center, but separate and grow as development progresses. (C) Transmission electron micrograph of an ommatidium from an adult wild type fly. A-A" and B were adapted from (Knust 2007).

different field of view than the neighboring rhabdomere, therefore each ommatidium can see pictures from 8 fields rather than just 1 in insects with a closed rhabdom. Additionally, the axons from each photoreceptor do not necessarily synapse with the same lamina cartridge. Instead, each cartridge contains axons from the 6 photoreceptors, R1-R6, which face the same point in the space but each axon is from the photoreceptor of a different ommatidium. These modifications arose throughout evolution and are thought to result in a significant improvement to the insect visual system.

Photoreceptor development

The photoreceptors begin to develop at the third instar larval stage. During this time, the photoreceptor precursors are located in a simple epithelium, called the eye disc, and they are connected by adherens junctions. During larval development, a wave of apically constricted cells moves through the eye disc, called the morphogenetic furrow (Ready et al. 1976), which leads to the expression of a large list of specification genes in its wake. This leads to the specification of R8 photoreceptors, followed by the specification of pairs of R1-6 photoreceptors sequentially and finally the specification of the R7 photoreceptor. Photoreceptor specification is a scientific field in itself, and it is nicely reviewed in (Kumar 2011; 2012). Before the photoreceptors are specified, the apical ends are located dorsally in the eye disc. Once the photoreceptors are specified and assembled behind the morphogenetic furrow, they undergo a 90° turn so that the apical ends turn toward the equator, resulting in the apical ends facing one another and attached at the center. This organization continues into the pupal stage. At early pupal development, the length of the cells begins to extend from distal to proximal, to the retinal floor. Additionally, microvilli begin to develop at the apical ends of the cell, which are all facing the center in a 20-cell cluster. Starting between 40-50% pupal development (PD), the microvillar membranes in the center begin to separate from one another and thicken while the photoreceptors continue to grow toward the retinal floor (Longley and Ready 1995). Shortly

before the flies eclose, about 90-95% PD, the development of the photoreceptors and the IRS is completed.

Genes involved in interrhabdomeral space formation

Studies to elucidate the mechanism of interrhabdomeral space (IRS) development are ongoing. Surprisingly, although vertebrate photoreceptors are not organized the same way as *Drosophila* photoreceptors, many of the genes involved in IRS formation are conserved. The first genes identified to play a role in IRS formation are *crumbs* (crb) and *chaoptin* (*chp*), and subsequently *eys, prom,* and *actin* (summarized in Figure 2-2).

Crumbs

Crumbs is a type I transmembrane protein involved in establishing apical basal polarity and adherens junctions, expressed apically on epithelial cells and required for embryonic development in *Drosophila* (Grawe et al. 1996; Knust et al. 1993; Tepass et al. 1990). Crumbs contains a short cytoplasmic domain, which is necessary and sufficient for Crb to establish apical basal polarity (Wodarz et al. 1993; Wodarz et al. 1995), and a large extracellular domain. The role of Crb in epithelial cell polarity is well studied, but its role in photoreceptor morphogenesis is less well understood. *Drosophila* photoreceptors require Crumbs, which is localized at the adherens junctions and stalk membrane, for proper morphogenesis (Pellikka et al. 2002; Tepass 1996). Loss of *crb* results in misshapen rhabdomeres, which frequently take an elongated, oval shape instead of their normal round shape. Additionally, stalk membranes are shorter and the photoreceptors do not extend the full length of the retina in *crb* mutant flies. Moreover, loss of *crb* results in light-induced photoreceptor degeneration in *Drosophila* (Johnson et al. 2002). Although *Drosophila* only have one *crb* homolog, mammals have three homologs: *CRB1, CRB2,* and *CRB3.* Interestingly, mutations in the extracellular domain of human CRB1, which is expressed exclusively in the brain and retina, cause autosomal recessive retinitis pigmentosa (arRP) and autosomal recessive Leber Congenital Amaurosis

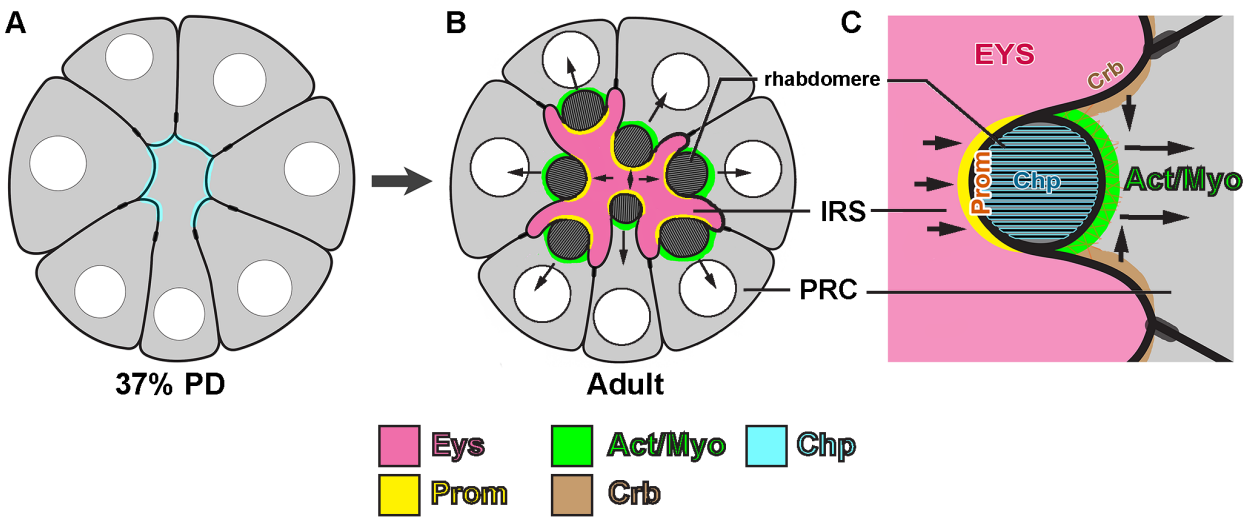

Adapted from Nie et al 2014

Figure 2-2. Proposed model of IRS separation. Eyes shut (Eys), expressed at ~55% PD, pushes against the rhabdomere surface where Prominin (Prom) is expressed. Prom expression begins around 45% PD, shortly before Eys expression begins. Crumbs (Crb), expressed before the pupal stage, restricts the rhabdomere width together with Actin/Myosin (Act/Myo), which pulls the rhabdomeres away from one another. All of these actions must overcome the adhesion properties of Chaoptin (Chp). Adapted from (Nie et al. 2014).

(LCA) (den Hollander et al. 2001; den Hollander et al. 1999). The role of the Crb extracellular domain in biology is slowly becoming clear. In the *Drosophila* eye, expression of the Crb intracellular domain in a *crb* null background cannot rescue the shortened stalk membrane defect, but expression of the Crb extracellular domain can (Richard et al. 2009). Moreover, the extracellular domain is required for the proper apical localization of Crb in neighboring cells and is required to mediate cell adhesion and for proper cell shape during embryonic development (Letizia et al. 2013). This group showed that both the extracellular and intracellular domains are required for normal polarity. Additionally, the extracellular domain is required for the prevention of light induced photoreceptor degeneration, and expression of the intracellular domain in a *crb* null background does not prevent degeneration (Johnson et al. 2002). This phenotype can be rescued by raising animals on vitamin A deficient media; vitamin A is the precursor for Rhodopsin synthesis, and raising animals on vitamin A deficient media reduces the level of rhodopsin by 97% (Nichols and Pak 1985)**.** This result demonstrates that Crb acts to maintain rhodopsin homeostasis, but the mechanism remained unknown until recently, when Pocha et al sought to determine the effect of Crb on rhodopsin (Pocha et al. 2011). This group found that Crb forms a complex with Myosin V, an unconventional myosin that is required for the post-Golgi transport of Rhodopsin to the rhabdomere (Li et al. 2007). Upon loss of Crb, Myosin V is mislocalized and degraded by the proteasome. Additionally, Rhodopsin is not transported to the rhabdomere properly upon loss of Crb. However, the function of Myosin V transport can be rescued with the expression of the Crb intracellular domain, so further studies will be required to determine the precise role of the extracellular domain in preventing light induced degeneration.

Eyes shut

The most important gene for IRS formation is *eyes shut* (*eys*), which is a secreted glycoprotein (Husain et al. 2006; Zelhof et al. 2006). Eys is secreted into the interrhabdomeral space in an Ire1 dependent but Sec6 independent manner (Coelho et al. 2013; Husain et al.

2006). Eys is expressed weakly in the embryonic and larval stages, and strongly in the pupal and adult stages (Husain et al. 2006). Moreover, Eys is not only expressed in the retina but also in the *Drosophila* mechanosensory organs (Husain et al. 2006; Zelhof et al. 2006). This gene was discovered by two groups simultaneously but independently in 2006, and both found that loss of Eys results in a complete loss of IRS, the only gene found so far that can transform an open rhabdom into what appears to be a closed rhabdom. Eys is conserved in some mammals including human (in whom it's called EYS) but is not conserved in mice or other rodents (Abd El-Aziz et al. 2008). The *eys* locus is about 40 kb in *Drosophila* and about 2 Mb in humans, the largest gene expressed in the human eye (Abd El-Aziz et al. 2008). In humans, EYS is expressed in the spinal cord, skeletal muscle, and brain in addition to the retina. Eyes shut is mutated in about 5-15% of patients with autosomal recessive retinitis pigmentosa (arRP), whereas most other arRP causative genes account for <5% of patients (Abd El-Aziz et al. 2008; Abd El-Aziz et al. 2010; Audo et al. 2010; Bandah-Rozenfeld et al. 2010; Barragan et al. 2010; Collin et al. 2008; Littink et al. 2010). Analysis done by one group shows that porcine EYS localizes to the outer segment of mammalian photoreceptors, which is the segment where Rhodopsin is localized to and is homologous to the rhabdomeres in *Drosophila* photoreceptors (Abd El-Aziz et al. 2008). Additionally, EYS is mutated in patients with cone-rod dystrophy (Katagiri et al. 2014). Very little is known about EYS function. One group showed that expression of human EYS in *eys* null *Drosophila* cannot rescue the *eys* phenotype (Nie et al. 2012), and the rhabdomeres remain fused, although pockets of IRS can be seen at the stalk membrane when coexpressed with human Prom (discussed below). However, many isoforms of human EYS exist, and the reference does not mention which isoform was used in its rescue experiments. Therefore, it is possible that the shorter isoform was expressed and the longest isoform is needed to rescue the phenotype.

Although the involvement of Eys in photoreceptors is the best studied function of Eys, it has other functions as well. Mutations in *eys* cause a temperature-sensitive loss of coordination in *Drosophila* (Cook et al. 2008). Eys is required in the mechanosensory organs, and loss of

eys reduces the function of mechanosensory organs when animals are raised at 37°C. *eys* null animals exhibit deformed mechanoreceptor neurons, and this is due to a loss of water from the mechanoreceptors when animals are shifted to higher temperatures. Animals raised at high temperatures but high humidity do not display the same phenotype, suggesting that Eys is required at the surface of or in the extracellular fluid that surrounds the neurons in the mechanosensory organs to preserve their shape and function under stress. Interestingly, single nucleotide polymorphisms (SNPs) in *EYS* have been associated with statin-induced myopathy in some patients (Isackson et al. 2011). It is possible that EYS is required to protect skeletal muscle under stress, similar to the protection of mechanosensory organs in *Drosophila*.

Prominin

Prominin (PROM1) was first discovered as an apically located protein in mouse neuroepithelial cells, hematopoietic stem cells, and retinoblastoma cells, and is frequently referred to as antigen AC133 (Corbeil et al. 2001; Miraglia et al. 1997; Weigmann et al. 1997). Prom is a pentaspan transmembrane protein with multiple glycosylation sites on its two large extracellular loops (Corbeil et al. 2001), and it associates with microvilli and epithelial membrane protrusions (Corbeil et al. 1998; Weigmann et al. 1997). The function lies in the extracellular loops, and the cytoplasmic tail with variable sequence between *Drosophila* and human Prom is not required for function in the context of *Drosophila* (Nie et al. 2012). PROM1 has been frequently used as a stem cell marker and a prognostic marker in cancers such as colorectal cancer and non-small cell lung cancer (Ren et al. 2013; Wang et al. 2014; Wu et al. 2014). Mutations in *PROM1* cause autosomal recessive and autosomal dominant retinal degeneration in humans (Maw et al. 2000), and *PROM1* is mutated in autosomal recessive retinitis pigmentosa, autosomal dominant Stargardt disease 4 and autosomal dominant bull's eye macular dystrophy (Kniazeva et al. 1999; Michaelides et al. 2003; Yang et al. 2008; Zhang et al. 2007). PROM1 localizes to the outer segment in mice and *Xenopus* photoreceptors (Han et al. 2012; Maw et al. 2000), and it is thought that PROM1 is required for proper disk formation

of the outer segment of the mammalian eye (analogous to *Drosophila* rhabdomeres). However, the function of Prom in the photoreceptors or other tissues remains unknown.

The *Drosophila* homolog of human PROM1 is prominin-like (Prom, also called Eyes closed, or Eyc) and is another player required for proper rhabdomere separation (Sang and Ready 2002). The overall sequence homology between human *PROM1* and *Drosophila prom* is rather low, with 18% identity and 44% similarity (Nie et al. 2012). *Drosophila* ommatidia with null mutations in *prom* have many fused rhabdomeres at the center, though not all rhabdomeres are fused as they are in *eys* mutant *Drosophila,* and some IRS can still be seen in *prom* mutants (Sang and Ready 2002). The Ready lab first discovered *Drosophila prom*, and although the mutant alleles they used were indeed *prom* mutant alleles, the gene they identified as *prom* was incorrect. The gene was correctly identified by the Zuker group (Zelhof et al. 2006). The rhabdomeres never fully separate from the beginning of IRS development upon loss of *prom* (Husain et al. 2006; Zelhof et al. 2006). Prom localizes to the rhabdomeres and stalk membrane just before rhabdomere separation (~45% PD) and shortly thereafter becomes restricted to the rhabdomere (Zelhof et al. 2006). Moreover, human PROM1 (hereafter referred to as hProm) expressed in *Drosophila* localizes to the same structure. However, it fails to rescue the *Drosophila prom* (*prom*) null phenotype (Nie et al. 2012). The group who performed these studies suggests that this may be due to the low expression level of hProm in transgenic flies. When hProm is overexpressed using a stronger promoter in *prom* mutant *Drosophila,* a certain amount of rescue can be achieved, but not 100%. These results demonstrate that there is at least some degree of functional conservation between *Drosophila* and human Prom. Additionally, mutation of all of the *N*-glycosylation sites in dProm or hProm results in the retention of both in the cell and a failure of each to be transported to or kept at the cell membrane. Indeed, neither of these mutant proteins can rescue the *prom* mutant phenotype. Moreover, the group sought to use *Drosophila* to model the disease-causing hProm mutation, R373C, identified by the Zhang lab, which disrupts murine outer segments when expressed in a wild type background (Yang et al. 2008). Interestingly, expression of this variant in *Drosophila*

results in a disruption in the rhabdomeric microvilli, but expression in a *prom* mutant background shows normal microvilli, although it fails to rescue the *prom* mutant rhabdomere attachment phenotype. Moreover, loss of *prom* causes retinal degeneration in a recessive manner in *Drosophila* (Gurudev et al. 2014). These studies highlight the evolutionary conservation of human and *Drosophila* prom in maintaining the integrity of cilia/microvilli of photoreceptors. Further studies are required to elucidate the mechanism through which Prominin prevents photoreceptor degeneration.

Although the mechanism behind retinal degeneration caused by loss of *prom* remains to be determined, studies attempting to elucidate the mechanism underlying the formation of IRS have revealed that Eys and Prom cooperate to separate the rhabdomeres (Zelhof et al. 2006). *eys*, *prom* double heterozygous flies show a mild but nearly 100% penetrant rhabdomere attachment defect, despite the fact that both the genes are recessive. Additionally, co-expression of Eys and Prom in S2 cells results in the recruitment of Eys to decorate the outside of Prom-expressing cells, suggesting that the two bind to one another, which may be the mechanism for rhabdomere separation. Surprisingly, although loss of *crb* and loss of *prom* show severe morphological and rhabdomere attachment defects, loss of both *crb* and *prom* in the same animal suppresses the phenotypes of the single mutants (Gurudev et al. 2014). This suggests an important genetic network of *eys, prom,* and *crb* in promoting rhabdomere separation.

Chaoptin

Chaoptin (Chp) is a glycosylphosphatidylinositol (GPI) anchored, photoreceptor-specific cell adhesion glycoprotein with 41 leucine rich repeats (LLRs) (Reinke et al. 1988; Van Vactor et al. 1988). Chp expression begins in the photoreceptor cells in the third instar larval stage and continues throughout pupal and adult life (Zipursky et al. 1984). Expression of Chp in S2 cells causes aggregates to form, confirming its role as a cell adhesion protein and suggesting that Chp's adhesive activity is homotypic (Krantz and Zipursky 1990). Chp has 16 sites for potential

glycosylation, and removal of these *N*-glycosylation sites affects Chp function in an additive manner (Hirai-Fujita et al. 2008). Mutating a few of the glycosylation sites throughout the protein results in reduced protein levels, but mutations in all of the glycosylation sites results in increased protein levels. This suggests that *N*-glycosylation is required for protein degradation. Additionally, mutating only 4 or 6 glycosylation of Chp and expressing this form in S2 cells leads to reduced cell-cell adhesion, indicating that the glycosylation sites are required for the adhesive activity of Chp.

Drosophila with mutations in *chp* are viable and fertile but have severe defects in rhabdomere microvilli (Van Vactor et al. 1988). Loss of *chp* causes loss of microvilli organization, suggesting that *chp* normally acts to adhere the individual microvilli together. If *chp* is a strong adhesion molecule, one would predict that the rhabdomeres would adhere together inherently to form a closed rhabdom. However, Zelhof et al discovered that Eys and Prom oppose the adhesive activity of Chp, and that Eys is not expressed in the eyes of insects with closed rhabdoms (Zelhof et al. 2006). Although *eys* and *prom* mutant photoreceptors degenerate when placed in constant light (~1800 lux), *chp* null photoreceptors do not show signs of apoptosis in these conditions (Gurudev et al. 2014). This suggests that, although these three genes and *crb* participate in a genetic network to separate the rhabdomeres, *chp* does not protect the rhabdomeres from light induced degeneration. Additionally, the degeneration defects of *crb, eys* and *prom* null photoreceptors can be rescued by vitamin A deficient media. Therefore, *crb, eys*, and *prom* all play a role in Rhodopsin homeostasis.

Actomyosin network

Recently, Nie et al sought to determine other players of IRS formation to further elucidate the mechanism of IRS development (Nie et al. 2014). In their study, they used a sensitized background, the *prom eys* double heterozygous, which they had established previously. In this background, some rhabdomeres of each ommatidium are attached. They used this background to perform a deficiency screen for modulators of IRS size and number of

rhabdomere attachments. They identified Actin5C in their screen, one of the 2 ubiquitously expressed Actin genes (Fyrberg et al. 1981; Fyrberg et al. 1983; Wagner et al. 2002). Reduction of Actin5C in the sensitized background results in increased rhabdomere attachments. Subsequently, they identified non-muscle myosin II heavy and light chains as modulators of the phenotype, similar to actin. Moreover, reduction of myosin II heavy and light chains alone, in a wild-type background, results in increased rhabdomere attachments and decreased IRS, demonstrating the importance of myosin II in IRS development. Additionally, players involved in the activation and phosphorylation of myosin II are also involved in IRS formation, such as Rho-kinase and the small GTPase Rho1 (Amano et al. 1996; Matsui et al. 1996). The authors suggest a mechanism in which Actin5C and non-muscle myosin II provide a contractile force inside the cell to pull the rhabdomeres away from one another, while Eys and Prom interact to push the rhabdomeres apart from the outside.

CHAPTER III

THE PROTEIN *O*-GLUCOSYLTRANSFERASE RUMI MODIFIES EYES SHUT TO PROMOTE RHABDOMERE SEPARATION IN *DROSOPHILA*

This chapter is based upon Haltom, A. R.*, Lee, T. V.*, Harvey, B. M., Leonardi, L., Chen, Y., Hong, Y., Haltiwanger, R. S., Jafar-Nejad, H. (2014). "The protein O-glucosyltransferase Rumi modifies eyes shut to promote rhabdomere separation in Drosophila." PLoS Genet **10**(11): e1004795.

* These authors contributed equally to this work.

INTRODUCTION

Diurnal insects possess “apposition eyes” in which ommatidia are optically isolated from each other (Borst 2009; Nilsson 1990). In most diurnal insects like honeybee and butterflies, the apical rhodopsin-housing structures of each ommatidium—the rhabdomeres—are fused at the center. This allows the group of photoreceptors in each ommatidium to act as a single optical device (Borst 2009). A modification of the apposition eye arose during insect evolution in dipteran flies, where an extracellular lumen called the inter-rhabdomeral space (IRS) forms to separate and optically isolate the rhabdomeres in each ommatidium from one another. Due to this structural modification and the accompanying regrouping of photoreceptor axons among neighboring ommatidia, information from photoreceptor cells that receive light from the same point in the space merge on the same postsynaptic targets in the lamina (Clandinin and Zipursky 2000). This type of eye is referred to as a neural superposition eye, and these improvements allow for increased light sensitivity without sacrificing resolution (Borst 2009; Kirschfeld 1967b).

Separation of the rhabdomeres in flies requires an evolutionarily conserved secreted glycoprotein called Eyes shut (Eys; also called Spacemaker). *eys* mutant flies lack the IRS and exhibit an altered photoreceptor organization that resembles the closed rhabdom of other insects like honeybees and mosquitos (Husain et al. 2006; Zelhof et al. 2006). Eys is secreted from the stalk membrane of the photoreceptor cells in an Ire1-dependent but Sec6-independent manner to separate the rhabdomeres and open the IRS (Coelho et al. 2013; Husain et al. 2006). *Drosophila eys* functions together with three other genes, *crumbs* (*crb*), *prominin* (*prom*) and *chaoptin* (*chp*), to regulate rhabdomere separation and IRS size (Gurudev et al. 2014; Husain et al. 2006; Nie et al. 2012; Zelhof et al. 2006). Genetic experiments have established that *prom* and *eys* promote rhabdomere separation but *chp* and *crb* promote rhabdomere adhesion, and that the balance between their activities results in proper IRS formation (Gurudev et al. 2014; Nie et al. 2012; Zelhof et al. 2006).

The Crb extracellular domain and the Eys protein are primarily composed of epidermal growth factor-like (EGF) repeats and Laminin G domains (Husain et al. 2006; Pellikka et al. 2002; Tepass et al. 1990; Zelhof et al. 2006). However, the role of these protein domains and their posttranslational modifications in the function Eys and Crb is unknown. Five of the Eys EGF repeats and seven of the Crb EGF repeats contain the $C^1X\underline{S}X(P/A)C^2$ consensus sequence, which predicts the addition of an *O*-linked glucose by the protein *O*-glucosyltransferase Rumi (POGLUT1 in mammals) (Acar et al. 2008; Rana et al. 2011). Mutations in *rumi* were first isolated in a genetic screen for regulators of sensory organ development in *Drosophila* (Acar et al. 2008). When raised at 18°C, *rumi* mutants are viable and only show a mild loss of Notch signaling in certain contexts including bristle lateral inhibition and leg joint formation (Acar et al. 2008; Leonardi et al. 2011). However, when raised at higher temperatures the mutant animals show a broad and severe loss of Notch signaling, until 28-30°C, at which loss of *rumi* becomes larval lethal (Acar et al. 2008; Leonardi et al. 2011; Perdigoto et al. 2011). Mice lacking the Rumi homolog POGLUT1 die at early embryonic stages (at or before E9.5) and some of the defects observed in mutant embryos are characteristic of loss of Notch signaling (Fernandez-Valdivia et al. 2011). Moreover, transgenic expression of human POGLUT1 in flies rescues the *rumi* null phenotypes, indicating that the function of Rumi is conserved (Takeuchi et al. 2011). *Drosophila* Notch has 18 Rumi target sites in its extracellular domain, most of which have been confirmed to harbor *O*-glucose residues (Acar et al. 2008; Lee et al. 2013). Moreover, serine-to-alanine mutations in the Rumi target sites of Notch result in a temperature-sensitive loss of Notch signaling (Leonardi et al. 2011), establishing Notch as a biologically-relevant target of Rumi in flies. However, whether Rumi and its glucosyltransferase activity are required for the function of its other potential targets like Eys and Crb and for rhabdomere separation remained unknown.

Here, we present evidence indicating that the enzymatic activity of Rumi is required for the separation of rhabdomeres in the *Drosophila* eye. When raised at 18°C, animals homozygous for a null allele of *rumi* or for a missense mutation that abolishes its protein *O*-

glucosyltransferase activity show a highly penetrant rhabdomere attachment phenotype that cannot be explained by loss of *O*-glucose from Notch. Mass spectral analysis indicates that both Crb and Eys harbor *O*-glucose when expressed in a fly cell line. However, genetic experiments rule out Crb as a target of Rumi during rhabdomere separation. Our data indicate that *O*-glucosylation of Eys by Rumi promotes Eys folding and stability and thereby ensures that enough Eys is secreted into the IRS in a critical time window during the mid-pupal stage to fully separate the rhabdomeres.

MATERIALS AND METHODS

Drosophila strains and genetics

The following strains were used in this study: 1) *Canton-S*, 2) *y w*, 3) *w; noc^{Sco}/CyO; TM3, Sb^{1}/TM6, Tb^{1}*, 4) *y w; D/TM6, Tb^{1}*, 5) *N^{55e11}/FM7c*, 6) *y^{1} w^{67c23} P{Crey}1b; D*/TM3, Sb^{1}*, 7) *y^{1} M{vas-int.Dm}ZH-2A w*; VK31*, 8) *y^{1} M{vas-int.Dm}ZH-2A w*; VK22*, 9) *w^{67} c^{23}P{lacW}Hsc70-3^{G0102}/FM7c*, 10) *GMR-GAL4* (on 2) (Bloomington *Drosophila* Stock Center), 11) *GMR-GAL4* (on 3) (Xu et al. 2006), 12) *eys^{734}* (Husain et al. 2006), 13) *P{rumi$^{gt\text{-}FLAG}$}* (*rumi* rescue transgene), 14) *y w; FRT82B rumi^{79}/TM6, Tb^{1}*, 15) *y w; FRT82B rumi$^{\Delta 26}$/TM6, Tb^{1}* (Acar et al. 2008), 16) *y w; PBac{N$^{gt\text{-}4\text{-}35}$}attVK22* (Leonardi et al. 2011), 17) *eys^{734}/CyO; FRT82B rumi$^{\Delta 26}$/TM6, Tb^{1}*, 18) *y w; crb$^{1\text{-}7}$::HA-A* (*crb$^{1\text{-}7\text{-}HA}$*), 19) *UAS-attB-eys^{wt}-VK31*, 20) *UAS-attB-eys$^{1\text{-}4}$-VK31*, 21) *UAS-attB-eys$^{1\text{-}5}$-VK31*, 22) *UAS-attB-rumi$^{wt\text{-}FLAG}$-VK22*, 23) *UAS-attB-rumi$^{79\text{-}FLAG}$-VK22* (this study), 24) *y w; crb^{wt}::HA-A* (*crb$^{wt\text{-}HA}$*) (Huang et al. 2009), 25) *crb^{11A22}/TM6, Tb^{1}* (Tepass et al. 1990).

All *rumi* mutant crosses were raised at 18°C to minimize the temperature-dependent defects in Notch signaling unless otherwise specified. To obtain *N^{55e11}/Y; PBac{N$^{gt\text{-}4\text{-}35}$}attVK22/+* animals, *N^{55e11}/FM7c* females were crossed to *y w/Y; PBac{N$^{gt\text{-}4\text{-}35}$}attVK22* males and the male progeny were selected based on the absence of the *FM7* bar eye phenotype.

To remove one copy of *Hsc70-3* in *rumi$^{-/-}$* animals, *w^{67} c^{23}P{lacW}Hsc70-3^{G0102}/FM7c* females were first crossed to *y w; FRT82B rumi$^{\Delta 26}$/TM6, Tb^{1}* males. The *w^{67} c^{23}P{lacW}Hsc70-*

3^{G0102}/y w; FRT82B rumi$^{\Delta 26}$/+ female progeny from this cross were backcrossed to *y w; FRT82B rumi$^{\Delta 26}$/TM6, Tb^{1}* males. *w^{67} c^{23}P{lacW}Hsc70-3^{G0102}/y w; FRT82B rumi$^{\Delta 26}$/FRT82B rumi$^{\Delta 26}$* progeny were selected based on the eye color from the *Hsc70-3* allele and the *rumi* mutant bristle phenotype (Leonardi et al. 2011) and used for TEM analysis.

_O_-Glucose site mapping on _Drosophila_ Crb and Eys fragments expressed in S2 cells

A construct encoding EGF1-5 from *Drosophila* Eys (harboring four out of the five Rumi target sites of Eys) was synthesized (Genewiz, Inc.). EGF12-17 from *Drosophila* Crb (harboring five out of the seven Rumi targets sites of Crb) was amplified using region-specific primers from genomic DNA extracted from flies carrying a *UAS-crb-full-length* transgene (Izaddoost et al. 2002). The genomic DNA was obtained using a DNA purification kit from Promega. The Eys fragment was cloned in frame to an N-terminal signal peptide from *Drosophila* Acetylcholine esterase and C-terminal V5 and 6X-Histidine tags in the *pMT/V5-HisB-ACE* vector (Acar et al. 2008). The Crb fragment was cloned into a pMT/BiP/3xFLAG vector using *EcoRI* and *XbaI* (Okajima et al. 2003). Eys-EGF1-5-V5-His and Crb-EGF12-17-3xFLAG were expressed in *Drosophila* S2 cells, purified from medium by Nickel column or anti-FLAG resin, respectively, reduced and alkylated, and subjected to in-gel protease digests as described (Nita-Lazar and Haltiwanger 2006; Xu et al. 2007) with minor modifications. *O*-Glucose modified glycopeptides were identified by neutral loss of the glycans during collision-induced dissociation (CID) using nano-LC-MS/MS as described (Rana et al. 2011).

Dissections, staining, processing, image acquisition and quantification

For dissection at 55% and 65% pupal development, animals were selected at the white prepupal stage and aged for 4.5 days (55%) and 5.5 days (65%) at 18°C. For animals raised at higher temperatures, the white prepupae were placed at 25°C at zero hours APF for 1 day and subsequently placed at 30°C until 55% or 75% PD for dissection. The pupal case was removed and heads were pierced to allow proper fixation. Corneas were removed from the eyes in PBS.

Tissues were fixed using 4% formaldehyde for 30-40 minutes, and then washed in 0.3-0.5% Triton X-100 in PBS. Blocking and antibody incubations were performed in PBS containing 0.5% Triton X-100 and 5% Serum (Donkey or Goat).The following antibodies were used: mouse anti-Eys (21A6) 1:250 and mouse anti-ELAV (9F8A9) 1:200 (Developmental Studies Hybridoma Bank), guinea pig anti-Eys 1:1000 (Husain et al. 2006), guinea pig anti-Boca 1:1000 (Culi and Mann 2003), rat anti-Crb 1:500 (Pellikka et al. 2002), rabbit anti-Lava lamp 1:2000 (Sisson et al. 2000), rabbit anti-Rab11 1:1000 (Satoh et al. 2005), Rabbit anti-Rab7 1:100 (Chinchore et al. 2009), mouse anti-Rab11 1:100 (BD Biosciences), guinea pig anti-Senseless 1:2000 (Nolo et al. 2000), goat anti-mouse-Cy3 1:500, goat anti-mouse-Cy5 1:500, donkey anti-mouse-Dylight649 1:500, donkey anti-mouse-Cy3 1:500, donkey anti-rabbit-Cy3 1:500, donkey anti-guinea pig-Dylight649 1:500 (Jackson ImmunoResearch Laboratories). Phalloidin Alexa488 conjugated 1:500 (Life Technologies) was used to visualize rhabdomeres. Confocal images were taken with either a Leica TCS-SP5 microscope with an HCX-PL-APO oil 63x, NA 1.25 objective and an HCX-PL-APO 20x, 0.7 NA objective with a PMT SP confocal detector, or a TCS-SP8 microscope with an HC-PL-APO glycerol 63x, NA 1.3 objective and HyD SP GaAsp detector. All images were acquired using Leica LAS-SP software. Amira 5.2.2 and Adobe Photoshop CS4 were used for processing and figures were assembled in Adobe Illustrator CS5.1.

To quantify IRS size, the electron micrographs were opened using “Fiji is just ImageJ” open source image processing software. The scale was set by tracing the scale bar in the image using the line tool and using the "set scale" function. The IRS was traced using the freehand selection tool and the area was measured using the "measure" function.

To quantify total pixel intensity, the Amira 5.2.2 image processing software was used. A single ommatidium was cropped, which was done twice for each image to obtain data from 2 different ommatidia per animal. The desired channel for quantification was labeled with the "label field" function, and the "segmentation editor" was opened. The IRS was traced using the lasso freehand tool, placed in a separate "material", and the rest of the pixels in the channel

were selected using the threshold tool and placed in a separate “material”. The same threshold was used for all ommatidia. In the "object pool" module, the total pixel intensities for IRS and the rest of the ommatidium were obtained using the "material statistics" option.

Western blotting

Proteins were extracted by lysing the heads in RIPA buffer (Boston BioProducts) containing a dissolved protease inhibitor cocktail tablet (Roche Diagnostics). Approximately 10 µL RIPA buffer was used per fly head. The following antibodies were used: guinea pig anti-Hsc70-3 1:5000 (Ryoo et al. 2007), guinea pig anti-Eys 1:10000 (Husain et al. 2006), mouse anti-FLAG 1:1000 (M2, Sigma-Aldrich), mouse anti-Tubulin 1:1000 (Santa Cruz Biotech), goat anti-guinea pig-HRP 1:5000 and goat anti-mouse-HRP 1:5000 antibodies (Jackson ImmunoResearch Laboratories). Western blots were developed using Pierce ECL Western Blotting Substrates (Thermo Scientific). The bands were detected and quantified using an ImageQuant LAS 4000 system and ImageQuant TL software, respectively, from GE Healthcare. At least two independent immunoblots were performed for each experiment.

Transmission electron microscopy

To process flies using transmission electron microscopy, heads were dissected and fixed overnight at 4°C in paraformaldehyde, glutaraldehyde and cacodylic acid and processed as previously described (Fabian-Fine et al. 2003). Briefly, after fixation, heads were post fixed with 1-2% OsO_4, dehydrated with ethanol and propylene oxide, and then embedded in Embed-812 resin. Thin sections (~50 nm thick) were stained with 1-2% uranyl acetate as the negative stain and then stained with Reynold’s lead citrate. Images were obtained using three different transmission electron microscopes: 1) Hitachi H-7500 with a Gatan US100 camera: images were captured using Digital Micrograph, v1.82.366 software; 2) JEOL 1230 with a Gatan Ultrascan 1000 camera: images were captured with Gatan Digital Micrograph software; 3)

JEOL JEM 1010 with an AMT XR-16 camera: images were captured using AMT Image Capture Engine V602. All images were processed using Adobe Photoshop CS4 and figures were assembled in Adobe Illustrator CS5.1.

Generation of the knock-in and transgenic animals

To generate the *crb$^{1\text{-}7}$::HA-A* knock-in allele (*crb$^{1\text{-}7\text{-}HA}$*), a *crb* mutant founder line was used in which 10 kb of the *crb* locus harboring most of the coding region is replaced with an *attP* and a *loxP* site (Huang et al. 2009). Multiple rounds of end overlap PCR were used to introduce serine-to-alanine mutations in all seven Rumi target sites of Crb in the *pGE-attB^{GMR}-crb^{wt}::HA-A* targeting vector (Huang et al. 2009) to generate the *pGE-attB^{GMR}-crb$^{1\text{-}7}$::HA-A* targeting construct. ΦC31-mediated integration was used to introduce the *crb$^{1\text{-}7}$::HA-A* fragment into the *crb* locus of the *crb* mutant founder line. A Cre-expressing transgene (Siegal and Hartl 1996) was used to remove the *GMR-hsp::white* and the remaining vector sequences from the knock-in allele and to obtain the *white^{-}* allele *crb$^{1\text{-}7}$::HA-A* used in our study. Genomic PCR with multiple primer pairs in the region was performed to confirm correct integration and Cre-mediated recombination, as described previously (Huang et al. 2009). Primer sequences are available upon request.

To generate the wild-type and mutant *eys* transgenes, the full length *eys* cDNA was retrieved from the *pUAST-eys* construct (Zelhof et al. 2006) using restriction digestion and cloned into the *pUASTattB* vector (Bischof et al. 2007), resulting in *pUASTattB-eys^{wt}*. To generate the mutant *eys* transgenes, a 603-bp cDNA fragment containing EGF1-5 of Eys with serine-to-alanine mutations in the four target sites in this region (EGF1-3 and EGF5) was synthesized (Genewiz, Inc.). The wild-type EGF1-5 region in *pUASTattB-eys^{wt}* construct was replaced with the synthesized mutant version using two rounds of end-overlap PCR (Higuchi et al. 1988) with three overlapping fragments. The resulting 1.2-kb fragment containing the first four mutant Rumi target sites was placed in *pUASTattB-eys^{wt}* by using *BglII* and *SacII* restriction enzymes to generate *pUASTattB-eys$^{1\text{-}4}$*. To mutate the fifth (last) Rumi target site in

eys, a 4-kb fragment of the *eys* cDNA containing the target site (EGF9) and flanked by *NdeI* and *KpnI* restriction sites was PCR amplified using Phusion DNA polymerase (New England Biolabs). The PCR product was cloned into *pSC-B* using the Strataclone blunt PCR cloning kit (Agilent Technologies) to generate *pSC-B-Eys-EGF9*. Site-directed mutagenesis was performed using complementary primers and Phusion DNA polymerase to introduce the serine-to-alanine mutation. The wild-type 4-kb fragment from *pUASTattB-eys*$^{1-4}$ was replaced with the mutant version by using *NdeI* and *KpnI* to generate *pUASTattB-eys*$^{1-5}$. All three constructs were integrated into the *VK31* docking site using standard methods (Bischof et al. 2007; Venken et al. 2006). Correct integration was confirmed by PCR.

To generate wild-type and mutant *rumi* transgenes, FLAG-tagged versions of *rumi*^{wt} and *rumi*^{79} (G189E) ORF were excised from *pUAST-rumi*$^{wt\text{-}FLAG}$ and *pUAST-rumi*$^{79\text{-}FLAG}$ (Acar et al. 2008) by using *EcoRI-KpnI* double digestion and were cloned into the *pUAST-attB* vector (Bischof et al. 2007). After verification by sequencing, the constructs were integrated into the *VK22* docking site using standard methods and verified by PCR (Bischof et al. 2007; Venken et al. 2006).

Statistical analysis

Data are presented as mean ± SEM. To compare the number of rhabdomere clusters per ommatidium, ANOVA with Scheffé or Tukey multiple comparisons or *t*-test was performed. To compare the IRS size between wild-type and *rumi* ommatidia at 65% PD, unpaired *t*-test was used.

RESULTS

Mutations in *rumi* result in a rhabdomere attachment phenotype which starts in the mid-pupal stage

When raised at 18°C, *rumi* mutant animals are viable and show only a mild loss of Notch signaling in some contexts (Acar et al. 2008; Leonardi et al. 2011). To explore whether Rumi plays a role in rhabdomere morphogenesis and IRS formation, we raised animals homozygous for the protein-null allele $rumi^{\Delta 26}$ ($rumi^{-}$) in ambient light at 18°C and performed transmission electron microscopy (TEM) on adult fly eyes. In cross sections of wild-type retinas, the rhabdomeres of the seven visible photoreceptor cells are separated from neighboring rhabdomeres by the IRS (Longley and Ready 1995) (Figure 3-1A, Figure 3-2A). However, 1-day old $rumi^{-/-}$ animals exhibited a moderate, yet 100% penetrant, rhabdomere attachment phenotype, i.e. attachment of two or more rhabdomeres per ommatidium (Figure 3-1B, Figure 3-2B). This phenotype can be fully rescued by $P\{rumi^{gt\text{-}FLAG}\}$, a genomic transgene expressing a FLAG-tagged version of Rumi (Acar et al. 2008), indicating that attachment of rhabdomeres observed in $rumi^{-/-}$ flies is due to the loss of *rumi*. Sections of $rumi^{-/-}$ animals at 15 and 40 days of age show a similar degree of rhabdomere attachment, suggesting that the phenotype is not age-dependent (Figure 3-1D-E, Figure 3-2C-D). Together, these observations indicate that Rumi is required for optical isolation of individual photoreceptors in the *Drosophila* eye.

We have previously shown that Rumi primarily regulates Notch signaling through its protein *O*-glucosyltransferase activity (Acar et al. 2008; Leonardi et al. 2011). We wondered whether the enzymatic activity of Rumi is also required for rhabdomere separation. To test this, we performed TEM on adult *Drosophila* homozygous for $rumi^{79}$, a severe hypomorphic allele harboring a missense mutation which abolishes the enzymatic activity of Rumi but does not affect its expression level or stability (Acar et al. 2008; Takeuchi et al. 2011). $rumi^{79/79}$ animals raised at 18°C also exhibit rhabdomere attachment in all ommatidia examined (Figure 3-3A and C; n>50). Surprisingly, the average number of separate rhabdomeres per ommatidium was somewhat lower in $rumi^{79/79}$ animals (3.41±0.15) compared to $rumi^{-/-}$ animals (4.11±0.08), indicating that the rhabdomere attachment phenotype is slightly more severe in $rumi^{79/79}$ animals compared to $rumi^{-/-}$ animals. Statistical analysis indicated that the difference between $rumi^{79/79}$ and $rumi^{-/-}$ average rhabdomere number per ommatidia is significant (P<0.0001).

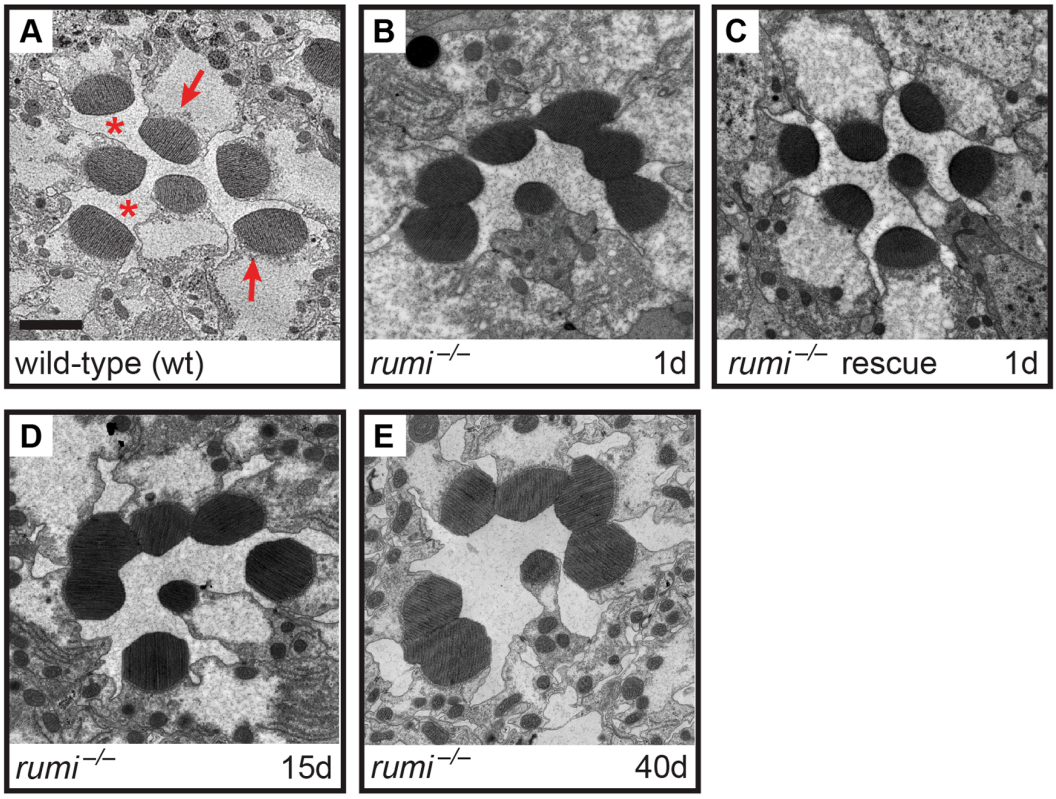

Figure 3-1. Loss of Rumi results in rhabdomere adhesion. Shown are electron micrographs of a single ommatidium from adult animals. (A) Wild-type. Arrows indicate rhabdomeres and asterisks indicate the IRS. Scale bar: 2 μm. (B) 1-day old *rumi*$^{-/-}$. Note the attachment in the neighboring rhabdomeres. (C) 1-day old *rumi*$^{-/-}$ expressing a wild-type *P{rumi*$^{gt\text{-}FLAG}$*}* genomic transgene. (D,E) The *rumi*$^{-/-}$ rhabdomere attachment phenotype does not change with age, since 15-day old (D) and 40-day old (E) animals show a similar degree of attachment. Sample processing for images in B-E was done by Tom Lee, PhD, and images were obtained by Claire Haueter in the lab of Hugo Bellen.

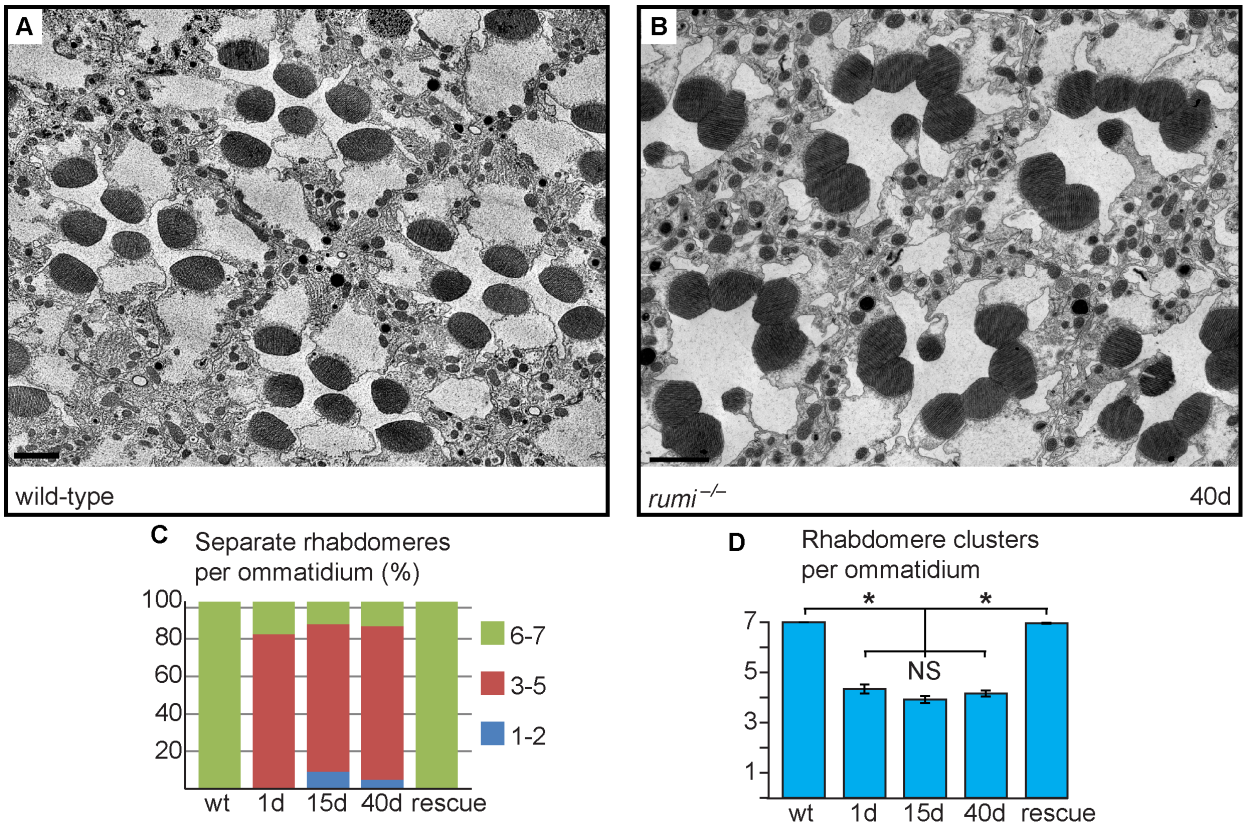

Figure 3-2. Loss of *rumi* results in a highly penetrant and statistically significant degree of rhabdomere adhesion. Images showing many ommatidia from (A) wild type and (B) *rumi*$^{-/-}$ animals. (C) Percentage of number of individual rhabdomeres per ommatidia for various genotypes. At least three animals were used for each genotype. The number of ommatidia examined for each genotype is as follows: wt (50), 1d (35), 15d (66), 40d (85), rescue (126). Scale bar: 2 μm. (D) Quantification of average individual rhabdomere number per ommatidium for the data shown in C. Rhabdomere attachments in 1-day, 15-day and 40-day old *rumi* animals are not significantly different from one another, but are significantly different from wild-type and rescued animals (*P<0.0001). NS, not significant. *rumi*$^{-/-}$ animals in (B) were processed by Tom Lee, PhD, and images were obtained by Claire Haueter in the lab of Hugo Bellen.

Given that *rumi*$^{\Delta 26}$ is a protein-null allele (Acar et al. 2008), these data suggest that *rumi*^{79} might have a dominant negative effect in the context of rhabdomere separation. However, one copy of the *P{rumi*$^{gt\text{-}FLAG}$*}* genomic transgene was able to fully rescue the rhabdomere attachment phenotype of *rumi*$^{79/79}$ animals (Figure 3-3B, n>50). Moreover, overexpression of Rumi-G189E, which is the protein product of *rumi*^{79} (Acar et al. 2008), did not result in any rhabdomere separation defects, similar to overexpression of wild-type Rumi (Figure 3-4). These observations suggest that *rumi*^{79} is not likely to be a dominant negative allele. Since *rumi*^{79} was generated in an EMS screen but *rumi*$^{\Delta 26}$ is the product of *P*-element excision, the modest worsening of the rhabdomere attachment in *rumi*^{79} might be due to a genetic background effect. Taken together, these observations indicate that enzymatic activity of Rumi is required for the separation of rhabdomeres in the fly eye.

Rhabdomere morphogenesis and IRS formation occur during the second half of pupal development (Longley and Ready 1995). Until 37% pupal development (PD), the apical surfaces of photoreceptors are attached to one another and do not exhibit any microvillar structures (Longley and Ready 1995). Around 55% PD, short microvilli and neighboring stalk membranes can be seen at the apical surfaces of the developing photoreceptors, and a thin IRS has formed (Figure 3-5A) (Longley and Ready 1995). By 65% PD, the rhabdomeres are clearly separated from one another by the IRS (Figure 3-5C). Because one-day old adult *rumi* retinas have a well-formed IRS but exhibit rhabdomere attachment, we asked whether absence of Rumi prevents rhabdomere separation during pupal development, or whether they initially separate but subsequently attach as the pupal eye assumes its adult structure. To address this question, we performed TEM on 55% and 65% PD *rumi*$^{-/-}$ retinas grown at 18°C. At 55% PD, *rumi* and wild type premature rhabdomeres appear too close in proximity to determine attachment status, although *rumi* rhabdomere microvilli and IRS appear more disorganized than wild type (Figure 3-5A and B). However, by 65% PD, each *rumi* photoreceptor harbors distinct stalk membrane and rhabdomere structures (Figure 3-5D). The IRS has formed but the average IRS size in mutant ommatidia (3.52 ± 0.20 μm^2) is 59% of the average IRS size in

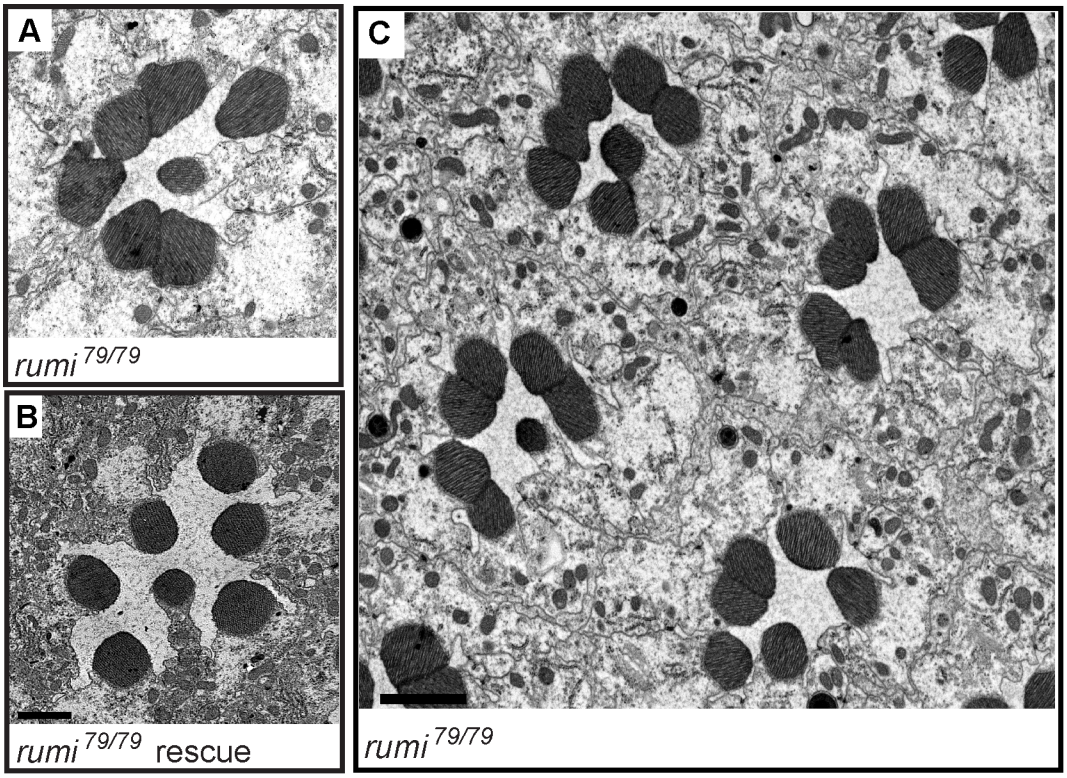

Figure 3-3. Loss of the enzymatic activity of Rumi results in rhabdomere adhesion. The enzymatically inactive allele *rumi*^{79} also shows rhabdomere a attachment phenotype (A,C), which can be rescued by one copy of the wild-type *P{rumi*$^{gt\text{-}FLAG}$*}* genomic transgene (B).

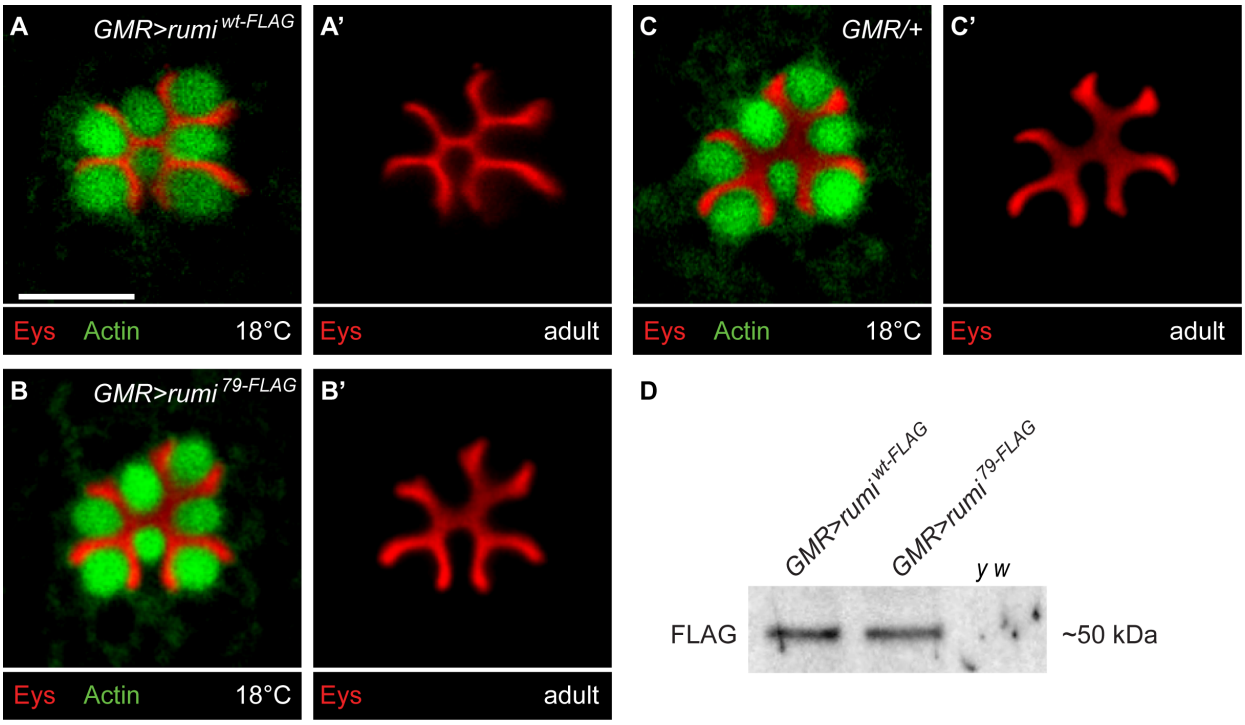

Figure 3-4. *rumi*^{79} is not likely to be a dominant negative allele. (A-C') Overexpression of FLAG-tagged versions of wild-type Rumi (A,A') or Rumi^{79} (B,B'; G189E) by *GMR-GAL4* does not impair rhabdomere separation. Note the absence of attachments between rhabdomeres marked by Phalloidin (green) and the continuous expression of Eys (red) in animals overexpressing wild-type and mutant Rumi (A-B'), similar to the control *GMR-GAL4/+* animals (C,C'). Scale bar in A is 5 μm and applies to (A-C'). (D) Western blotting with anti-FLAG antibody shows that wild-type and G189E Rumi are overexpressed at comparable levels in *GMR>rumi*$^{wt\text{-}FLAG}$ and *GMR>rumi*$^{79\text{-}FLAG}$ animals.

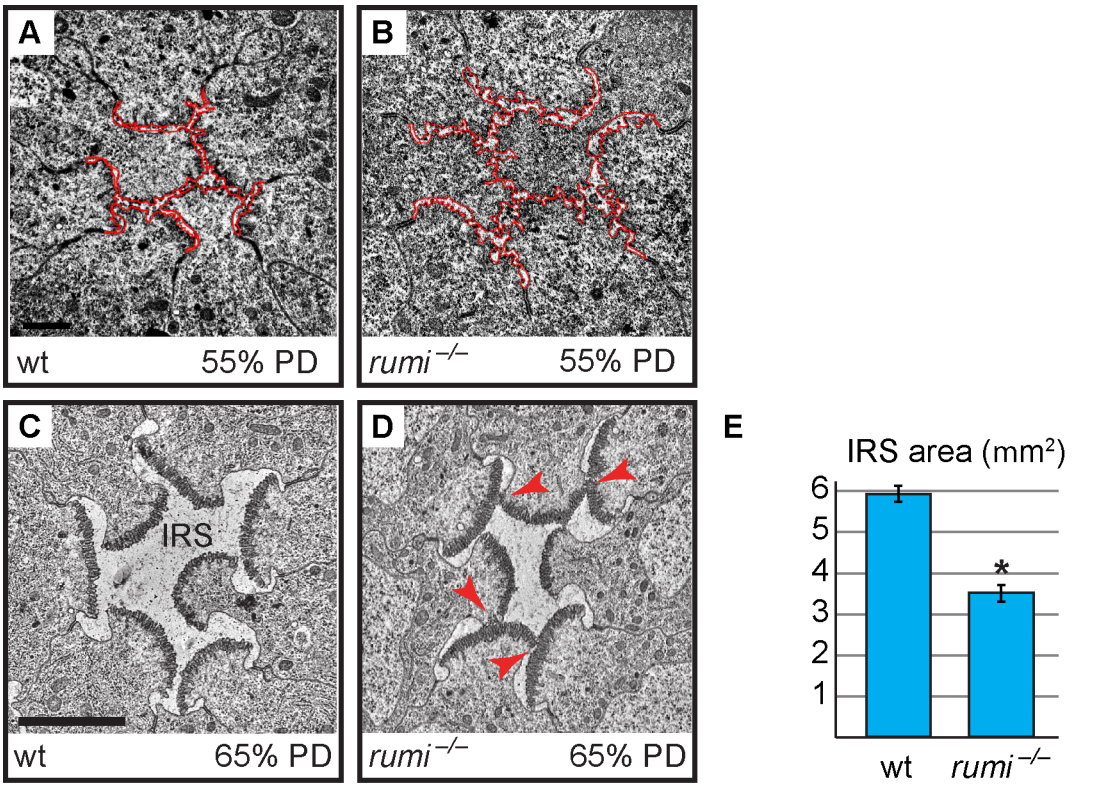

Figure 3-5. The rhabdomere attachment phenotype in *rumi*$^{-/-}$ begins early in pupal development. (A,B) Ommatidia from animals at 55% PD from wild-type (A) and *rumi*$^{-/-}$ (B). Rhabdomere attachments cannot be discerned at this stage although the microvilli of *rumi*$^{-/-}$ rhabdomeres appear more disorganized. (C,D) Images 65% PD from wild-type (C) and *rumi*$^{-/-}$ (D). Arrowheads in (D) indicate points of rhabdomere attachment. (E) Means ± SEM of IRS area in wild-type and *rumi*$^{-/-}$ at 65% PD. IRS areas were measured using ImageJ software. Unpaired *t*-test was used to compare wt (n=14) and *rumi*$^{-/-}$ (n=24) IRS, **P*<0.0001.

wild-type ommatidia (5.95 ± 0.19 μm^2) at a similar stage raised at the same temperature (Figure 3-5E, *P*<0.0001). Although the apical surfaces of photoreceptors adjacent to the IRS appear separated from one another, multiple local adhesions persist between the microvillar membranes of neighboring rhabdomeres (and occasionally opposing rhabdomeres) in each ommatidium (Figure 3-5D, arrowheads). These observations indicate that the *rumi* rhabdomere attachment phenotypes are evident early during rhabdomere morphogenesis and strongly suggest that proper rhabdomere separation never occurs in *rumi*$^{-/-}$ animals.

Loss of *O*-glucose from Notch cannot explain the rhabdomere attachment phenotype of *rumi* animals.

If Rumi regulates rhabdomere spacing via its protein *O*-glycosyltransferase (Poglut) activity, lack of glucose on Rumi target proteins is likely to be responsible for the observed phenotype. To identify all fly proteins with a potential Rumi target site, we used the MOTIF search engine (http://motif.genome.jp/MOTIF2.html) to search the Swiss-Prot and KEGG-GENES databases for *Drosophila* proteins harboring one or more EGF repeats with the $C^1XSX(P/A)C^2$ consensus sequence (Rana et al. 2011). Based on this search, 14 *Drosophila* proteins have at least one EGF repeat with a predicted Rumi target site (Table 1), with Notch harboring the largest number of *O*-glucosylation sites, most of which have been confirmed to be efficiently *O*-glucosylated by Rumi (Acar et al. 2008; Lee et al. 2013; Rana et al. 2011). *rumi* null animals raised at 18°C do not show photoreceptor specification defects characteristic of loss of Notch signaling (Figure 3-6A-C'), suggesting that Notch signaling is not significantly affected in *rumi*$^{-/-}$ developing photoreceptors at this temperature. Moreover, to our knowledge, Notch signaling has not been implicated in rhabdomere spacing. Nevertheless, given the broad roles that Notch plays in multiple developmental contexts, we sought to examine whether the rhabdomere spacing defects observed in *rumi* mutants can be explained by loss of *O*-glucose from Notch EGF repeats. To this end, we used a *Notch* genomic transgene (*PBac{N*$^{gt\text{-}4\text{-}35}$*}*) in which serine-to-alanine mutations are introduced in all 18 Rumi target sites and therefore expresses a Notch

Potential target	# of sites
Notch	18
Crumbs	7
Eyes shut (Spam)	5
Uninflatable	4
Weary	4
Kugelei (Fat2)	2
Starry night (Fmi)	2
CG32072	1
CG42255	1
Delta	1
Dumpy	1
Fat	1
Neurexin IV	1
Trol	1

Table 3-1. List of proteins in *Drosophila* that harbor the Rumi consensus sequence.

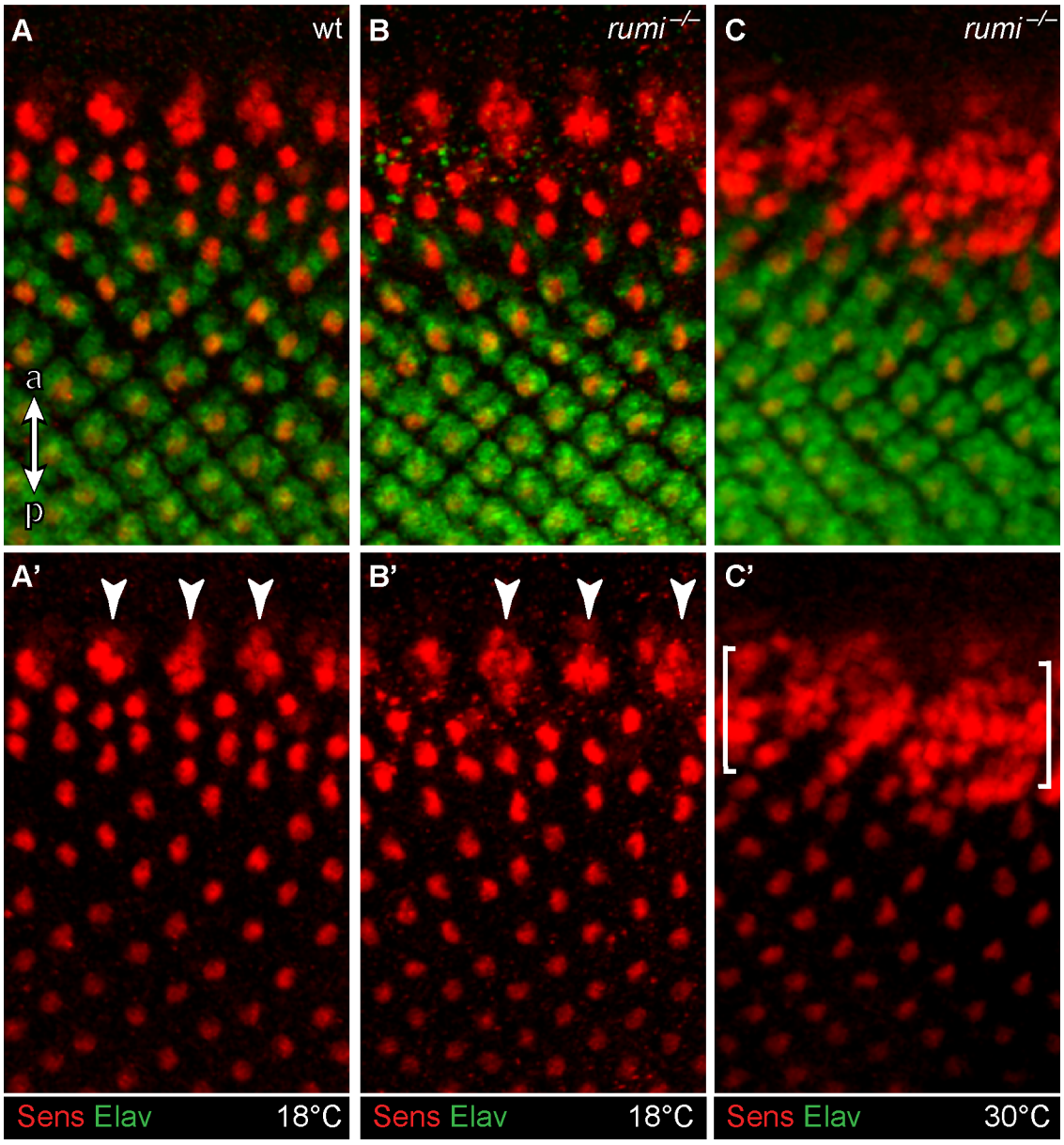

Figure 3-6. Photoreceptor specification is normal in *rumi*$^{-/-}$ animals raised at 18°C. (A-C') Close-ups of the third instar larval eye discs showing the developing photoreceptors in wt (A,A'), *rumi*$^{-/-}$ animals raised at 18°C (B,B') and *rumi*$^{-/-}$ animals raised at 18°C and shifted to 30°C for 4 hours before dissection (C,C'). R8 photoreceptors are marked with Senseless (Sens, red) and all photoreceptors are marked with Elav (green). 'a' and 'p' in panel B show anterior and posterior, respectively, and apply to A-C'. Arrowheads in A' and B' mark the R8 proneural clusters before a single R8 is selected through Notch-mediated lateral inhibition. In *rumi*$^{-/-}$ animals raised at 18°C (B,B'), the R8 proneural clusters are refined into single Sens^{+} R8 cells, which themselves recruit other photoreceptors, similar to the wild-type animal (A,A'). In contrast, raising the *rumi* larvae at 30°C results in the specification of multiple R8 photoreceptor

cells (the area between the brackets), indicating an impairment of the Notch-mediated lateral inhibition at this temperature (C,C'). Note that R8 selection and photoreceptor recruitment is not impaired in the area posterior to the brackets because the animal was raised at 30°C only for four hours.

protein which cannot be *O*-glucosylated by Rumi (Leonardi et al. 2011) (Figure 3-7A). When reared at 18°C, the *PBac{N$^{gt-4-35}$}* transgene rescues the lethality of *Notch* null mutations, and the *N^{-}; PBac{N$^{gt-4-35}$}/+* animals only show a mild loss of Notch signaling similar to *rumi* mutants (Leonardi et al. 2011). TEM revealed that adult *N^{-}; PBac{N$^{gt-4-35}$}/+* eyes raised at 18°C do not show any rhabdomere attachment phenotypes (Figure 3-7B), strongly supporting the notion that addition of *O*-glucose to Notch is not essential for proper rhabdomere spacing.

Crb is *O*-glucosylated but loss of *O*-glucose from Crb does not result in rhabdomere attachment

The fly protein with the second largest number of Rumi target sites is Crb (Table 1), an evolutionarily conserved transmembrane protein involved in the regulation of epithelial polarity, organ size, and photoreceptor development and maintenance (Chen et al. 2010; Izaddoost et al. 2002; Johnson et al. 2002; Ling et al. 2010; Pellikka et al. 2002; Richardson and Pichaud 2010; Tepass et al. 1990). Of note, *crb* mutant retinas exhibit attachment of neighboring rhabdomeres despite the presence of IRS (Izaddoost et al. 2002; Johnson et al. 2002). Seven of the *Drosophila* Crb EGF repeats, 13 of the human CRB1 EGF repeats and eight of the human CRB2 EGF repeats harbor Rumi target sites, suggesting that *O*-glucosylation might play an important role in the function of Crb (Figure 3-8A). We performed mass spectral analysis on peptides derived from a fragment of the Crb extracellular domain expressed in *Drosophila* S2 cells (Figure 3-8A, the red line) to examine whether Crb can be *O*-glucosylated in *Drosophila*. Indeed, peptides containing the predicted sites in this region are *O*-glucosylated (Figure 3-8B-F, Figure 3-9 and Figure 3-10). We next asked whether loss of *O*-glucose from Rumi target sites in Crb recapitulates the rhabdomere attachment phenotype observed in *rumi* mutants. Using a previously established platform (Huang et al. 2009; Ling et al. 2010; Robinson et al. 2010), we generated a knock-in allele of *crb* (*crb^{1-7-HA}*) with serine-to-alanine mutations in all seven Rumi target sites (Figure 3-8A). Animals homozygous for this allele or trans-heterozygous for this allele and the null allele *crb^{11A22}* are viable and do not exhibit any gross

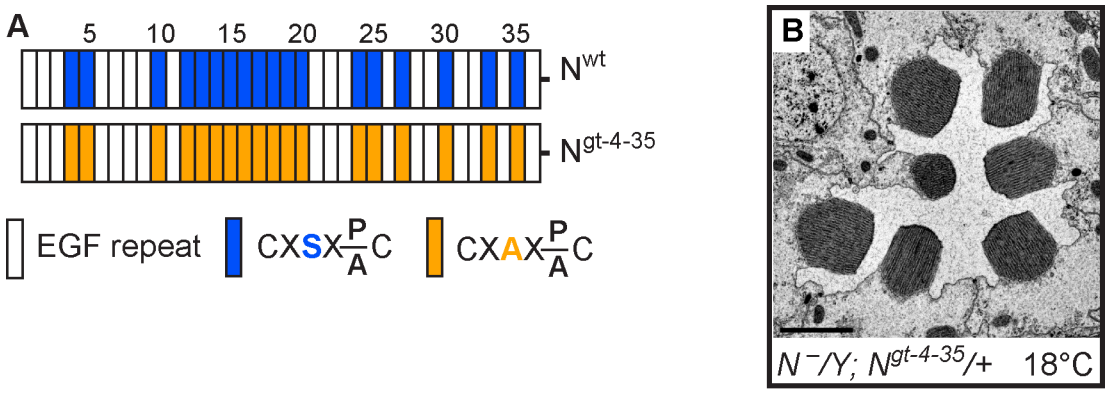

Figure 3-7. Loss of *O*-glucose on Notch does not cause rhabdomere attachment and cannot explain the *rumi*$^{-/-}$ phenotype. (A) Schematic of the EGF repeats of the Notch genomic transgene used in the study. Blue and orange boxes indicate EGF repeats harboring wt and mutant Rumi consensus sequences, respectively. (B) Electron micrograph of an ommatidium of an animal expressing the mutated *PBac{Notch*$^{gt\text{-}4\text{-}35}$*}* transgene in a *Notch* null background raised at 18°C. Scale bar: 2 μm.

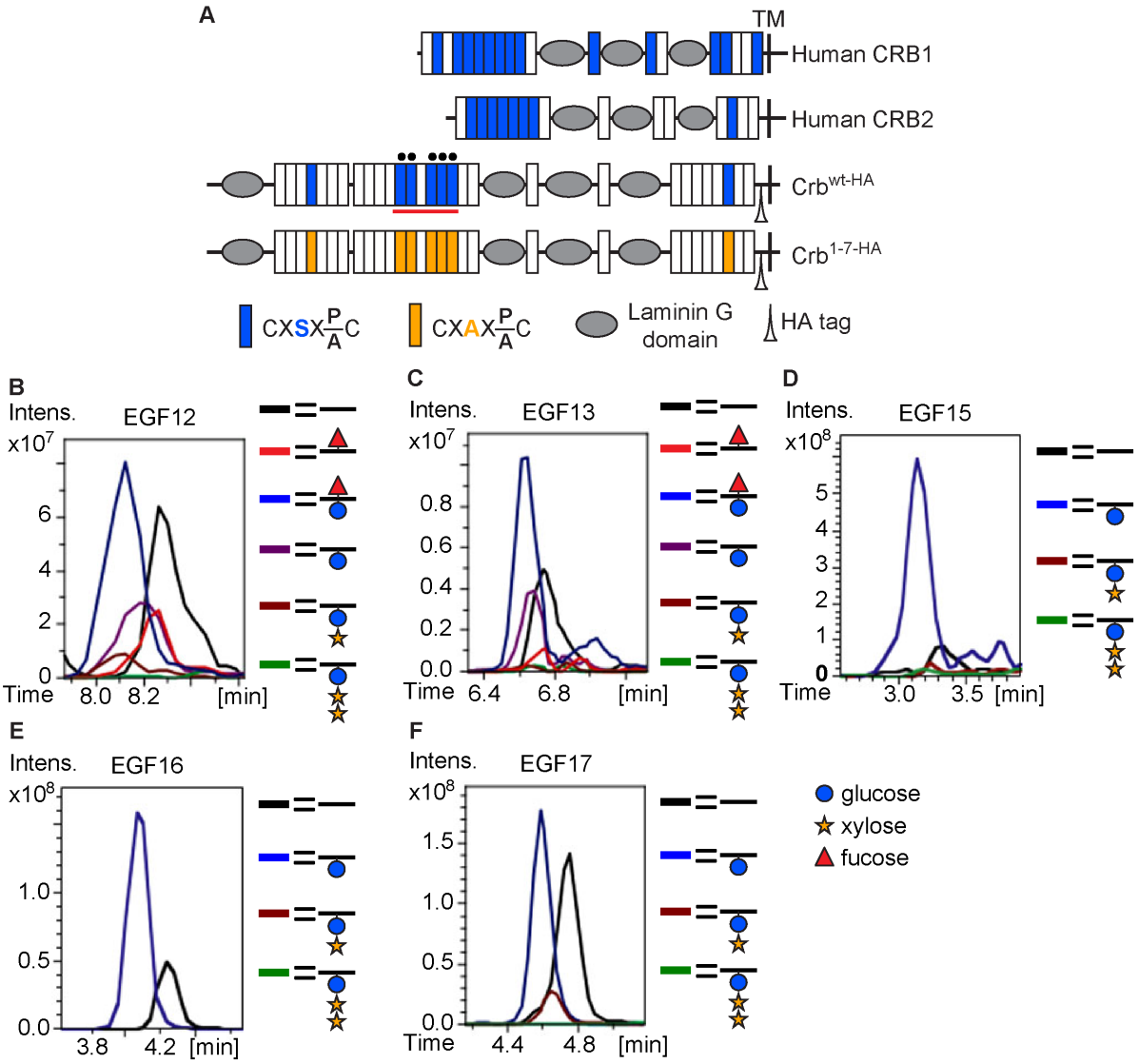

Figure 3-8. Crb contains *O*-glucose modifications. (A) Schematic of the human CRB1, human CRB2, and wt and mutant, HA-tagged *Drosophila* Crb based on the Crb-PA polypeptide (FlyBase ID: FBpp0083987). Blue and orange boxes indicate EGF repeats harboring wt and mutant Rumi consensus sequences, respectively. TM, transmembrane domain. . (B-F) Extracted Ion Chromatogram (EIC) data for peptides containing the *O*-glucose consensus site from Crb EGF12 (B), EGF13 (C), EGF15 (D), EGF16 (E) and EGF17 (F) obtained from mass spectrometry on a Crb fragment indicated by the red line in (A). Note the presence of *O*-glucose (blue circle) on all five EGF repeats, some of which are elongated by xylose (yellow star). Peptides from EGF12 and EGF13 also harbor *O*-fucose (red triangle) added to the consensus *O*-fucosylation sites present in these two EGF repeats. Mass spectrometry data was collected by collaborators Robert Haltiwanger and Beth Harvey.

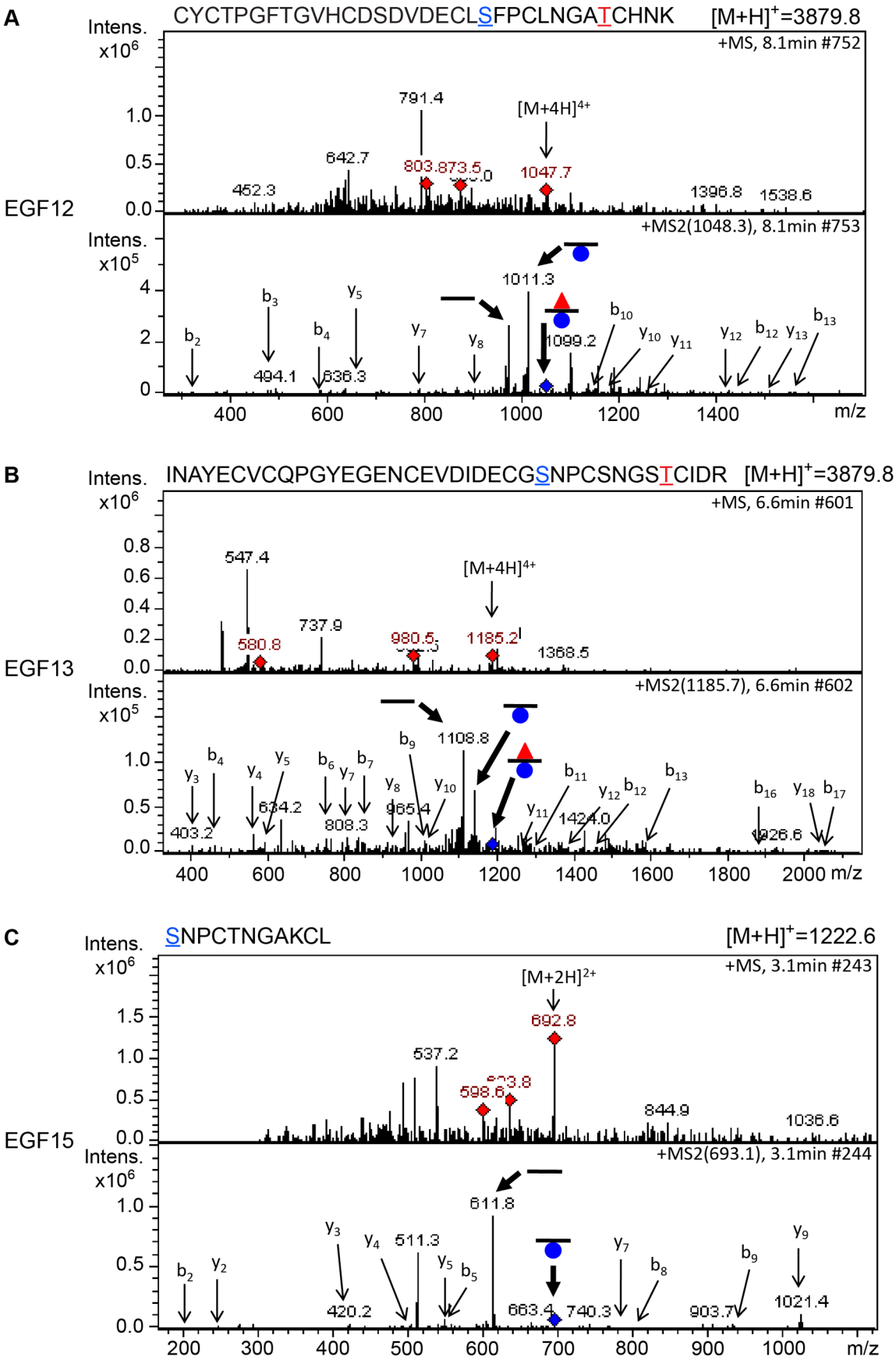
A
CYCTPGFTGVHCDSDVDECLSFPCLNGATCHNK [M+H]+=3879.8
EGF12
Intens. x10^6
+MS, 8.1min #752
[M+4H]4+
791.4
642.7
803.873.5
1047.7
452.3
1396.8
1538.6
Intens. x10^5
+MS2(1048.3), 8.1min #753
1011.3
1099.2
494.1
636.3
m/z
B
INAYECVCQPGYEGENCEVDIDECGSNPCSNGSTCIDR [M+H]+=3879.8
EGF13
Intens. x10^6
+MS, 6.6min #601
[M+4H]4+
547.4
737.9
580.8
980.5
1185.2
1368.5
Intens. x10^5
+MS2(1185.7), 6.6min #602
1108.8
403.2
624.2
808.3
965.4
1424.0
1926.6
m/z
C
SNPCTNGAKCL [M+H]+=1222.6
EGF15
Intens. x10^6
+MS, 3.1min #243
[M+2H]2+
692.8
537.2
598.6
844.9
1036.6
Intens. x10^6
+MS2(693.1), 3.1min #244
611.8
511.3
420.2
663.4
740.3
903.7
1021.4
m/z

Figure 3-9. Rumi target sites in Crb EGF12, EGF13 and EGF15 are *O*-glucosylated. (A) Identification of the peptide ^{671}CYCTPGFTGVHCDSDVDECLSFPCLNGATCHNK^{703} from Crb EGF12. Amino acid numbering for all Crb peptides is based on the Crb-PA polypeptide (FlyBase ID: FBpp0083987). The top panel shows a full MS spectrum of material eluting at 8.1 min. The ion labeled $[M+4H]^{4+}$ matches the predicted mass for quadruply charged form of the peptide modified with *O*-fucose monosaccharide and *O*-glucose monosaccharide. Other ions are from co-eluting material. CID fragmentation of the quadruply charged form of this peptide, m/z 1048.3 (top panel, $[M+4H]^{4+}$), resulted in the MS/MS spectrum shown in the bottom panel. Numerous sequence fragment ions (arrows) are observed that confirm the identity of the peptide. The position of the parent ion fragmented in the MS/MS spectrum is identified with a blue diamond. The blue underlined S is the glucosylated serine, and the red underlined T is the fucosylated threonine. (B) Identification of the peptide ^{704}INAYECVCQPGYEGENCEVDIDECGSNPCSNGSTCIDR^{741} from Crb EGF13. The top panel shows a full MS spectrum of material eluting at 6.6 min. The ion labeled $[M+4H]^{4+}$ matches the predicted mass for quadruply charged form of the peptide modified with *O*-fucose monosaccharide and *O*-glucose monosaccharide. Other ions are from co-eluting material. CID fragmentation of the quadruply charged form of this peptide, m/z 1185.7 (top panel, $[M+4H]^{4+}$), resulted in the MS/MS spectrum shown in the bottom panel. Numerous sequence fragment ions (arrows) are observed that confirm the identity of the peptide. The position of the parent ion fragmented in the MS/MS spectrum is identified with a blue diamond. (C) Identification of the peptide ^{806}SNPCTNGAKCL^{816} from Crb EGF15. The top panel shows a full MS spectrum of material eluting at 3.1 min. The ion labeled $[M+2H]^{2+}$ matches the predicted mass for doubly charged form of the peptide modified with *O*-glucose monosaccharide. Other ions are from co-eluting material. CID fragmentation of the doubly charged form of this peptide, m/z 693.1 (top panel, $[M+2H]^{2+}$), resulted in the MS/MS spectrum shown in the bottom panel. Numerous sequence fragment ions (arrows) are observed that confirm the identity of the peptide. The position of the parent ion fragmented in the MS/MS spectrum is identified with a blue diamond.

In all MS/MS spectra, ions representing glycopeptides are indicated by black lines modified with *O*-glucose (blue circle) and *O*-fucose (red triangle). Ions representing the glycopeptides in the MS spectra were used to generate EIC in Figure 3-8B-D. Data was collected by collaborators Robert Haltiwanger and Beth Harvey.

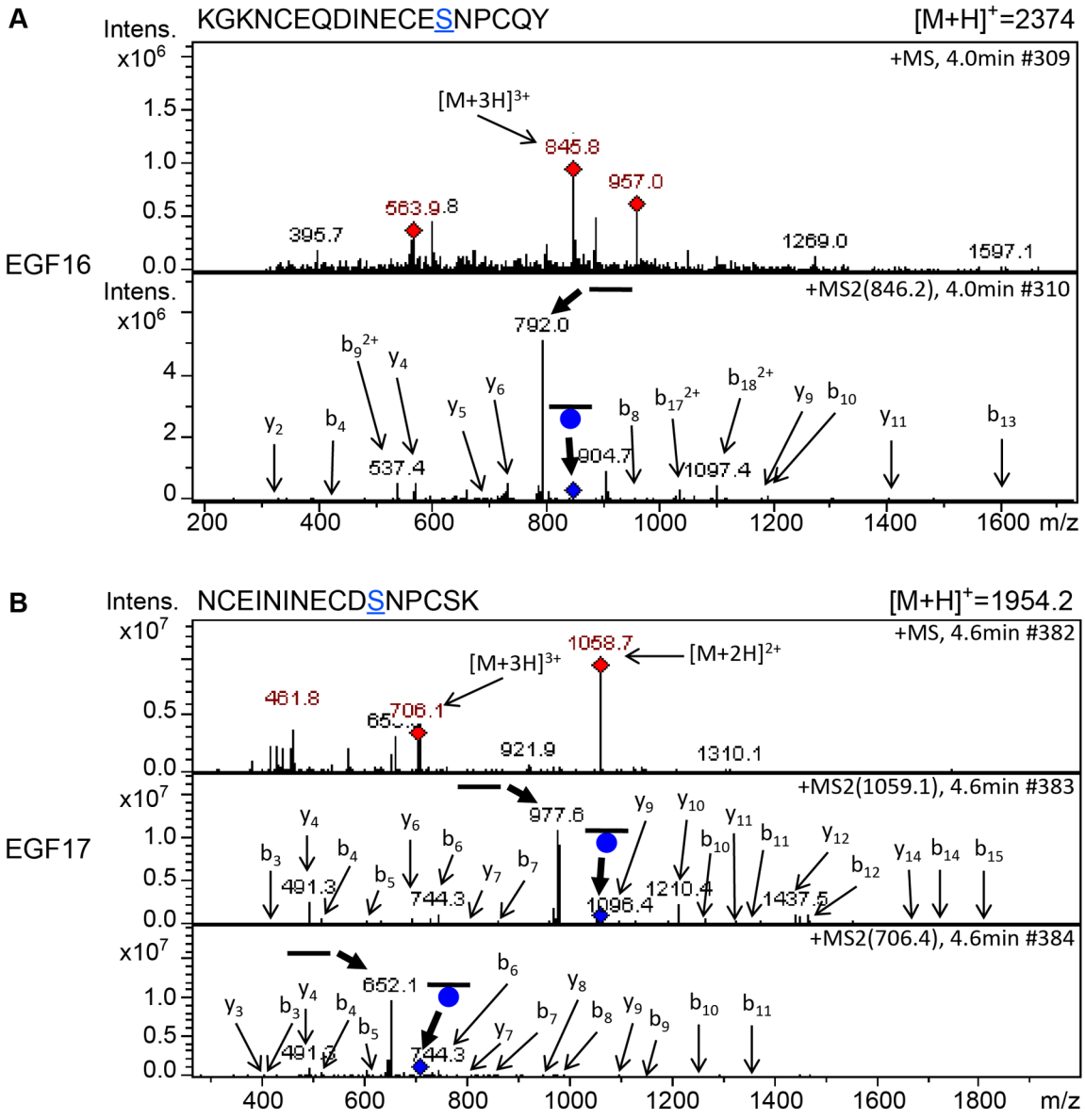

Figure 3-10. Rumi target sites in Crb EGF16 and EGF17 are *O*-glucosylated. (A) Identification of the peptide ^{831}KGKNCEQDINECESNPCQY^{849} from Crb EGF16. The top panel shows a full MS spectrum of material eluting at 4 min. The ion labeled $[M+3H]^{3+}$ matches the predicted mass for triply charged form of the peptide modified with *O*-glucose monosaccharide. Other ions are from co-eluting material. CID fragmentation of the triply charged form of this peptide, m/z 846.2 (top panel, $[M+3H]^{3+}$), resulted in the MS/MS spectrum shown in the bottom panel. Numerous sequence fragment ions (arrows) are observed that confirm the identity of the peptide. Ions selected for fragmentation in the MS spectrum are identified by red diamonds. The position of the parent ion fragmented in the MS/MS spectrum is identified with a blue diamond. The blue underlined S is the glucosylated serine. (B) Identification of the

peptide ^{898}NCEININECDSNPCSK^{913} from Crb EGF17. The top panel shows a full MS spectrum of material eluting at 4.6 min. The ion labeled $[M+3H]^{3+}$ matches the predicted mass for triply charged form of the peptide modified with *O*-glucose monosaccharide, and the ion labeled $[M+2H]2^{+}$ matches the predicted mass for doubly charged form of the same peptide. Other ions are from co-eluting material. CID fragmentation of the doubly charged form of this peptide, m/z 1059.1 (top panel, $[M+2H]^{2+}$), resulted in the MS/MS spectrum shown in the middle panel. CID fragmentation of the triply charged form of this peptide, m/z 706.4 (top panel, $[M+3H]^{3+}$), resulted in the MS/MS spectrum shown in the bottom panel. Numerous sequence fragment ions (arrows) are observed that confirm the identity of the peptide. Ions selected for fragmentation in the MS spectrum are identified by red diamonds. The positions of the parent ions fragmented in the MS/MS spectrum are identified with blue diamonds. In all MS/MS spectra, ions representing glycopeptides are indicated by black lines modified with *O*-glucose (blue circle). Ions representing the glycopeptides in the MS spectra were used to generate EIC in Figure 3-8E and F. Data was collected by collaborators Robert Haltiwanger and Beth Harvey.

abnormalities when raised between 18°C and 25°C. Moreover, TEM indicates normal rhabdomere morphology and IRS formation with no defects in rhabdomere spacing in *crb*$^{1\text{-}7\text{-}HA/1\text{-}7\text{-}HA}$ animals raised at either 18°C or 25°C (Figure 3-11G and H). These observations indicate that absence of Crb *O*-glucosylation does not explain the rhabdomere spacing defects of *rumi* mutants. In agreement with these data, Crb appears to be properly localized to the stalk membrane in 65% PD *rumi*$^{-/-}$ retinas, although an increase in the number of Crb^{+} puncta is seen in *rumi* mutants raised at 25°C compared to control animals (Figure 3-11C-D', arrowheads). Together, these data indicate that although *O*-glucose modifications might affect the trafficking of Crb, they are not essential for the function of Crb during fly embryonic development and photoreceptor morphogenesis.

Eys is a biologically-relevant target of Rumi during rhabdomere morphogenesis

As mentioned above, another *Drosophila* protein with multiple predicted Rumi target sites and an IRS phenotype is Eys (Table 1 and Figure 3-12A) (Husain et al. 2006; Zelhof et al. 2006). To examine whether Eys is the biologically-relevant target of Rumi in the context of rhabdomere spacing, we first performed mass spectral analysis on peptides derived from an Eys fragment harboring four Rumi target sites expressed in S2 cells (Figure 3-12A, the red line). So far we have been able to identify peptides corresponding to three of these sites by mass spectrometric analysis and have identified *O*-glucose on all three sites (Figure 3-12B-D and Figure 3-13). The Rumi target site in EGF1 appears to be less efficiently *O*-glucosylated compared to those in other Eys EGF repeats. Nevertheless, these data indicate that *Drosophila* Eys contains several bona fide Rumi targets. We next performed genetic interaction studies between *rumi* and *eys* by using the protein-null allele *eys*^{734} (Husain et al. 2006). As reported previously, loss of one copy of *eys* does not cause any rhabdomere defects (Figure 3-14A) (Husain et al. 2006; Zelhof et al. 2006). However, removing one copy of *eys* in a *rumi*$^{-/-}$ background results in a strong enhancement of the *rumi*$^{-/-}$ rhabdomere attachment phenotype at 18°C (Compare Figure 3-14B and C to Figure 3-1B, D and E). In *eys*$^{+/-}$*; rumi*$^{-/-}$ animals,

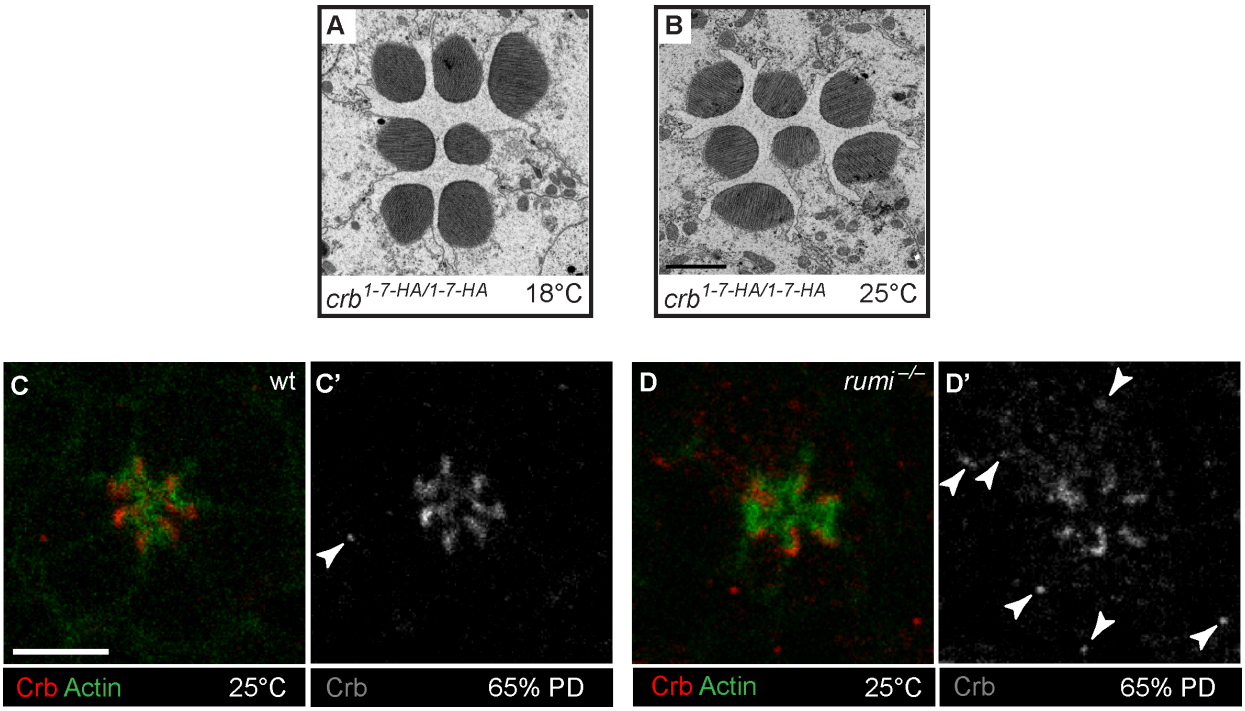

Figure 3-11. Loss of *O*-glucose on Crb cannot explain the *rumi*$^{-/-}$ rhabdomere attachment phenotype. (A,B) *crb* knock-in mutants lacking all Rumi target sites and raised at 18°C (A) or 25°C (B) do not show rhabdomere attachment. Scale bar in B applies to A and B and is 2 µm. (C-D') Loss of Rumi does not impair Crb localization to the stalk membrane. Increased Crb puncta, some of which are marked with arrowheads in D', are seen in the photoreceptor cell body of *rumi*$^{-/-}$ ommatidia raised at 25°C (D,D') compared to wild-type (C,C'). Actin (green) is used to mark the rhabdomeres. Crb is shown in red. Scale bar: 5 µm.

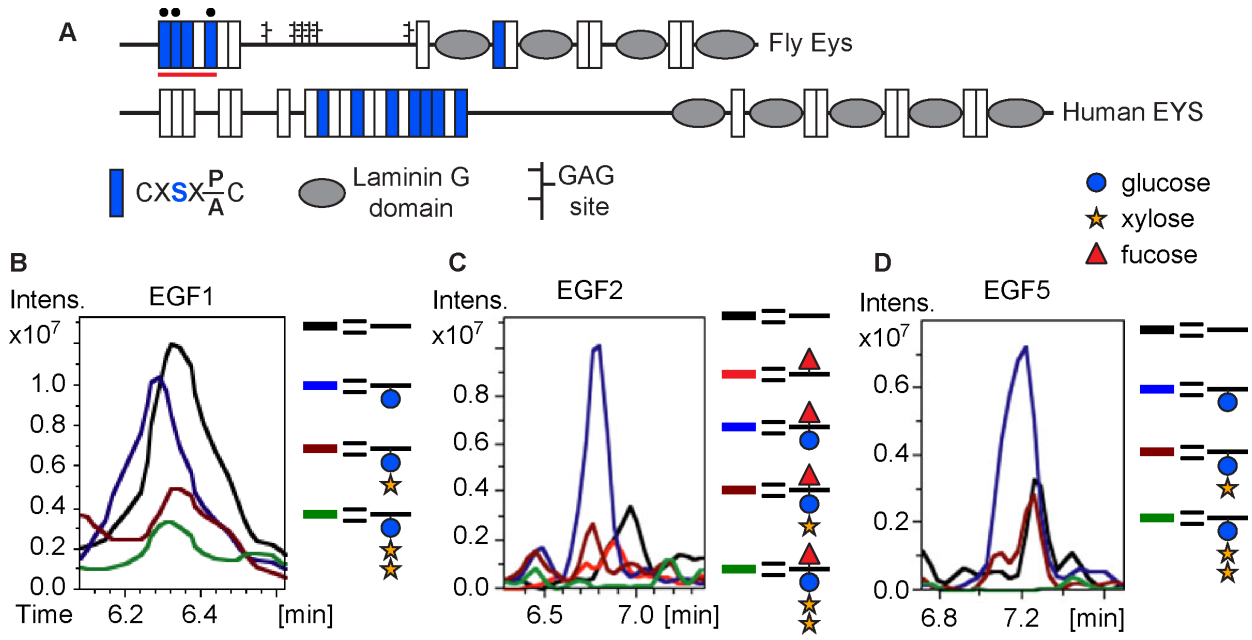

Figure 3-12. Eys contains *O*-glucose modifications. (A) Schematic of the fly and human Eys proteins. Red line indicates the EGF repeats used for mass spectrometry analysis. Black circles mark EGF repeats shown in B-D. (B-D) EIC data from mass spectral analysis of EGF1 (B), EGF2 (C), and EGF5 (D). Blue peak indicates the addition of *O*-glucose (blue circle) onto the EGF repeat. EGF2 is also modified by *O*-fucose (red triangle). Rumi appears to be less efficient in *O*-glucosylating EGF1 of Eys compared to the other EGF repeats when expressed in S2 cells. Mass spectrometry data was collected by collaborators Robert Haltiwanger and Beth Harvey.

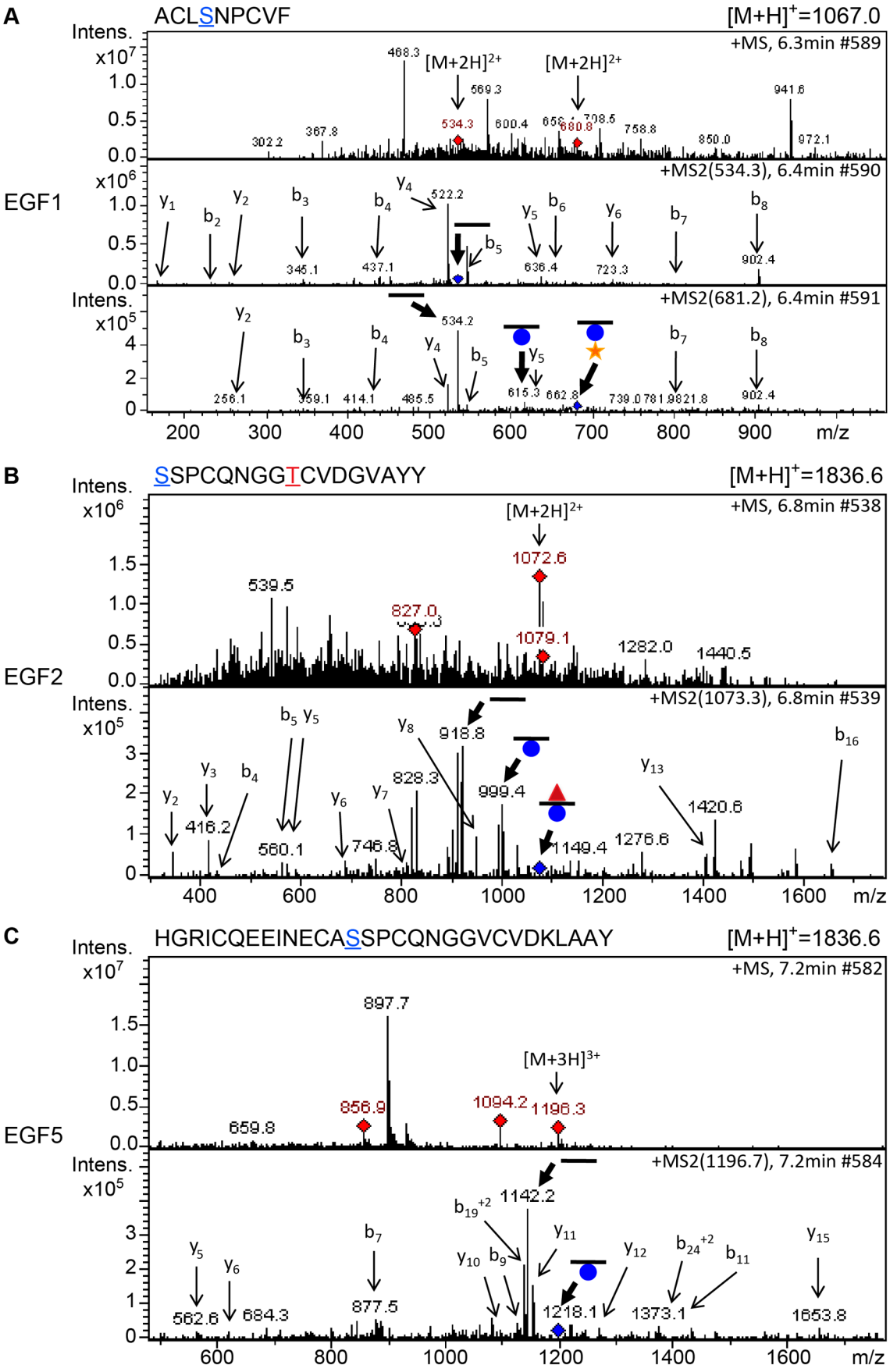
A
ACLSNPCVF
[M+H]+=1067.0
EGF1
+MS, 6.3min #589
+MS2(534.3), 6.4min #590
+MS2(681.2), 6.4min #591
B
SSPCQNGGTCVDGVAYY
[M+H]+=1836.6
EGF2
+MS, 6.8min #538
+MS2(1073.3), 6.8min #539
C
HGRICQEEINECASSPCQNGGVCVDKLAAY
[M+H]+=1836.6
EGF5
+MS, 7.2min #582
+MS2(1196.7), 7.2min #584
Intens.
m/z

Figure 3-13. Rumi target sites in Eys EGF1, EGF2 and EGF5 are *O*-glucosylated. (A-C) Top: full MS spectra of Eys EGF1 (A), EGF2 (B) and EGF5 (C) peptides. Bottom: CID fragmentation of the doubly charged (A and B) or triply charged (C) forms of the identified peptide. The blue underlined S is the glucosylated serine, and the red underlined T is the fucosylated threonine. (A) Identification of the peptide ^{147}ACLSNPCVF^{155} from Eys EGF1. Amino acid numbering for all Eys peptides is based on Eys-PE polypeptide (FlyBase ID: FBpp0311004). The top panel shows a full MS spectrum of material eluting at 6.3 min. The ions labeled $[M+2H]^{2+}$ match the predicted mass for doubly charged forms of the unmodified peptide (m/z 534.3) and the peptide modified with an *O*-glucose and a xylose (m/z 680.8). Other ions are from co-eluting material. CID fragmentation of the doubly charged form of the unmodified peptide, m/z 534.3 (top panel, $[M+2H]^{2+}$ to the left), resulted in the MS/MS spectrum shown in the middle panel. CID fragmentation of the doubly charged form of the glycosylated peptide, m/z 680.8 (top panel, $[M+2H]^{2+}$ to the right), resulted in the MS/MS spectrum shown in the bottom panel. Numerous sequence fragment ions (arrows) are observed that confirm the identity of the peptides. (B) Identification of the peptide ^{188}SSPCQNGGTCVDGVAYY^{204} from Eys EGF2. The top panel shows a full MS spectrum of material eluting at 6.8 min. The ion labeled $[M+2H]^{2+}$ matches the predicted mass for doubly charged form of the peptide modified with *O*-glucose monosaccharide and *O*-fucose monosaccharide. Other ions are from co-eluting material. CID fragmentation of the doubly charged form of this peptide, m/z 1073.3 (top panel, $[M+2H]^{2+}$), resulted in the MS/MS spectrum shown in the bottom panel. Numerous sequence fragment ions (arrows) are observed that confirm the identity of the peptide. (C) Identification of the peptide ^{282}HGRICQEEINECASSPCQNGGVCVDKLAAY^{322} from Eys EGF5. The top panel shows a full MS spectrum of material eluting at 7.2 min. The ion labeled $[M+3H]^{3+}$ matches the predicted mass for triply charged form of the peptide modified with *O*-glucose monosaccharide. Other ions are from co-eluting material. CID fragmentation of the triply charged form of this peptide, m/z 1196.7 (top panel, $[M+3H]^{3+}$), resulted in the MS/MS spectrum shown in the bottom panel. Numerous sequence fragment ions (arrows) are observed that confirm the

identity of the peptide. Ions selected for fragmentation in the MS spectrum are identified by red diamonds. The position of the parent ion fragmented in the MS/MS spectrum is identified with a blue diamond. In all MS/MS spectra, ions representing glycopeptides are indicated by black lines modified with *O*-glucose (blue circle) and *O*-fucose (red triangle). Ions representing the glycopeptides in the MS spectra shown here were used to generate the EICs in Figure 3-12B-C. Data was collected by collaborators Robert Haltiwanger and Beth Harvey.

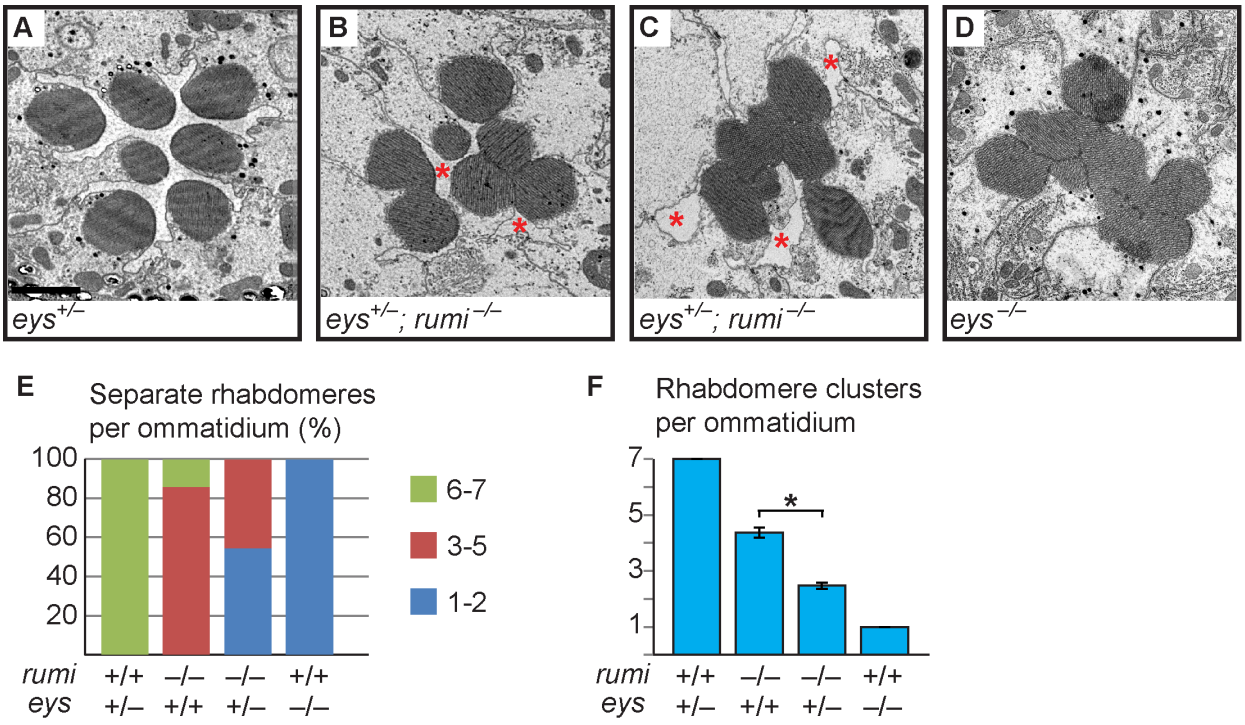

Figure 3-14. *eys* genetically interacts with *rumi*. (A) An *eys* heterozygous ommatidium with normal rhabdomere separation. Scale bar: 2 μm. (B,C) $eys^{+/-}$ $rumi^{-/-}$ ommatidia show a dramatic enhancement of the $rumi^{-/-}$ phenotype. In severe cases, all the rhabdomeres are attached (C). Pockets of IRS are marked by asterisks. (D) *eys* null ommatidia completely lack IRS. (E) Percentage of number of individual rhabdomeres per ommatidium for various genotypes. At least three animals were used for each genotype. (F) Quantification of average individual rhabdomere number per ommatidium for the data shown in E. All pairs are significantly different from each other (*P<0.0001).

multiple rhabdomeres collapse into one another in each ommatidium, and there is a dramatic decrease in the IRS size (Figure 3-14B, C, E and F). Of note, pockets of IRS can still be recognized in all *eys*$^{+/-}$*; rumi*$^{-/-}$ ommatidia (Figure 3-14B and C, asterisks), in contrast to *eys*$^{-/-}$ ommatidia, which completely lack IRS (Figure 3-14D and F) (Husain et al. 2006). This dosage-sensitive genetic interaction strongly suggests that Rumi is critical for the function of Eys, especially when Eys levels are limiting.

Loss of Rumi results in a decrease in the extracellular level of Eys in a temperature-dependent manner

Secretion of Eys from the apical surface of the photoreceptor cells at the mid-pupal stage separates the rhabdomeres from one another and generates the IRS (Husain et al. 2006; Zelhof et al. 2006). Based on the modENCODE Temporal Expression Data accessed on FlyBase (http://flybase.org/reports/FBgn0031414.html), expression of *eys* sharply increases at mid-pupal stage and gradually decreases in later pupal stages. Following the initial burst of Eys expression between 50-70% PD (Husain et al. 2006) and rhabdomere separation, Eys continues to be secreted into the IRS, which gradually enlarges and assumes its adult size late in the pupal stage (Husain et al. 2006; Longley and Ready 1995). Given the increased degree of rhabdomere attachment and the severe decrease in the IRS size in adult animals simultaneously lacking *rumi* and one copy of *eys*, we examined whether loss of Rumi affects Eys levels in the IRS. We first compared Eys expression in the early stages of IRS development between *rumi*$^{-/-}$ and control pupae raised at 18°C. At 55% PD, the rhabdomeres of control animals are separated from one another by a thin but continuous IRS filled with Eys, and only low levels of Eys can be detected in photoreceptor cell bodies (Figure 15A and 15A', Figure 16A and A') (Husain et al. 2006). In contrast, *rumi*$^{-/-}$ ommatidia almost invariably show some degree of rhabdomere attachment and a decreased and interrupted pattern of Eys expression in the IRS (Figure 3-15B and B', Figure 3-16B-C'). In the majority of *rumi*$^{-/-}$

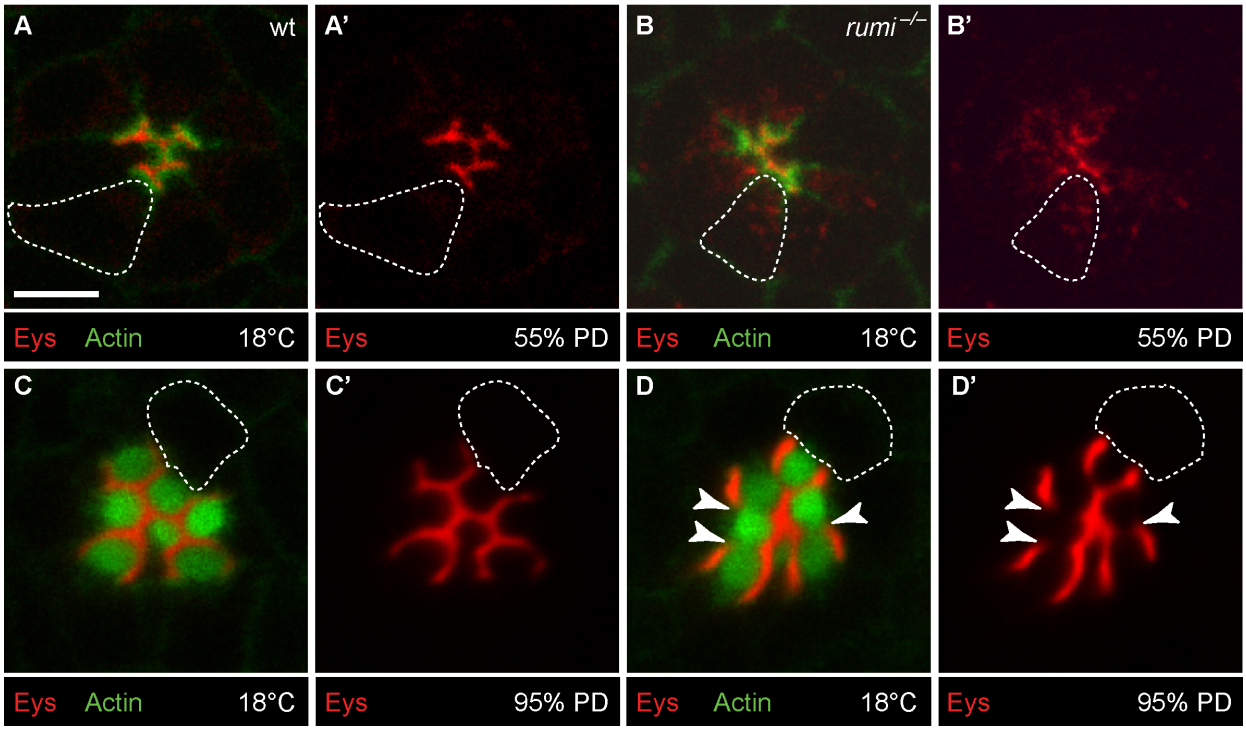

Figure 3-15. Loss of Rumi leads to intracellular accumulation and decreased IRS levels of Eys at the mid-pupal stage. (A-D') Confocal micrographs each showing a single ommatidium from the indicated genotypes. Phalloidin (green) marks Actin and is concentrated in rhabdomeres; Eys is shown in red. The dotted shapes mark the outline of a single photoreceptor cell body in each micrograph. The scale bar in A applies to A-G' and is 5 μm. (A,A') A wild-type ommatidium at 55% PD raised at 18°C. Note that Eys is primarily localized to the IRS. (B,B') A *rumi*$^{-/-}$ ommatidium at 55% PD raised at 18°C. Note the decreased level of Eys in the IRS and its accumulation in the cell body. (C,C') A wild-type ommatidium at 95% PD raised at 18°C. (D,D') A *rumi*$^{-/-}$ ommatidium at 95% PD raised at 18°C. Note the increased amount of Eys in the IRS at this stage and disappearance of Eys from the photoreceptor cell bodies compared to B. White arrowheads mark points of rhabdomere attachment and gaps in Eys.

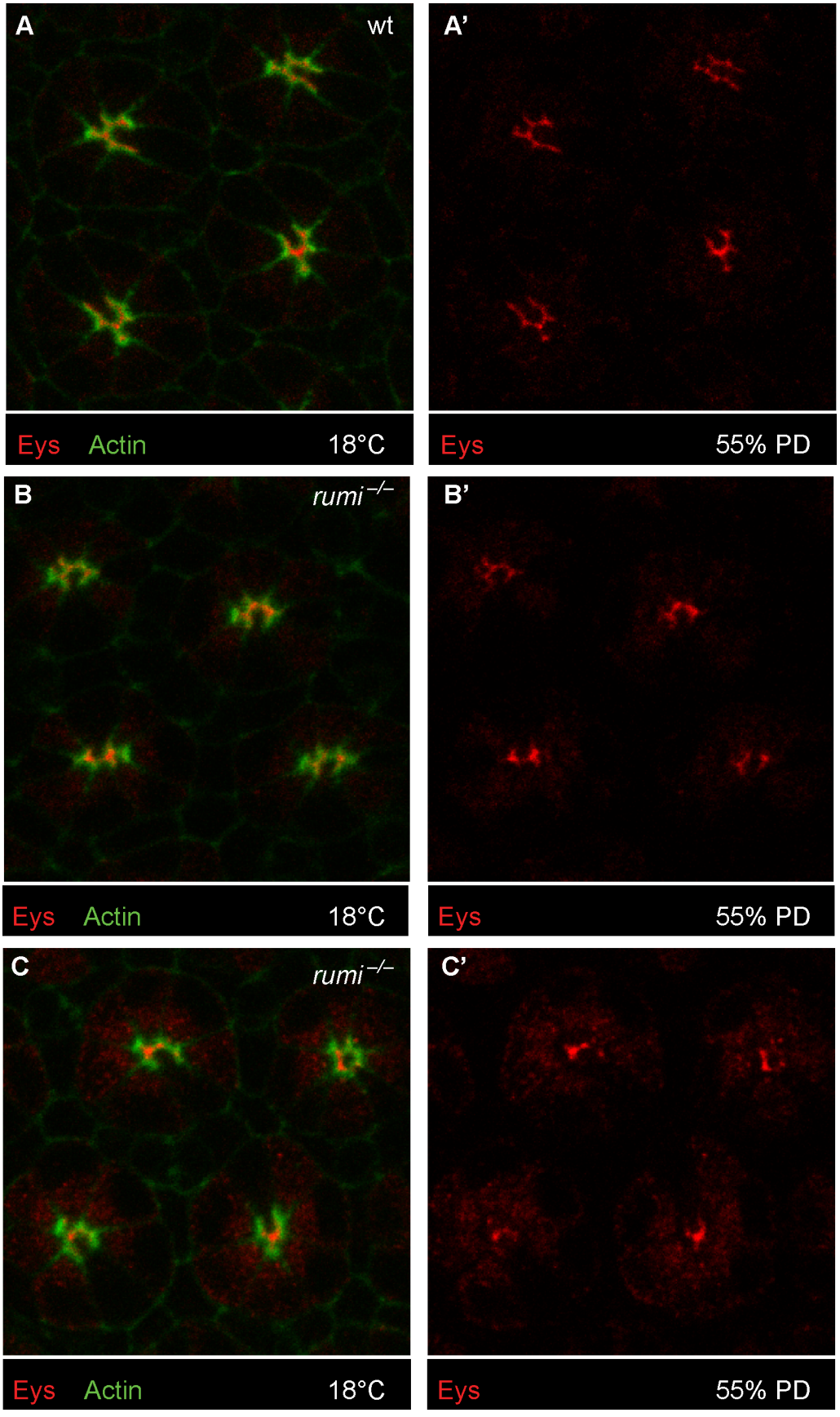
A
wt
A'
Eys Actin 18°C
Eys 55% PD
B
rumi−/−
B'
Eys Actin 18°C
Eys 55% PD
C
rumi−/−
C'
Eys Actin 18°C
Eys 55% PD

Figure 3-16. Loss of *rumi* results in intracellular accumulation of Eys. Images showing 4 ommatidia of (A,A') wild type and (B-C') *rumi*$^{-/-}$ animals. Note that the intracellular accumulation of Eys in *rumi*$^{-/-}$ can vary between animals, as (B,B') shows less accumulation than (C,C'). ommatidia examined, decreased levels of Eys in the IRS are accompanied by increased Eys levels in the photoreceptor cell bodies (Figure 3-15B and B', Figure 3-16C and C'), although the intracellular accumulation varies between animals (Figure 3-16B and B').

Quantification of the total pixel intensity of Eys at 55% PD in animals raised at 18°C shows that in wild-type ommatidia, 87.1±2.0% of total Eys is found in the IRS and the rest is in photoreceptor cell bodies. However, there is a statistically significant decrease in the percentage of Eys found in the IRS in *rumi*$^{-/-}$ ommatidia (63.6±6.5%, P=0.01). These data indicate that during early stages of IRS formation, a significant amount of Eys remains inside the photoreceptor cells in *rumi* mutants, unlike wild-type animals, in which most of the Eys is efficiently secreted into the IRS.

As shown above, *rumi* mutants raised at 18°C show rhabdomere attachment and a significantly decreased IRS size in the mid-pupal stage (Figure 3-5D). However, in *rumi*$^{-/-}$ adults, even though the rhabdomere attachments persist, the IRS in the center of the ommatidia appears similar to that in control ommatidia (Figure 3-1A-E), suggesting that enough Eys is secreted in later pupal stages to expand the IRS. To test this notion, we examined Eys expression in wild-type and *rumi* null animals at 95% PD. In wild-type animals, Eys fills the IRS in an uninterrupted manner and cannot be seen in the cell body (Figure 3-15C and C'). In *rumi* mutants, Eys is properly localized to the IRS at levels similar to that found in wild-type IRS and is not visible in the cell body (Figure 3-15D and D'). However, multiple gaps in the Eys expression domain are seen in the IRS, coinciding with rhabdomere attachments (Figure 3-15D and D', white arrowheads). These data suggest that the rhabdomere attachments in *rumi* mutants result from decreased levels of Eys in the IRS in a critical period during the mid-pupal stage and that these attachments are not resolved later in pupal development despite continued secretion of Eys.

Since the loss of Notch signaling in *rumi* mutants is temperature-sensitive (Acar et al. 2008; Leonardi et al. 2011; Perdigoto et al. 2011), we next examined whether the IRS defect observed in *rumi* animals becomes worse at higher temperatures. To bypass the larval lethality and photoreceptor specification defects of *rumi* mutants at 30°C, we kept *rumi* mutant and control animals at 18°C until the end of the third instar stage and shifted them to 30°C at zero hours after puparium formation (APF) so that they are kept at high temperature at mid-pupal

stage, when *eys* expression starts (Husain et al. 2006). However, these animals died by mid-pupal stage, precluding the study of Eys secretion and IRS formation. Therefore, we modified our temperature shift regimen by transferring *rumi*$^{-/-}$ and control animals to 25°C at zero h APF, shifted them to 30°C at 24 h APF and kept them at this temperature until 55%-75% pupal development, when we dissected them for staining or TEM. The patterns of Phalloidin and Eys staining in control animals looked similar to those raised at 18°C (Figure 3-17A and A'). In contrast, *rumi* mutants either lacked Eys in the IRS (Figure 3-17B and B') or had small Eys-containing regions (Figure 3-17C and C'). Most *rumi* mutant ommatidia showed high levels of Eys in the photoreceptor cells (Figure 3-17B-C'). Additionally, raising animals homozygous for the enzymatic null *rumi*^{79} allele at 30°C resulted in a severe intracellular accumulation of Eys (Figure 3-18), reinforcing our conclusion that loss of the enzymatic function of Rumi causes the rhabdomere attachment defects. TEM on *rumi*$^{-/-}$ animals reared under the above mentioned conditions showed multiple sites of rhabdomere attachment and a small IRS at 75% PD compared to control animals raised under the same conditions (Figure 3-17D and E). These observations indicate that in *rumi* mutants grown at higher temperatures, a higher fraction of Eys remains inside the cell and the level of Eys in the IRS is further reduced.

To examine whether Eys accumulates in a specific subcellular compartment in *rumi* mutant photoreceptor cells, we performed colocalization studies between Eys and markers of ER (Figure 3-19A-A''), Golgi (Figure 3-19B-B''), recycling endosome (Figure 3-20A-A''), and the late endosome (Figure 3-20B-B'') in *rumi* null animals shifted to 25°C at zero h APF and later to 30°C at 24 h APF as explained above. Eys was transported to all cellular compartments examined, as shown by occasional colocalization with each marker (Figure 3-19A-B''', Figure 3-20A-B'''), white arrowheads), indicating that Eys trafficking is not blocked at a single step in the secretion pathway but is likely slowed down through the secretory pathway, causing it to accumulate in the cell body as it travels to the membrane.

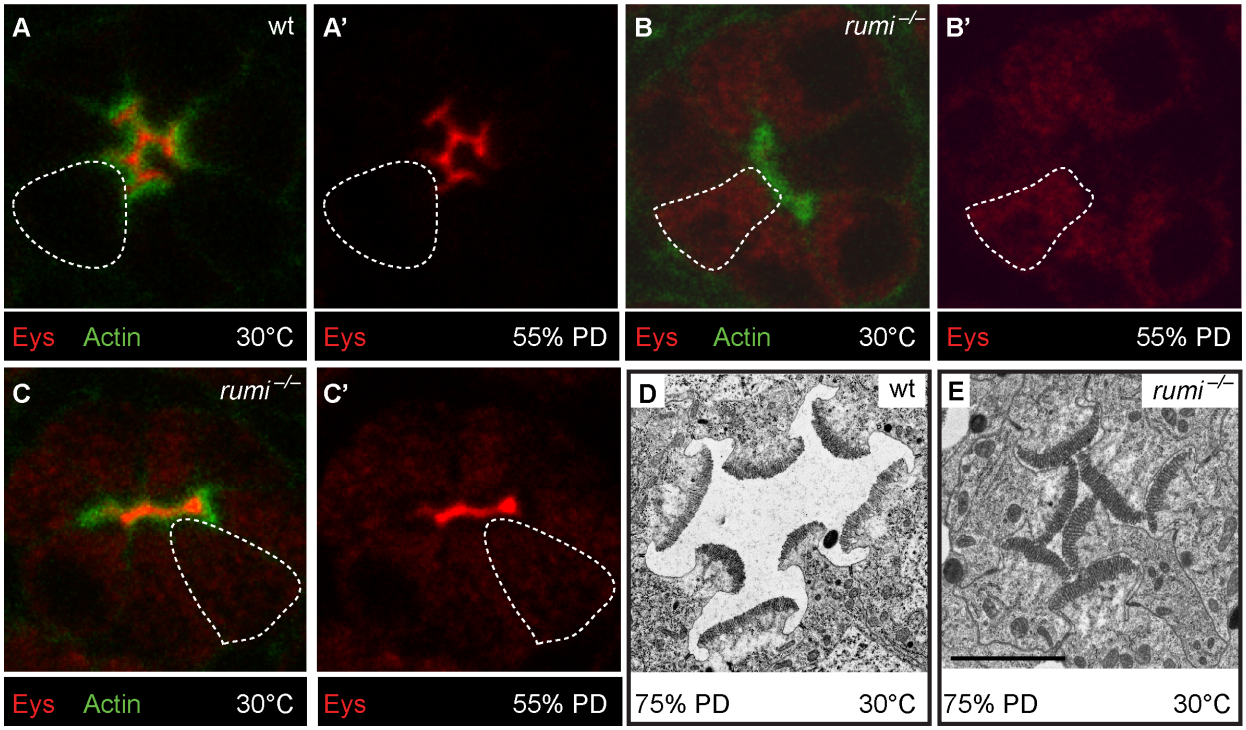

Figure 3-17. The intracellular accumulation of Eys in *rumi*$^{-/-}$ becomes worse with increasing temperature. (A,A') A single ommatidium from a wild-type animal at 55% PD shifted to 30°C during IRS formation. (B-C') Ommatidia from *rumi*$^{-/-}$ animals at 55% PD shifted to 30°C during IRS formation show severe Eys accumulation in the cell body, with either a complete lack of Eys in the IRS (B,B') or a thin line of Eys in the IRS (C,C'). (D,E) Electron micrographs showing wild-type (D) and *rumi*$^{-/-}$ (E) ommatidia from 75% PD animals shifted to 30°C during IRS formation. Red: Eys, Green: Actin which marks the rhabdomeres. The scale bar in E applies to D and E and is 2 μm.

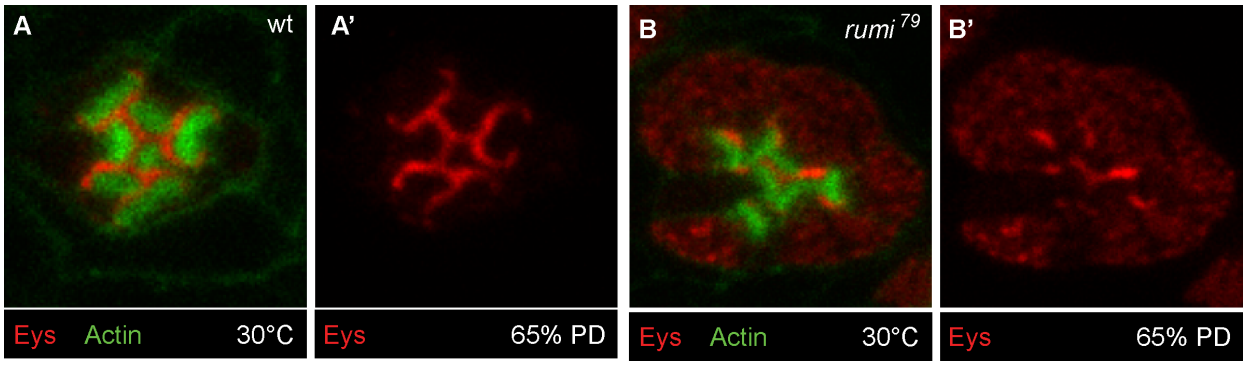

Figure 3-18. Enzymatic null *rumi* allele also shows intracellular accumulation of Eys. Confocal micrographs depicting antibody stainings of single ommatidia from (A,A') wild-type and (B,B') *rumi*^{79} mutant animals. The animals, shifted to 30°C during IRS formation, show severe accumulation of Eys in the photoreceptor cell body, indicating that the defect is due to loss of *O*-glucose. Red: Eys, Green: Actin which marks the rhabdomeres.

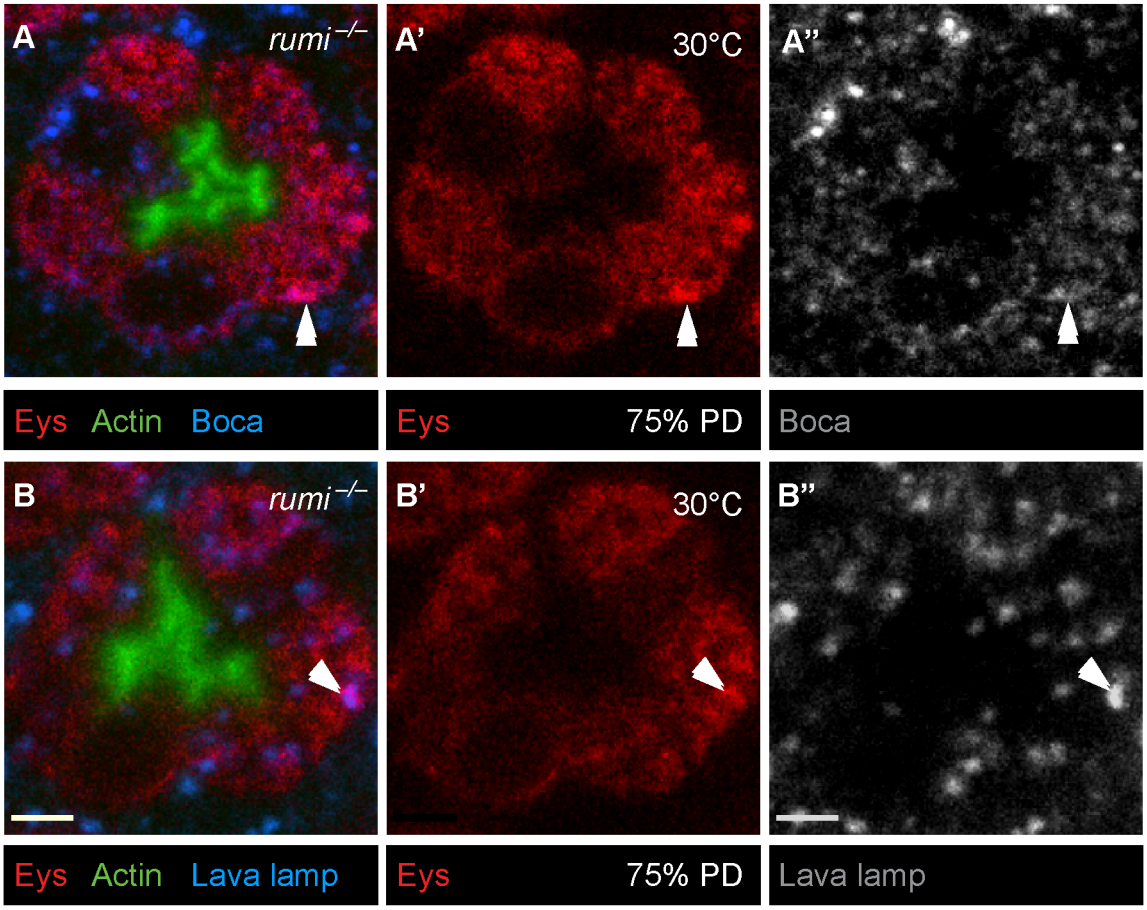

Figure 3-19. Eys does not accumulate in the ER or the Golgi in *rumi*$^{-/-}$ photoreceptors raised at 30°C. Confocal micrographs from 75% PD *rumi*$^{-/-}$ ommatidia colabeled with Eys and the ER marker Boca (A-A''), the Golgi marker Lava lamp (B-B''). Arrows indicate points of colocalization, which occurs only occasionally, suggesting that Eys does not accumulate in a single compartment. Scale bar: 5 μm.

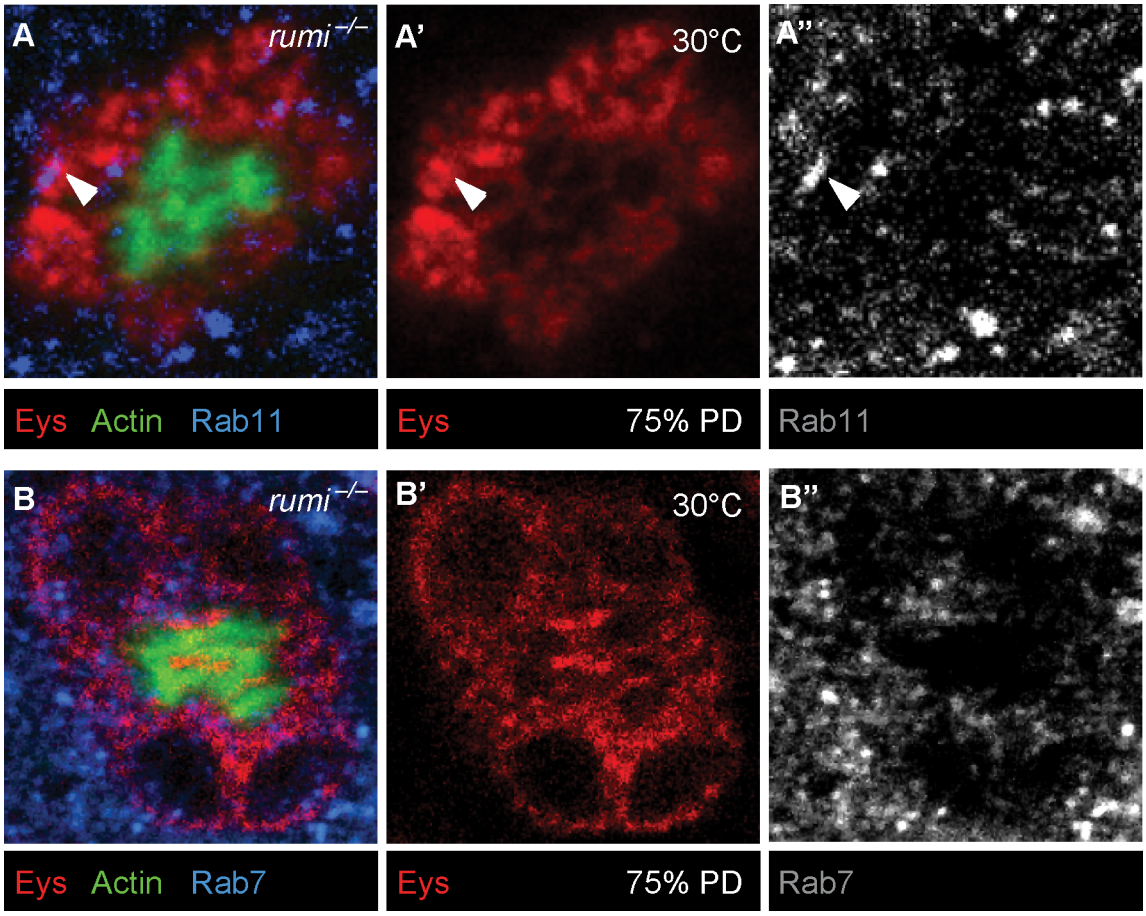

Figure 3-20. Eys does not accumulate in recycling endosomes or the late endosomes in *rumi*$^{-/-}$ photoreceptors raised at 30°C. Confocal micrographs from 75% PD *rumi*$^{-/-}$ ommatidia colabeled with Eys and the recycling endosomal marker Rab11 (C-C''), and the late endosomal marker Rab7 (D-D''). White arrowheads mark colocalization between Eys and the respective subcellular compartment. Eys only shows occasional colocalization with each marker, strongly suggesting that Eys does not accumulate in a single compartment.

Worsening of the IRS defect and further decrease in the extracellular levels of Eys in *rumi* mutant animals raised at higher temperature suggest that in the absence of Rumi, Eys is misfolded. To assess the effects of loss of Rumi on Eys protein levels at low and high temperatures, we performed Western blots on head extracts from 80% PD wild-type and $rumi^{-/-}$ animals. When raised at 18°C throughout development, wild-type and $rumi^{-/-}$ pupae did not show a significant difference in the level of Eys (Figure 3-21A and B, left panel, P=0.57). However, when the animals were raised at 18°C until mid-pupal stage and shifted to 30°C during IRS formation, there was a significant decrease in the level of Eys in $rumi^{-/-}$ pupal heads (Figure 3-21A and B, right panel, P<0.05). These data support the notion that loss of Rumi decreases the ability of Eys to fold properly and to be secreted at a normal rate. The data also suggest that at higher temperatures, misfolding results in degradation of Eys and worsening of IRS defects in *rumi* mutant animals.

If rhabdomere attachments observed in *rumi* mutants result from Eys misfolding, decreasing the level of chaperone proteins might enhance this phenotype. To test this hypothesis, we examined whether removing one copy of the ER chaperone *Hsc70-3* (BiP) affects rhabdomere attachment in $rumi^{-/-}$ animals. As shown in Figure 3-22A, animals double heterozygous for a lethal *P*-element inserted in the coding region of *Hsc70-3* ($Hsc70\text{-}3^{G0102}$) and *rumi* do not exhibit any rhabdomere attachment. However, $Hsc70\text{-}3^{G0102/+}$; $rumi^{-/-}$ animals raised at 18°C show an enhancement of rhabdomere attachment phenotype observed in $rumi^{-/-}$ animals raised at the same temperature (Figure 3-22B; compare to Figure 1). The average number of separate rhabdomeres in $Hsc70\text{-}3^{G0102/+}$; $rumi^{-/-}$ animals is significantly different from $rumi^{-/-}$ animals (Figure 3-22C, 2.85±0.11 vs. 4.11±0.08, P<0.0001). This observation further supports the conclusion that Eys is misfolded in *rumi* mutants. We next asked whether loss of Rumi triggers the unfolded protein response (UPR) in the pupal eye. One of the hallmarks of the UPR is the induction of chaperones, including Hsc70-3 (Ryoo et al. 2007). Western blotting using anti-Hsc70-3 antibody did not show an increase in the level of Hsc70-3 expression in *rumi* mutants raised at 18°C or 30°C compared to control animals (Figure 3-23A and B). This

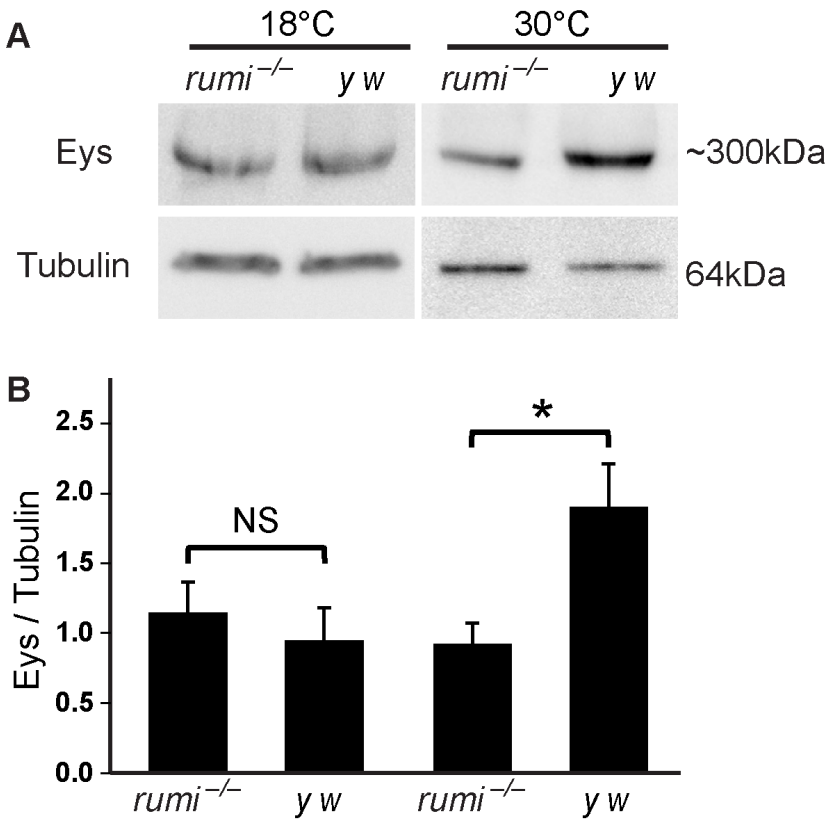

Figure 3-21. *rumi*$^{-/-}$ animals show a temperature-dependent decrease in Eys levels. (A) Western blots showing Eys levels in *rumi*$^{-/-}$ and *y w* heads grown at 18°C (left) and 30°C (right). (B) Graph showing densitometry quantifications from the bands in (A). There is a statistically significant decrease in Eys levels in *rumi*$^{-/-}$ head raised at 30°C (P<0.05; lower panel).

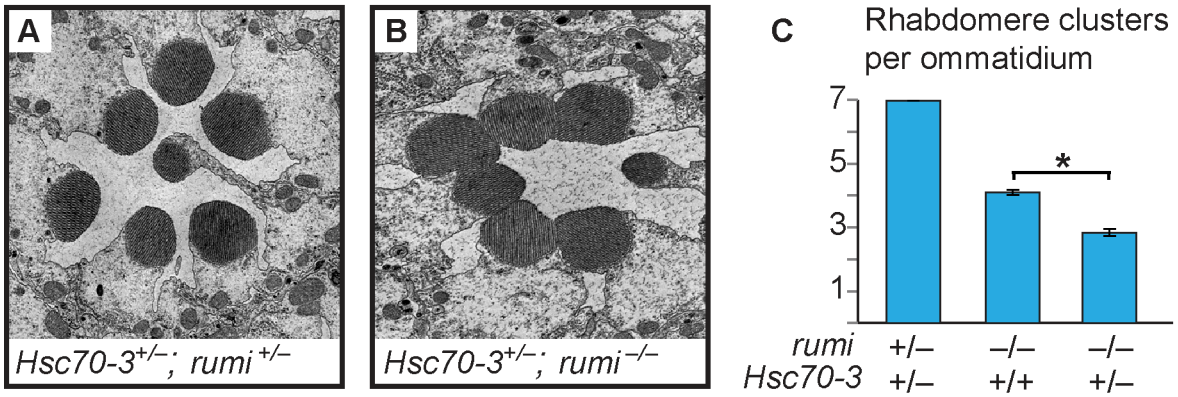

Figure 3-22. *rumi*$^{-/-}$ animals show a dosage-sensitive genetic interaction with an ER chaperone. (A,B) *Hsc70-3*$^{+/-}$*; rumi*$^{-/-}$ ommatidia show an enhancement of the *rumi*$^{-/-}$ phenotype. (A) Electron micrograph showing a single ommatidium from an *Hsc70-3*$^{+/-}$*; rumi*$^{+/-}$ control animal. (B) Electron micrograph showing an *Hsc70-3*$^{+/-}$*; rumi*$^{-/-}$ ommatidium. Frequently, all rhabdomeres but one are attached. (C) Quantification of average individual rhabdomere number per ommatidium for the indicated genotypes. **P*<0.0001.

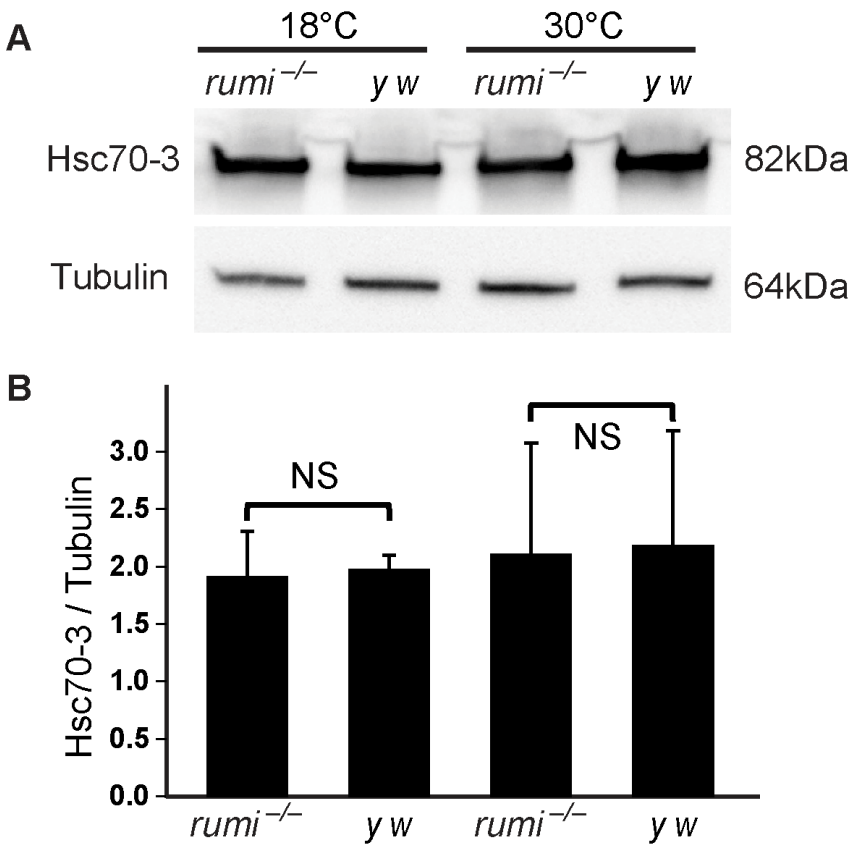

Figure 3-23. Unfolded protein response is not induced in *rumi*$^{-/-}$ animals. Levels of Hsc70-3, which is induced upon UPR, do not change between *rumi*$^{-/-}$ and *y w* animals raised at different temperatures. (A) western blot showing Hsc70-3 levels and Tubulin loading control. (B) ratio of Hsc70-3/Tubulin levels, which do not change between genotypes. NS, not significant.

indicates that UPR is not induced in the pupal eyes upon loss of Rumi, in agreement with a previous report on lack of UPR induction in *rumi*$^{-/-}$ clones in wing imaginal discs raised at 28°C despite accumulation of the Notch protein (Acar et al. 2008).

Mutations in Eys *O*-glucosylation sites result in its intracellular accumulation

If loss of the Poglut activity results in intracellular accumulation of Eys in the mid-pupal stage, mutating the Rumi target sites on Eys should affect its trafficking as well. To test this, we generated *UAS-attB* transgenes capable of overexpressing wild-type Eys (Eys^{wt}) or Eys with serine-to-alanine mutations in four (Eys$^{1-4}$) or in all five Rumi target sites of Eys (Eys$^{1-5}$) (Figure 3-24A). To minimize the expression variability associated with random insertion of transgenes, we used ΦC31 transgenesis and integrated all three constructs in the same docking site (*VK31*) in the fly genome (Bischof et al. 2007; Venken et al. 2006). We used *GMR-GAL4* to overexpress wild-type and mutant Eys in the developing photoreceptors and kept the animals at 18°C to avoid the very high levels of GAL4-driven transgene expression at high temperatures. In animals overexpressing wild-type Eys, the IRS is expanded and the majority of the Eys is within the IRS, although low levels of Eys are seen in photoreceptor cells (Figure 3-24B-C'). Overexpression of Eys$^{1-4}$ and Eys$^{1-5}$ also expands the IRS (Figure 3-24D-E', compare to Figure 3-15). However, unlike the wild-type protein, *O*-glucose mutant versions of Eys protein accumulate in the photoreceptor cells (Figure 3-24D-E', white arrowheads). These data support a role for *O*-glucose residues in the proper folding and trafficking of Eys.

DISCUSSION

We have previously shown that the extracellular domains of *Drosophila* and mammalian Notch proteins are efficiently *O*-glucosylated, and have provided strong evidence that Rumi/POGLUT1 is the only protein *O*-glucosyltransferase capable of adding *O*-glucose to EGF repeats in animals (Acar et al. 2008; Fernandez-Valdivia et al. 2011; Lee et al. 2013; Moloney et al. 2000b; Rana et al. 2011). The data presented here indicate that *Drosophila* Crb and Eys

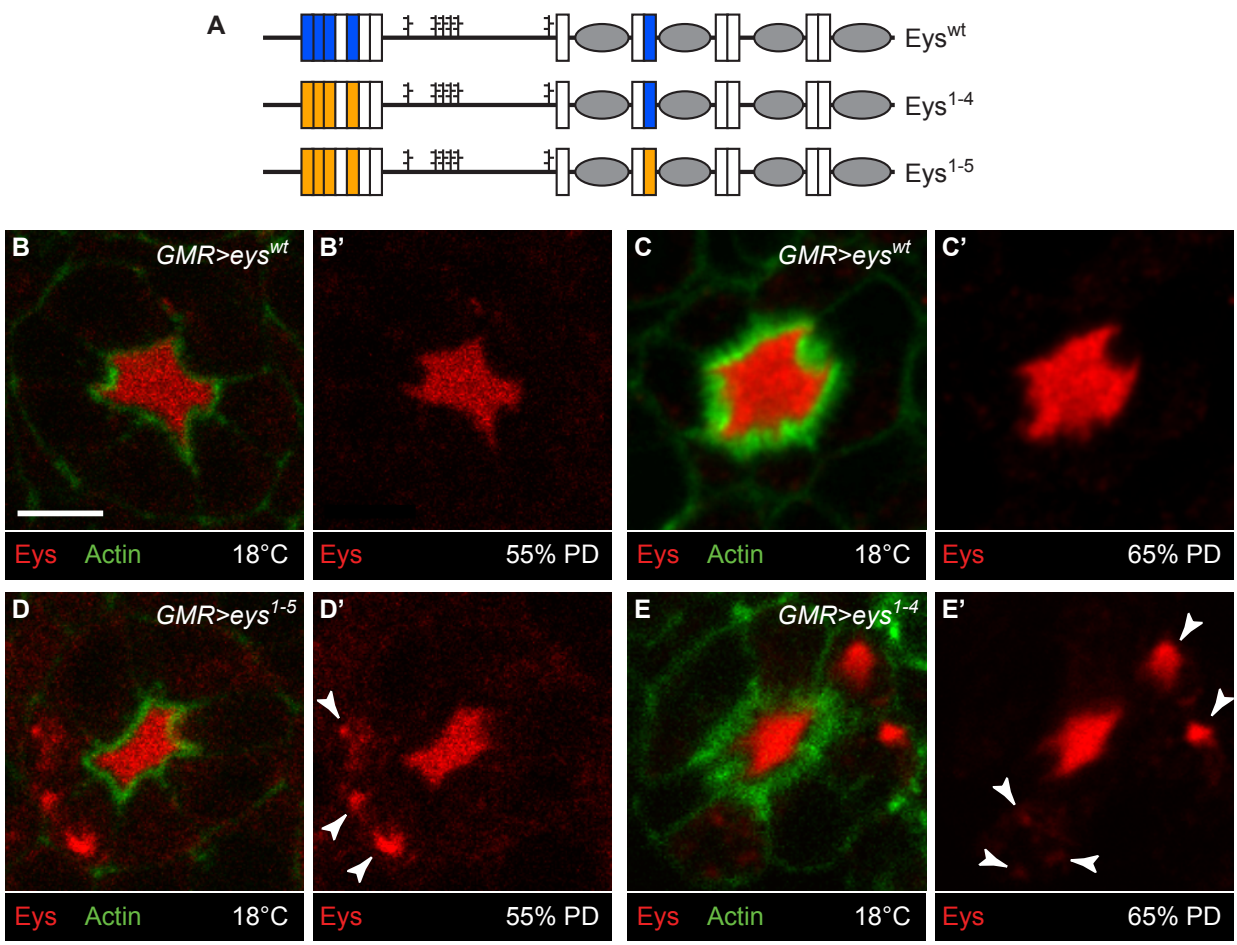

Figure 3-24. Loss of *O*-glucose on Eys results in its intracellular accumulation. (A) Schematic of Eys^{wt}, Eys^{1-4}, in which 4 out of 5 Rumi target sites are mutated, and Eys^{1-5}, in which all Rumi target sites are mutated. (B-E') Overexpression of Eys^{1-5} (D,D') and Eys^{1-4} (E,E'), but not Eys^{wt} (B-C'), results in intracellular Eys accumulation (arrowheads). The *GMR-GAL4* driver was used and all animals were raised at 18°C. Note that the *GMR>eys*^{wt} animal shown in (B,B') and the *GMR>eys*$^{1-5}$ animal (D,D') are younger than the *GMR>eys*^{wt} animal shown in (C,C') and the *GMR>eys*$^{1-4}$ animal (E,E'). Scale bar: 5 µm.

also harbor *O*-glucose residues, yet the impact of loss of Rumi and loss of *O*-glucose from these three target proteins, which harbor the highest number of Rumi target sites among all *Drosophila* proteins, is not equivalent. Loss of Rumi and mutations in Rumi target sites in a *Notch* genomic transgene both result in a temperature-dependent loss of Notch signaling (Acar et al. 2008; Leonardi et al. 2011), indicating that the Notch protein becomes sensitive to temperature alterations in the absence of *O*-glucose. Although the Notch loss-of-function phenotypes in *rumi* mutants raised at 18°C are mild and limited to certain contexts, raising animals homozygous for *rumi* or harboring *rumi* mitotic clones at 30°C phenocopies *Notch*-null phenotypes (Acar et al. 2008; Perdigoto et al. 2011; Takeuchi et al. 2011), indicating that *O*-glucose is indispensable for the function of *Drosophila* Notch at the restrictive temperature. At a functional level, loss of Rumi affects Eys similarly, with a moderate rhabdomere attachment phenotype at 18°C which becomes more severe when *rumi* animals are raised at 30°C during IRS formation. However, even when raised at 30°C, *rumi* does not phenocopy an *eys*-null phenotype in the eye, as rhabdomeres show some degree of separation in the mid-pupal stage. The function of Crb, in contrast, does not seem to be significantly affected by loss of *O*-glucose, as flies homozygous for a mutant allele of *crb* which contains no intact Rumi consensus sequences are viable and fertile, and do not exhibit any obvious phenotypes in rhabdomere morphogenesis. The divergent effects of *O*-glucose on the function of these proteins does not seem to be correlated with the number of Rumi target sites or the overall structure of these proteins, as Notch and Crb are transmembrane proteins but Eys is secreted, Crb and Eys both have a combination of EGF repeats and Laminin G domains but Notch does not have Laminin G domains, and Crb has a higher number of Rumi target sites (7) compared to Eys (5). In summary, our data indicate that although the $C^1XSX(P/A)C^2$ motif is highly predictive for the addition of *O*-glucose to EGF repeats of *Drosophila* proteins, the functional importance of *O*-glucose depends on additional parameters beyond the number of *O*-glucose sites and the overall domain structure of a given target protein.

In *rumi* mutant ommatidia, a significant amount of Eys remains inside the photoreceptor cells, while the extracellular levels of Eys in the IRS decrease. At the restrictive temperature, these phenotypes are enhanced and the total level of Eys in *rumi* mutant heads is significantly decreased. Moreover, removing one copy of an important ER chaperone enhances the rhabdomere attachment phenotype in *rumi* mutants. Finally, animals homozygous for the catalytically-inactive allele $rumi^{79}$ also show rhabdomere attachment, and mutating the *O*-glucose sites of Eys results in its intracellular accumulation. Together, these observations strongly suggest that loss of *O*-glucosylation results in Eys misfolding and a decrease in its extracellular levels. In contrast, despite the almost complete loss of Notch signaling in *rumi* clones raised at 28-30°C, surface expression of Notch is not decreased upon loss of Rumi; in contrast, Notch accumulates inside and at the surface of *rumi* mutant epithelial cells raised at the restrictive temperature (Acar et al. 2008). Moreover, cell-based and genetic experiments suggest that in the absence of Rumi, Notch is able to bind ligands at the cell surface but fails to be cleaved properly by the ADAM10 metalloproteinase Kuzbanian (Acar et al. 2008; Leonardi et al. 2011). Therefore, although these reports cannot rule out a redundant role for *O*-glucose in promoting the cell surface expression of Notch, they indicate that *O*-glucose is required for Notch signaling independently of its exocytic trafficking. Nevertheless, the temperature-dependent enhancement of loss of Notch signaling and Notch accumulation in *rumi* mutants (Acar et al. 2008; Leonardi et al. 2011) suggests that folding of Notch might also be affected by the loss of *O*-glucose. Similarly, the increase in the number of Crb^{+} puncta observed in $rumi^{-/-}$ photoreceptors raised at 25°C suggests that, although the function of *Drosophila* Crb does not depend on *O*-glucosylation, loss of *O*-glucose affects Crb trafficking. Therefore, while we cannot rule out that *O*-glucosylation affects each of these targets differently at molecular and cell biological levels, we favor a scenario in which the folding of all three targets is affected by loss of *O*-glucose. In this scenario, the degree of functional defects observed for each target and the cellular compartment where the defect is observed varies depending on the extent of misfolding, the sensitivity of the target protein to lack of *O*-glucose and the cellular context

where the target operates. It is intriguing to note that Rumi/POGLUT1 only glucosylates properly folded EGF repeats *in vitro* (Takeuchi et al. 2012), suggesting that Rumi/POGLUT1 may exert its effects on folding at the level of individual EGF repeats.

Analysis of rhabdomere separation and IRS size in mid-pupal and late pupal/adult *rumi*$^{-/-}$ animals raised at 18°C suggests two temporally distinct steps for the function of Eys during IRS formation. In the early stages of IRS formation, some of the rhabdomeres in each ommatidium fail to separate from each other, and the mutant IRS is significantly smaller than control IRS. In late pupal stages, the level of Eys in the IRS of *rumi*$^{-/-}$ ommatidia is comparable to that in control ommatidia, in agreement with the more or less normal IRS size observed in adult *rumi* ommatidia. Nevertheless, rhabdomere attachments are not resolved. These observations suggest that Eys generates the IRS in two steps. At ~45-55% PD, Eys secretion is required to sever the attachments among the rhabdomeres in each ommatidium (step 1), likely by opposing the adhesive forces mediated by Chaoptin (Zelhof et al. 2006). Rhabdomere separation in turn generates conduits between stalk membranes—from which Eys is likely secreted (Husain et al. 2006) —and the central IRS, and thereby allows Eys to increase the IRS size after rhabdomeres are separated (step 2). We propose that in *rumi* mutants, the Eys protein fails to fold properly and as a result, a significant fraction of Eys remains inside the cell instead of being secreted into the extracellular space. Therefore, at the mid-pupal stage Eys fails to fully separate the rhabdomeres from one another. Once the critical time window between 45-55% PD (step 1) passes, continued Eys secretion in step 2 (IRS expansion) cannot separate rhabdomeres anymore. However, since in each *rumi* ommatidium some rhabdomeres separate from one another, Eys can reach the central IRS and can gradually increase the IRS size. This two-step model of rhabdomere separation and IRS expansion is further supported by the observation that overexpression of Eys in an *eys* null background after 65% PD fails to separate the rhabdomeres (Zelhof et al. 2006).

Lack of photoreceptor abnormalities in *crb* mutants with no intact Rumi target sites was somewhat surprising, given that Crb has the second highest number of *O*-glucosylation motifs

in all fly proteins and that multiple EGF repeats in human CRB1 and CRB2 contain the Rumi consensus sequence. Our data indicate that *O*-glucosylation of Crb is not required for viability, fertility and photoreceptor morphogenesis in flies, at least in a laboratory setting. The Crb extracellular domain is dispensable for proper apical-basal polarity in embryos (Wodarz et al. 1995), but is required in other contexts, such as stalk membrane formation (Pellikka et al. 2002), regulation of the head size (Richardson and Pichaud 2010), prevention of light-induced photoreceptor degeneration (Johnson et al. 2002) and invagination of the salivary gland placode in embryos (Roper 2012). While the stalk membrane formation is not impaired upon mutating all Crb *O*-glucose sites, it remains to be determined whether *O*-glucosylation of Crb is required for the regulation of other processes regulated by the Crb extracellular domain, and whether *O*-glucosylation of mammalian CRB proteins is required for their function.

Although a number of mammalian species including mice, rats, guinea pigs and sheep have lost Eys during evolution (Abd El-Aziz et al. 2008), humans have an Eys homolog (EYS), which shows an overall protein domain organization similar to the fly Eys (Figure 4) (Collin et al. 2008). Transgenic expression of human EYS in a *Drosophila eys* null background produces pockets of IRS, presumably at the location of secretion, but fails to rescue the rhabdomere attachment phenotype (Nie et al. 2012). However, when human EYS is coexpressed in $eys^{-/-}$ animals with a human homolog of the *Drosophila* Prom called PROM1, some rhabdomeres separate from their neighbors (Nie et al. 2012). Since binding between *Drosophila* Eys and Prom is important for IRS formation (Zelhof et al. 2006), these rescue experiments highlight the evolutionary conservation of the Eys-Prom interaction in the visual system. Of note, mutations in human *EYS* and *PROM1* cause several forms of retinal degeneration including autosomal recessive retinitis pigmentosa, rod-cone dystrophies and cone-rod dystrophy (Abd El-Aziz et al. 2008; Audo et al. 2010; Beryozkin et al. 2014; Collin et al. 2008; Iwanami et al. 2012; Katagiri et al. 2014; Littink et al. 2010; Permanyer et al. 2010; Pras et al. 2009; Zhang et al. 2007). Human EYS contains seven target sites for *O*-glucosylation, 4-5 of which are clustered similar

to the Rumi target sites in EGF1-5 of *Drosophila* Eys. Therefore, *O*-glucosylation might play an important role in the function of the human EYS.

CHAPTER IV

SUMMARY AND FUTURE DIRECTIONS

PART 1: SUMMARY AND DISCUSSION

The functions of *O*-linked glycosylation are an area of active study. Many of the discovered functions of *O*-linked glycosylation on EGF repeats have been characterized with respect to Notch signaling. Rumi was discovered and initially characterized as the *O*-glucosyltransferase that modifies Notch to promote Notch signaling (Acar et al. 2008). Although other proteins, such as coagulation factors, contain *O*-glucose modifications, no other targets of Rumi had been characterized. The data presented in chapter III demonstrates that Rumi has other targets in *Drosophila* besides the Notch extracellular domain. I have shown that the enzymatic function of Rumi is required for the separation of rhabdomeres independently of its role in Notch signaling. The two candidate targets responsible for this phenotype are Crb and Eys, and both of these harbor *O*-glucose modifications on every Rumi consensus sequence tested. I have shown that, surprisingly, loss of *O*-glucose on Crb appears to have no effect on *Drosophila* development, including eye and rhabdomere morphology. However, slightly increased Crb^{+} puncta are visible in $rumi^{-/-}$ photoreceptors, suggesting that Rumi plays some role on Crb in the secretory pathway. My data strongly suggest that addition of *O*-glucose by Rumi to Eys is likely required to promote the complete separation of rhabdomeres during pupal development. The role of *O*-glucose on Crb is less clear, as mutations in the Rumi target sequences of Crb cause no obvious developmental phenotypes. Loss of the enzymatic activity of Rumi results in severe intracellular accumulation of Eys, especially when animals are raised at higher temperatures, which corresponds with a decrease in IRS size in $rumi^{-/-}$ animals. Mutations in the Rumi target sites in Eys also cause intracellular accumulation of Eys, suggesting that this defect is due to loss of *O*-glucose on Eys. Somewhat surprisingly, accumulated Eys is not located exclusively in the ER, where Rumi resides, or in any other cellular compartment. This corresponds with the Notch data when Rumi is absent; Notch accumulates intracellularly but is not accumulated in the ER (Acar et al. 2008). This suggests that Eys secretion through the secretory pathway is slow upon loss of *O*-glucose, and the

temperature sensitivity suggests that Eys may be misfolded, blocking smooth transport through the secretory pathway. Conversely, unfolded protein response is not induced in *rumi*$^{-/-}$ animals, but again this is consistent with the Notch data upon loss of Rumi (Acar et al. 2008). However, removing a copy of the ER chaperone *hsc70-3* in a *rumi*$^{-/-}$ animal worsens the rhabdomere attachment defect, suggesting that protein misfolding is the cause of rhabdomere attachment in *rumi*$^{-/-}$. Lastly, Eys levels decrease in *rumi*$^{-/-}$ raised at higher temperatures, which could be due to Eys misfolding and subsequent degradation. Collectively, these results suggest that Eys requires *O*-glucose to be properly folded and secreted into the IRS, where it can separate the rhabdomeres.

The differences between loss of *O*-glucose on Eys and Notch suggest that *O*-glucose is not required for all proteins equally. At a functional level, loss of *O*-glucose on Notch does not affect ligand binding or transport to the cell surface, but affects Notch at a step between S2 and S3 cleavage. At the protein level, loss of *O*-glucose leads to increased Notch levels both at the cell surface and intracellularly. One potential hypothesis is upon loss of *O*-glucose, the Notch extracellular domain binds the ligands but fail to undergo the conformational changes required to expose the S2 cleavage site due to a mild misfolding at the membrane. It is possible that the Notch accumulation is due to Notch misfolding, although Notch is not accumulated in the ER and the unfolded protein response is not induced (Acar et al. 2008). The same is true for Eys; the data presented here suggest that Eys is misfolded upon loss of *O*-glucose, although Eys does not accumulate in the ER and the unfolded protein response (UPR) is not induced. The reason for the accumulation of misfolded Notch and Eys remains to be determined. Cells have mechanisms such as the UPR to decrease the load of misfolded proteins and target them for degradation, but this does not seem to be happening, at least efficiently, upon loss of *O*-glucose from Notch and Eys. *O*-glucose may be required for misfolded protein degradation, but Eys levels are decreased at higher temperatures in *rumi* mutants, suggesting that at least some degradation is occurring in the case of Eys.

O-glucose is likely not required for the initial stages of protein folding, given that *O*-glucose must be added to an already folded EGF repeat (Ishio et al. 2014). It is possible that *O*-glucose is required to maintain the conformational stability of Eys in the secretory pathway, and this conformational stability is required for proper Eys secretion. When Eys is not *O*-glucosylated, it then lingers in the secretory pathway by an unknown mechanism before eventually moving through. It remains to be determined whether conformational stability prevents consistent Eys binding with an important chaperone in the secretory pathway, thereby preventing proper Eys secretion. However, it could also be true that chaperones bind more tightly to misfolded Eys in an attempt to correct the folding problem, which could lead to a slower Eys secretion. Notably, Ire1 recognizes misfolded proteins and loss of Ire1 results in defective Eys secretion (Coelho et al. 2013). It is possible that binding of Eys to Ire1 is required for secretion, and loss of *O*-glucose disrupts this binding.

Humans have an Eys homolog (EYS) that is required to prevent retinal degeneration (Abd El-Aziz et al. 2008). However, retinitis pigmentosa patients with mutations in EYS do not have any vision disruptions before the onset of retinal degeneration symptoms, suggesting a difference in the function of *Drosophila* Eys and human *EYS* in the context of development. However, it was recently discovered that mutations in *Drosophila eys* results in retinal degeneration (Gurudev et al. 2014).. Unfortunately, it remains difficult to study EYS since mice have lost EYS during evolution. One can speculate that mice have some compensatory mechanism for EYS function, but this remains to be determined.

The proposed mechanism of Eys function is that extracellular Eys binds to Prominin, a pentaspan transmembrane protein, to push apart the rhabdomeres during development (Zelhof et al. 2006). However, expression of Eys after ~60% PD fails to separate the rhabdomeres, indicating that other mechanisms exist for rhabdomere separation. Possibly at 55-60% PD, the microvilli of the rhabdomeres are premature and adhere less tightly than the microvilli of adults, and are therefore more easily pushed apart. After this time, the microvilli begin to elongate, and perhaps the microvilli of unseparated rhabdomeres interlock with the neighboring microvilli. In

my model, I propose that unglucosylated Eys is not rhabdomeres efficiently secreted into the IRS at the beginning of rhabdomere separation, marking a critical time window that must separate during development. After this time period, Eys is able to escape into the IRS, but at that time the microvilli is more mature and cannot be separated.

PART 2: FUTURE DIRECTIONS

Develop a rescue system to determine whether loss of O-glucose from Eys causes rhabdomere attachment

The data presented in chapter III suggests that Eys requires *O*-glucose for its function of rhabdomere separation. Further studies are required to prove this mechanism. To prove that loss of *O*-glucose on Eys is the actual cause of the rhabdomere attachment defect in *rumi* null animals, several techniques can be employed. First, the $eys^{1\text{-}5}$ construct used in the study will need to be expressed under the endogenous promoter. GMR is too strongly expressed and cannot be accurately used for rhabdomere separation experiments. Two commercially available MiMIC lines have the insertion in the first half of the *eys* gene: Mi00140 lies in the first intron of Eys, and MI09039 is inserted into the third intron of Eys (http://flypush.imgen.bcm.tmc.edu/pscreen/mimic.html) (Venken et al. 2011; Venken et al. 2009). These insertions can be replaced with a GAL4 by employing ϕC31-mediated integration, therefore driving Gal4 under the endogenous *eys* promoter. Using this method, Eys cDNA under the control of a UAS element (this study) could be driven by Gal4 expression with the natural promoter, the exact sequence of which is unknown.

A second method to test whether loss of *O*-glucose on Eys indeed causes rhabdomere attachment would be to generate a genomic transgene of *eys* with its natural promoter. This can be inserted into a VK line containing an *attP* site in a certain location on the genome which can be used to insert a construct with an *attB* site using ϕC31-mediated integration (Venken et al. 2006). Once a rescue system is established, the Rumi consensus sequences can be

mutated and subsequently used to determine the amount of rescue of the *eys* null phenotype. Our group previously used the same method for introducing mutations in *O*-glycosylation sites (Leonardi et al. 2011). However, this method would be much more inefficient and time consuming for Eys because the Rumi target sites in Eys are encoded by multiple rather distant exons. Regardless, we have used this method to inject two large BAC constructs into the VK31 site; CH321-59D21, and a shorter 50 kb construct that was generated by homologous recombination using homology arms close to the *eys* coding region. Flies carrying the larger 59D21 insertion, which we have named *PBac{eys$^{gt\text{-}59D21}$}attVK31,* are sick and it has been difficult to cross them onto an *eys* null background. Animals with the shorter transgene, however, have been crossed onto an *eys* null background. Although Eys is expressed in these animals, it fails to separate the rhabdomeres (Figure 25), suggesting that essential regulatory elements are present in the deleted upstream or downstream regions. It is possible that this construct is expressed too late in IRS development to separate the rhabdomeres.

Determine whether Eys is misfolded

Since the Eys intracellular accumulation phenotype is temperature-sensitive and since removing one copy of the chaperone *hsc70-3* in a *rumi*$^{-/-}$ background worsens the rhabdomere attachment in *rumi*$^{-/-}$, it is easy to speculate that Eys is misfolded upon loss of *O*-glucose. However, the methods employed in chapter III cannot prove protein misfolding. To determine this, a method called circular dichroism can be used (Greenfield 2006). This method measures the protein's unequal absorption of left-handed and right-handed circular polarized light. Proteins must be 95% pure and only 20 µg or less of protein is needed. Ideally, Eys protein from Rumi positive and Rumi negative cell lines (or flies) would be purified and the difference in absorption would be measured. Additionally, this system can be used to determine changes in protein conformation with varying temperature, which could be performed to determine if Eys misfolding is indeed increased at higher temperatures.

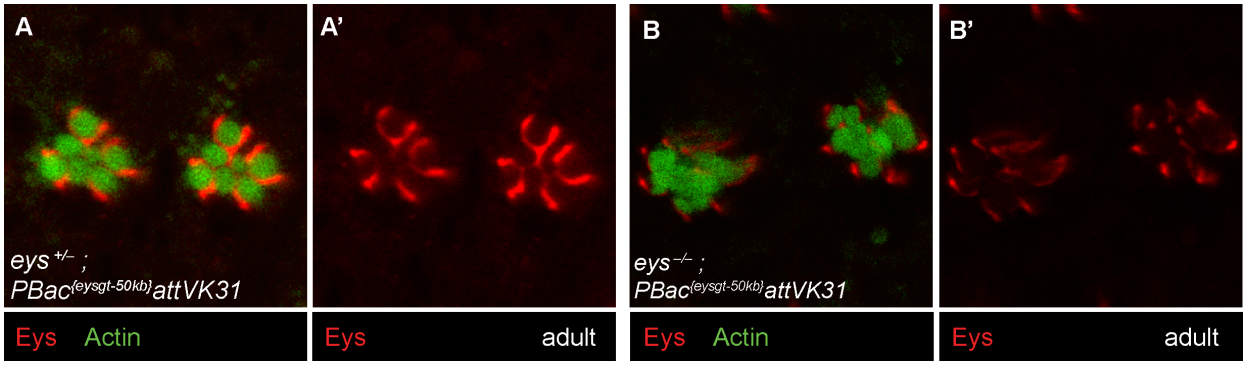

Figure 4-1. The shorter Eys genomic transgene does not rescue the *eys* null phenotype. Confocal micrographs of (A,A') heterozygous and (B,B') homozygous *eys* null animals expressing the shorter *eys* genomic transgene. Eys is concentrated at the stalk membrane on the outside of unseparated rhabdomeres. This construct is potentially lacking regulatory elements required for proper timing of Eys expression, and this expression pattern is consistent with late expression of Eys (Zelhof et al. 2006).

Potential cooperation of *O*-glucose with other *O*-linked glycans on Eys and Crb

Loss of *O*-glucose on Eys results in an Eys folding defect, which grows worse at higher temperatures, but never phenocopies the *eys* null phenotype. This is unlike the phenotype of loss of *O*-glucose on Notch, which mimics the *Notch* loss of function phenotype when animals are raised at higher temperatures (Acar et al. 2008). However, Ishio *et al* showed that loss of the *O*-fucose on Notch does not affect Notch signaling alone at lower temperatures, but affects Notch signaling at higher temperatures. The loss of both *O*-glucose and *O*-fucose on Notch causes severe defects even at lower temperatures, suggesting that glucose and fucose on Notch have a redundant function. It remains to be determined whether this is also true for Eys or Crb function. It is possible that loss of *O*-glucose and loss of *O*-fucose on Eys results in a complete loss of Eys function at higher temperatures. Additionally, loss of *O*-glucose surprisingly had no effect on Crb function. Given that Crb has a higher number of highly conserved *O*-glucose target sequences, it is strange that *O*-glucose is dispensable for Crb function. Interestingly, Crb contains seven *O*-glucose sites and ten *O*-fucose sites, whereas Eys possesses five *O*-glucose sites and four *O*-fucose sites. Since Crb has more *O*-fucose sites and *O*-glucose, and many more sites than Eys, possibly *O*-fucose and *O*-glucose cooperate in a slightly different redundant fashion in which *O*-fucose is more important for Crb function than *O*-glucose. This could be determined by mutating both the *O*-glucose and the *O*-fucose sites on Crb. Additionally, it is possible that we did not raise our $crb^{1\text{-}7\text{-}HA}$ animals at a high enough temperature as the highest we raised them was 25°C. Raising the animals at 30°C was lethal for both $crb^{1\text{-}7\text{-}HA}$ and $crb^{wt\text{-}HA}$, indicating that the HA tag disrupted Crb function at the higher temperature, so no conclusions about the temperature sensitive function of *O*-glucose could be reached at that temperature.

Comparing Pofut1/Ofut1 knockout phenotypes can provide clues to the relevant targets of the enzymes. Loss of *Pofut1/ofut1* results in embryonic lethality similar to loss of Notch function, suggesting Notch requires *O*-fucose to function (de la Pompa et al. 1997; Oka et al. 1995; Poulson 1937; Sasamura et al. 2003; Shi and Stanley 2003). Loss of *crb* in flies results in

a disruption of embryonic ectodermal derived epithelial cells (Tepass et al. 1990). While it is easy to relate loss of *Pofut1* to a global loss of Notch signaling because mutations in *RBPJ* result in a global loss of Notch signaling, it is more difficult for *CRB.* Loss of function mutations in *CRB1* result exclusively in eye phenotypes, involving loss of polarity, but animals survive (Mehalow et al. 2003). Loss of *CRB2* results in embryonic lethality at E12.5, later than global loss of Notch and loss of Pofut1 which die around E10.5 to E11.5 (Oka et al. 1995; Shi and Stanley 2003; Xiao et al. 2011). CRB3 is not required for mouse embryonic development, but is required for lung development as *CRB3* null mice die shortly after birth due to respiratory distress (Whiteman et al. 2014). However, CRB3 has a very short extracellular domain with no EGF repeats and therefore no sites for *O*-glycosylation(Makarova et al. 2003), so glycosylation likely does not play a role in CRB3 function. Additionally, loss of Pofut1/ofut1 has no reported phenotypes in epithelial polarity, which is the main function of Crb (Okamura and Saga 2008; Schuster-Gossler et al. 2009; Yao et al. 2011). Although glycosylation sites are conserved between *Drosophila* and mammalian Crb proteins, more studies will be required to determine the role of glycosylation in Crb function.

Determine whether *O*-glucose plays a role in the function of human EYS

Loss of *O*-glucose on *Drosophila* Eys results in a slow secretion into the IRS, leading to the lack of complete rhabdomere separation. It is tempting to speculate that *O*-glucose plays a role on human EYS as well since EYS possesses seven sites for *O*-glucose addition.. However, this is difficult to test since EYS is not conserved in mice and no mutations in Rumi have been reported in arRP patients (RetNet, https://sph.uth.edu/retnet/). One possibility is to generate the cDNA of human EYS, which spans about 10kb in length and is not available elsewhere. I have obtained fragments of human EYS from various sources and have been working to assemble them by overlap extension PCR. This construct, once assembled, can be transfected into mammalian cell lines, such as Y79 (a human retinoblastoma cell line) or Neuro2A (a murine neuroblastoma cell line), to determine whether the protein is secreted. The

construct can also be transfected into a cell lines with Rumi knocked down, which can be efficiently induced by RNAi (Fernandez-Valdivia et al. 2011). Furthermore, the construct can be injected into flies to make transgenic animals, and genetic experiments can subsequently be performed to determine whether human EYS can rescue the fly *eys* null phenotype or whether loss of *rumi* affects the function of human EYS in this context.

Modeling arRP mutations in flies

Mutations in human EYS cause autosomal recessive retinitis pigmentosa in several different populations across the world (Bandah-Rozenfeld et al. 2010; Barragan et al. 2010; Huang et al. 2010; Isackson et al. 2011; Iwanami et al. 2012; Littink et al. 2010), and mutations in EYS have been found in cone-rod dystrophy (Katagiri et al. 2014). According to http://www.hgmd.cf.ac.uk/ac/index.php, 34% of arRP-causing EYS mutations are missense mutations, and although they are highly associated with the disease, not all of them are predicted to be pathogenic by prediction programs (Oishi et al. 2014). Therefore, modeling these mutations in other organisms could provide insight on the pathogenic mechanism of these mutations. Mice do not contain an EYS homolog, and therefore cannot be used to model pathogenic EYS mutations. However, *Drosophila* can be used to model disease-causing EYS mutations; if a full-length EYS transgene is generated and a rescue system is created, mutations that are found in patients with retinitis pigmentosa can be introduced into the human construct, which can then be introduced into *Drosophila*. This method could be used to determine the effect of disease causing mutations on EYS biology *in vivo*. In one study, this same method was employed to model a retinitis pigmentosa disease causing mutation in *PROM1* to determine the effect on retinal biology (Nie et al. 2012). This resulted in an interesting phenotype in which the mutated PROM1 disrupted the function of endogenous *prom* in a dominant negative fashion, consistent with the fact that the disease-causing mutation is autosomal dominant. Additionally, the EYS construct with disease-causing mutations can be

introduced into mammalian cell lines to examine the effect of each mutation on trafficking and secretion.

Role of Rumi in mechano- and chemosensory organs

Cook *et al* found that Eys is required to prevent water loss in mechanosensory organs when animals are placed at higher temperatures (Cook et al. 2008), and that loss of Eys has no effect on mechanosensory organs when animals are raised at lower temperatures (Husain et al. 2006). If *O*-glucose is required on Eys in the context of rhabdomere spacing, it is possible that Eys requires *O*-glucose to function in the mechanosensory and chemosensory organs. To determine whether Rumi is required in the mechanosensory organs, adult *rumi*$^{-/-}$ would be placed at 37°C with *eys*$^{-/-}$ and wild type animals as controls, and loss of coordination would be assayed starting at 30 minutes and examined every 15 minutes thereafter. Animals that are *eys*$^{-/-}$ should lose the ability to walk and stand up after 30 minutes at 37°C according to previously published data (Cook et al. 2008). If *O*-glucose is required for Eys function, *rumi*$^{-/-}$ animals should lose ability to walk and stand in a similar manner. It is possible that *rumi* mutants behave like an *eys* hypomorph in this context, similar to the way they behave in the eye. If this is the case, perhaps *rumi*$^{-/-}$ animals will become more uncoordinated but still retain the ability to walk. In this case, climbing assays can be performed to determine how fast the flies can climb to the top of the vial. Wild type animals do this quickly since flies display negative geotaxis, i.e. move away from gravity.

Single nucleotide polymorphisms (SNPs) in EYS are associated with statin-induced myopathy, suggesting that EYS is important for human muscle function under environmental stress (Isackson et al. 2011). Only one copy of an EYS SNP is required to incur damage induced by statins. Isackson *et al* proposed that *EYS* is required for proper muscle regeneration in response to muscle damage. Additionally, they identified many isoforms of the EYS transcript in different tissues such as brain, spinal cord, and muscle, suggesting that each tissue has a wide variety of isoforms and complex splicing of EYS. It's possible that the

mechanism of statin-induced damage caused by EYS mutations is similar to the loss of mechanoreceptor function in *Drosophila* with *eys* mutations. Additionally, human EYS and *Drosophila* Eys have a similar protein organization to Notch, which is required to prevent premature satellite cell differentiation (Kopan et al. 1994; Kuroda et al. 1999; Schuster-Gossler et al. 2009). Both proteins contain multiple EGF repeats, which can mediate protein-protein interactions. It is possible, as Isackson *et al* suggests, that EYS is involved in muscle related Notch functions. *Drosophila* is a good model to study muscle since the *Drosophila* tubular body muscle is similar to mammalian muscle. To the best of my knowledge, it has not been tested whether Eys is expressed in *Drosophila* muscle. If it is indeed expressed, *Drosophila* would be a great model to study stress-induced muscle damage in animals lacking *eys*.

BIBLIOGRAPHY

Abd El-Aziz MM, Barragan I, O'Driscoll CA, Goodstadt L, Prigmore E, Borrego S, Mena M, Pieras JI, El-Ashry MF, Safieh LA, et al. 2008. EYS, encoding an ortholog of Drosophila spacemaker, is mutated in autosomal recessive retinitis pigmentosa. *Nat Genet*. 40: 1285-1287.

Abd El-Aziz MM, O'Driscoll CA, Kaye RS, Barragan I, El-Ashry MF, Borrego S, Antinolo G, Pang CP, Webster AR, Bhattacharya SS. 2010. Identification of Novel Mutations in the Ortholog of Drosophila Eyes Shut Gene (EYS) Causing Autosomal Recessive Retinitis Pigmentosa. *Invest Ophthalmol Vis Sci*. 51: 4266-4272.

Acar M, Jafar-Nejad H, Takeuchi H, Rajan A, Ibrani D, Rana NA, Pan H, Haltiwanger RS, Bellen HJ. 2008. Rumi is a CAP10 domain glycosyltransferase that modifies Notch and is required for Notch signaling. *Cell*. 132: 247-258.

Alfaro JF, Gong CX, Monroe ME, Aldrich JT, Clauss TR, Purvine SO, Wang Z, Camp DG, 2nd, Shabanowitz J, Stanley P, et al. 2012. Tandem mass spectrometry identifies many

mouse brain O-GlcNAcylated proteins including EGF domain-specific O-GlcNAc transferase targets. *Proc Natl Acad Sci U S A*. 109: 7280-7285.

Amano M, Ito M, Kimura K, Fukata Y, Chihara K, Nakano T, Matsuura Y, Kaibuchi K. 1996. Phosphorylation and activation of myosin by Rho-associated kinase (Rho-kinase). *J Biol Chem*. 271: 20246-20249.

Aoki K, Porterfield M, Lee SS, Dong B, Nguyen K, McGlamry KH, Tiemeyer M. 2008. The diversity of O-linked glycans expressed during Drosophila melanogaster development reflects stage- and tissue-specific requirements for cell signaling. *J Biol Chem*. 283: 30385-30400.

Appella E, Weber IT, Blasi F. 1988. Structure and function of epidermal growth factor-like regions in proteins. *FEBS Lett*. 231: 1-4.

Arikawa K, Hicks JL, Williams DS. 1990. Identification of actin filaments in the rhabdomeral microvilli of Drosophila photoreceptors. *J Cell Biol*. 110: 1993-1998.

Artavanis-Tsakonas S, Muskavitch MA. 2010. Notch: the past, the present, and the future. *Curr Top Dev Biol*. 92: 1-29.

Arteaga CL. 2001. The epidermal growth factor receptor: from mutant oncogene in nonhuman cancers to therapeutic target in human neoplasia. *J Clin Oncol*. 19: 32S-40S.

Asano M, Furukawa K, Kido M, Matsumoto S, Umesaki Y, Kochibe N, Iwakura Y. 1997. Growth retardation and early death of beta-1,4-galactosyltransferase knockout mice with augmented proliferation and abnormal differentiation of epithelial cells. *EMBO J*. 16: 1850-1857.

Audo I, Sahel JA, Mohand-Said S, Lancelot ME, Antonio A, Moskova-Doumanova V, Nandrot EF, Doumanov J, Barragan I, Antinolo G, et al. 2010. EYS is a major gene for rod-cone dystrophies in France. *Hum Mutat*. 31: E1406-1435.

Balzar M, Briaire-de Bruijn IH, Rees-Bakker HA, Prins FA, Helfrich W, de Leij L, Riethmuller G, Alberti S, Warnaar SO, Fleuren GJ, et al. 2001. Epidermal growth factor-like repeats

mediate lateral and reciprocal interactions of Ep-CAM molecules in homophilic adhesions. *Mol Cell Biol*. 21: 2570-2580.

Bandah-Rozenfeld D, Littink KW, Ben-Yosef T, Strom TM, Chowers I, Collin RW, den Hollander AI, van den Born LI, Zonneveld MN, Merin S, et al. 2010. Novel null mutations in the EYS gene are a frequent cause of autosomal recessive retinitis pigmentosa in the Israeli population. *Invest Ophthalmol Vis Sci*. 51: 4387-4394.

Barbacci EG, Guarino BC, Stroh JG, Singleton DH, Rosnack KJ, Moyer JD, Andrews GC. 1995. The structural basis for the specificity of epidermal growth factor and heregulin binding. *J Biol Chem*. 270: 9585-9589.

Barragan I, Borrego S, Pieras JI, Gonzalez-del Pozo M, Santoyo J, Ayuso C, Baiget M, Millan JM, Mena M, Abd El-Aziz MM, et al. 2010. Mutation spectrum of EYS in Spanish patients with autosomal recessive retinitis pigmentosa. *Hum Mutat*. 31: E1772-1800.

Bennett EP, Mandel U, Clausen H, Gerken TA, Fritz TA, Tabak LA. 2012. Control of mucin-type O-glycosylation: a classification of the polypeptide GalNAc-transferase gene family. *Glycobiology*. 22: 736-756.

Beryozkin A, Zelinger L, Bandah-Rozenfeld D, Shevach E, Harel A, Storm T, Sagi M, Eli D, Merin S, Banin E, et al. 2014. Identification of mutations causing inherited retinal degenerations in the israeli and palestinian populations using homozygosity mapping. *Invest Ophthalmol Vis Sci*. 55: 1149-1160.

Bischof J, Maeda RK, Hediger M, Karch F, Basler K. 2007. An optimized transgenesis system for Drosophila using germ-line-specific phiC31 integrases. *Proc Natl Acad Sci U S A*. 104: 3312-3317.

Bjoern S, Foster DC, Thim L, Wiberg FC, Christensen M, Komiyama Y, Pedersen AH, Kisiel W. 1991. Human plasma and recombinant factor VII. Characterization of O-glycosylations at serine residues 52 and 60 and effects of site-directed mutagenesis of serine 52 to alanine. *J Biol Chem*. 266: 11051-11057.

Blass DH, Hunt DM. 1980. Pyrimidine biosynthesis in the dumpy mutants of Drosophila melanogaster. *Mol Gen Genet*. 178: 437-442.

Bonafede RP, Beighton P. 1979. Autosomal dominant inheritance of scalp defects with ectrodactyly. *Am J Med Genet*. 3: 35-41.

Borst A. 2009. Drosophila's view on insect vision. *Curr Biol*. 19: R36-47.

Boschek CB. 1971. On the fine structure of the peripheral retina and lamina ganglionaris of the fly, Musca domestica. *Z Zellforsch Mikrosk Anat*. 118: 369-409.

Braitenberg V. 1967. Patterns of projection in the visual system of the fly. I. Retina-lamina projections. *Exp Brain Res*. 3: 271-298.

Breloy I, Schwientek T, Gries B, Razawi H, Macht M, Albers C, Hanisch FG. 2008. Initiation of mammalian O-mannosylation in vivo is independent of a consensus sequence and controlled by peptide regions within and upstream of the alpha-dystroglycan mucin domain. *J Biol Chem*. 283: 18832-18840.

Brou C, Logeat F, Gupta N, Bessia C, LeBail O, Doedens JR, Cumano A, Roux P, Black RA, Israel A. 2000. A novel proteolytic cleavage involved in Notch signaling: the role of the disintegrin-metalloprotease TACE. *Mol Cell*. 5: 207-216.

Bruckner K, Perez L, Clausen H, Cohen S. 2000. Glycosyltransferase activity of Fringe modulates Notch-Delta interactions. *Nature*. 406: 411-415.

Burton BK, Hauser L, Nadler HL. 1976. Congenital scalp defects with distal limb anomalies: report of a family. *J Med Genet*. 13: 466-468.

Chen CL, Gajewski KM, Hamaratoglu F, Bossuyt W, Sansores-Garcia L, Tao C, Halder G. 2010. The apical-basal cell polarity determinant Crumbs regulates Hippo signaling in Drosophila. *Proc Natl Acad Sci U S A*. 107: 15810-15815.

Chen J, Lu L, Shi S, Stanley P. 2006. Expression of Notch signaling pathway genes in mouse embryos lacking beta4galactosyltransferase-1. *Gene Expr Patterns*. 6: 376-382.

Chen J, Moloney DJ, Stanley P. 2001. Fringe modulation of Jagged1-induced Notch signaling requires the action of beta 4galactosyltransferase-1. *Proc Natl Acad Sci U S A*. 98: 13716-13721.

Chinchore Y, Mitra A, Dolph PJ. 2009. Accumulation of rhodopsin in late endosomes triggers photoreceptor cell degeneration. *PLoS Genet*. 5: e1000377.

Clandinin TR, Zipursky SL. 2000. Afferent growth cone interactions control synaptic specificity in the Drosophila visual system. *Neuron*. 28: 427-436.

Coelho DS, Cairrao F, Zeng X, Pires E, Coelho AV, Ron D, Ryoo HD, Domingos PM. 2013. Xbp1-Independent Ire1 Signaling Is Required for Photoreceptor Differentiation and Rhabdomere Morphogenesis in Drosophila. *Cell Rep*.

Cohen B, Bashirullah A, Dagnino L, Campbell C, Fisher WW, Leow CC, Whiting E, Ryan D, Zinyk D, Boulianne G, et al. 1997. Fringe boundaries coincide with Notch-dependent patterning centres in mammals and alter Notch-dependent development in Drosophila. *Nat Genet*. 16: 283-288.

Cohen I, Silberstein E, Perez Y, Landau D, Elbedour K, Langer Y, Kadir R, Volodarsky M, Sivan S, Narkis G, et al. 2014. Autosomal recessive Adams-Oliver syndrome caused by homozygous mutation in EOGT, encoding an EGF domain-specific O-GlcNAc transferase. *Eur J Hum Genet*. 22: 374-378.

Collin RW, Littink KW, Klevering BJ, van den Born LI, Koenekoop RK, Zonneveld MN, Blokland EA, Strom TM, Hoyng CB, den Hollander AI, et al. 2008. Identification of a 2 Mb human ortholog of Drosophila eyes shut/spacemaker that is mutated in patients with retinitis pigmentosa. *Am J Hum Genet*. 83: 594-603.

Cook B, Hardy RW, McConnaughey WB, Zuker CS. 2008. Preserving cell shape under environmental stress. *Nature*. 452: 361-364.

Corbeil D, Roper K, Fargeas CA, Joester A, Huttner WB. 2001. Prominin: a story of cholesterol, plasma membrane protrusions and human pathology. *Traffic*. 2: 82-91.

Corbeil D, Roper K, Weigmann A, Huttner WB. 1998. AC133 hematopoietic stem cell antigen: human homologue of mouse kidney prominin or distinct member of a novel protein family? *Blood*. 91: 2625-2626.

Culi J, Mann RS. 2003. Boca, an endoplasmic reticulum protein required for wingless signaling and trafficking of LDL receptor family members in Drosophila. *Cell*. 112: 343-354.

de la Pompa JL, Wakeham A, Correia KM, Samper E, Brown S, Aguilera RJ, Nakano T, Honjo T, Mak TW, Rossant J, et al. 1997. Conservation of the Notch signalling pathway in mammalian neurogenesis. *Development*. 124: 1139-1148.

den Hollander AI, Heckenlively JR, van den Born LI, de Kok YJ, van der Velde-Visser SD, Kellner U, Jurklies B, van Schooneveld MJ, Blankenagel A, Rohrschneider K, et al. 2001. Leber congenital amaurosis and retinitis pigmentosa with Coats-like exudative vasculopathy are associated with mutations in the crumbs homologue 1 (CRB1) gene. *Am J Hum Genet*. 69: 198-203.

den Hollander AI, ten Brink JB, de Kok YJ, van Soest S, van den Born LI, van Driel MA, van de Pol DJ, Payne AM, Bhattacharya SS, Kellner U, et al. 1999. Mutations in a human homologue of Drosophila crumbs cause retinitis pigmentosa (RP12). *Nat Genet*. 23: 217-221.

Downing AK, Knott V, Werner JM, Cardy CM, Campbell ID, Handford PA. 1996. Solution structure of a pair of calcium-binding epidermal growth factor-like domains: implications for the Marfan syndrome and other genetic disorders. *Cell*. 85: 597-605.

Esmon NL, Owen WG, Esmon CT. 1982. Isolation of a membrane-bound cofactor for thrombin-catalyzed activation of protein C. *J Biol Chem*. 257: 859-864.

Evrard YA, Lun Y, Aulehla A, Gan L, Johnson RL. 1998. lunatic fringe is an essential mediator of somite segmentation and patterning. *Nature*. 394: 377-381.

Fabian-Fine R, Verstreken P, Hiesinger PR, Horne JA, Kostyleva R, Zhou Y, Bellen HJ, Meinertzhagen IA. 2003. Endophilin promotes a late step in endocytosis at glial invaginations in Drosophila photoreceptor terminals. *J Neurosci*. 23: 10732-10744.

Fehon RG, Kooh PJ, Rebay I, Regan CL, Xu T, Muskavitch MA, Artavanis-Tsakonas S. 1990. Molecular interactions between the protein products of the neurogenic loci Notch and Delta, two EGF-homologous genes in Drosophila. *Cell*. 61: 523-534.

Fernandez-Valdivia R, Takeuchi H, Samarghandi A, Lopez M, Leonardi J, Haltiwanger RS, Jafar-Nejad H. 2011. Regulation of the mammalian Notch signaling and embryonic development by the protein O-glucosyltransferase Rumi. *Development*. 138: 1925-1934.

Fleming RJ, Gu Y, Hukriede NA. 1997. Serrate-mediated activation of Notch is specifically blocked by the product of the gene fringe in the dorsal compartment of the Drosophila wing imaginal disc. *Development*. 124: 2973-2981.

Fyrberg EA, Bond BJ, Hershey ND, Mixter KS, Davidson N. 1981. The actin genes of Drosophila: protein coding regions are highly conserved but intron positions are not. *Cell*. 24: 107-116.

Fyrberg EA, Mahaffey JW, Bond BJ, Davidson N. 1983. Transcripts of the six Drosophila actin genes accumulate in a stage- and tissue-specific manner. *Cell*. 33: 115-123.

Gao S, Takemura SY, Ting CY, Huang S, Lu Z, Luan H, Rister J, Thum AS, Yang M, Hong ST, et al. 2008. The neural substrate of spectral preference in Drosophila. *Neuron*. 60: 328-342.

Grawe F, Wodarz A, Lee B, Knust E, Skaer H. 1996. The Drosophila genes crumbs and stardust are involved in the biogenesis of adherens junctions. *Development*. 122: 951-959.

Greenfield NJ. 2006. Using circular dichroism spectra to estimate protein secondary structure. *Nat Protoc*. 1: 2876-2890.

Gurudev N, Yuan M, Knust E. 2014. chaoptin, prominin, eyes shut and crumbs form a genetic network controlling the apical compartment of Drosophila photoreceptor cells. *Biol Open*. 3: 332-341.

Haines N, Irvine KD. 2005. Functional analysis of Drosophila beta1,4-N-acetylgalactosaminyltransferases. *Glycobiology*. 15: 335-346.

Hallgren P, Lundblad A, Svensson S. 1975. A new type of carbohydrate-protein linkage in a glycopeptide from normal human urine. *J Biol Chem*. 250: 5312-5314.

Haltom AR, Lee TV, Harvey BM, Leonardi J, Chen YJ, Hong Y, Haltiwanger RS, Jafar-Nejad H. 2014. The protein O-glucosyltransferase Rumi modifies eyes shut to promote rhabdomere separation in Drosophila. *PLoS Genet*. 10: e1004795.

Han Z, Anderson DW, Papermaster DS. 2012. Prominin-1 localizes to the open rims of outer segment lamellae in Xenopus laevis rod and cone photoreceptors. *Invest Ophthalmol Vis Sci*. 53: 361-373.

Harris RJ, Ling VT, Spellman MW. 1992. O-linked fucose is present in the first epidermal growth factor domain of factor XII but not protein C. *J Biol Chem*. 267: 5102-5107.

Harris RJ, Spellman MW. 1993. O-linked fucose and other post-translational modifications unique to EGF modules. *Glycobiology*. 3: 219-224.

Harris RJ, van Halbeek H, Glushka J, Basa LJ, Ling VT, Smith KJ, Spellman MW. 1993. Identification and structural analysis of the tetrasaccharide NeuAc alpha(2-->6)Gal beta(1-->4)GlcNAc beta(1-->3)Fuc alpha 1-->O-linked to serine 61 of human factor IX. *Biochemistry*. 32: 6539-6547.

Hase S, Kawabata S, Nishimura H, Takeya H, Sueyoshi T, Miyata T, Iwanaga S, Takao T, Shimonishi Y, Ikenaka T. 1988. A new trisaccharide sugar chain linked to a serine residue in bovine blood coagulation factors VII and IX. *J Biochem*. 104: 867-868.

Hassed SJ, Wiley GB, Wang S, Lee JY, Li S, Xu W, Zhao ZJ, Mulvihill JJ, Robertson J, Warner J, et al. 2012. RBPJ mutations identified in two families affected by Adams-Oliver syndrome. *Am J Hum Genet*. 91: 391-395.

Hicks C, Johnston SH, diSibio G, Collazo A, Vogt TF, Weinmaster G. 2000. Fringe differentially modulates Jagged1 and Delta1 signalling through Notch1 and Notch2. *Nat Cell Biol*. 2: 515-520.

Higuchi R, Krummel B, Saiki RK. 1988. A general method of in vitro preparation and specific mutagenesis of DNA fragments: study of protein and DNA interactions. *Nucleic Acids Res*. 16: 7351-7367.

Hirai-Fujita Y, Yamamoto-Hino M, Kanie O, Goto S. 2008. N-Glycosylation of the Drosophila neural protein Chaoptin is essential for its stability, cell surface transport and adhesive activity. *FEBS Lett*. 582: 2572-2576.

Hou X, Tashima Y, Stanley P. 2012. Galactose differentially modulates lunatic and manic fringe effects on Delta1-induced NOTCH signaling. *J Biol Chem*. 287: 474-483.

Huang J, Zhou W, Dong W, Watson AM, Hong Y. 2009. From the Cover: Directed, efficient, and versatile modifications of the Drosophila genome by genomic engineering. *Proc Natl Acad Sci U S A*. 106: 8284-8289.

Huang Y, Zhang J, Li C, Yang G, Liu M, Wang QK, Tang Z. 2010. Identification of a novel homozygous nonsense mutation in EYS in a Chinese family with autosomal recessive retinitis pigmentosa. *BMC Med Genet*. 11: 121.

Husain N, Pellikka M, Hong H, Klimentova T, Choe KM, Clandinin TR, Tepass U. 2006. The agrin/perlecan-related protein eyes shut is essential for epithelial lumen formation in the Drosophila retina. *Dev Cell*. 11: 483-493.

Irvine KD, Wieschaus E. 1994. fringe, a Boundary-specific signaling molecule, mediates interactions between dorsal and ventral cells during Drosophila wing development. *Cell*. 79: 595-606.

Isackson PJ, Ochs-Balcom HM, Ma C, Harley JB, Peltier W, Tarnopolsky M, Sripathi N, Wortmann RL, Simmons Z, Wilson JD, et al. 2011. Association of common variants in the human eyes shut ortholog (EYS) with statin-induced myopathy: Evidence for additional functions of EYS. *Muscle Nerve*.

Ishio A, Sasamura T, Ayukawa T, Kuroda J, Ishikawa HO, Aoyama N, Matsumoto K, Gushiken T, Okajima T, Yamakawa T, et al. 2014. O-fucose monosaccharide of Drosophila Notch

has a temperature-sensitive function and cooperates with O-glucose glycan in Notch transport and Notch signaling activation. *J Biol Chem*. in press.

Iwanami M, Oshikawa M, Nishida T, Nakadomari S, Kato S. 2012. High prevalence of mutations in the EYS gene in Japanese patients with autosomal recessive retinitis pigmentosa. *Invest Ophthalmol Vis Sci*. 53: 1033-1040.

Izaddoost S, Nam SC, Bhat MA, Bellen HJ, Choi KW. 2002. Drosophila Crumbs is a positional cue in photoreceptor adherens junctions and rhabdomeres. *Nature*. 416: 178-183.

Jafar-Nejad H, Leonardi J, Fernandez-Valdivia R. 2010. Role of glycans and glycosyltransferases in the regulation of Notch signaling. *Glycobiology*. 20: 931-949.

Johnson K, Grawe F, Grzeschik N, Knust E. 2002. Drosophila crumbs is required to inhibit light-induced photoreceptor degeneration. *Curr Biol*. 12: 1675-1680.

Johnston SH, Rauskolb C, Wilson R, Prabhakaran B, Irvine KD, Vogt TF. 1997. A family of mammalian Fringe genes implicated in boundary determination and the Notch pathway. *Development*. 124: 2245-2254.

Katagiri S, Akahori M, Hayashi T, Yoshitake K, Gekka T, Ikeo K, Tsuneoka H, Iwata T. 2014. Autosomal recessive cone-rod dystrophy associated with compound heterozygous mutations in the EYS gene. *Doc Ophthalmol*. 128: 211-217.

Kato Y, Tapping RI, Huang S, Watson MH, Ulevitch RJ, Lee JD. 1998. Bmk1/Erk5 is required for cell proliferation induced by epidermal growth factor. *Nature*. 395: 713-716.

Kentzer EJ, Buko A, Menon G, Sarin VK. 1990. Carbohydrate composition and presence of a fucose-protein linkage in recombinant human pro-urokinase. *Biochem Biophys Res Commun*. 171: 401-406.

Kim J, Irvine KD, Carroll SB. 1995. Cell recognition, signal induction, and symmetrical gene activation at the dorsal-ventral boundary of the developing Drosophila wing. *Cell*. 82: 795-802.

Kim ML, Chandrasekharan K, Glass M, Shi S, Stahl MC, Kaspar B, Stanley P, Martin PT. 2008. O-fucosylation of muscle agrin determines its ability to cluster acetylcholine receptors. *Mol Cell Neurosci*. 39: 452-464.

Kirschfeld K. 1967a. [The projection of the optical environment on the screen of the rhabdomere in the compound eye of the Musca]. *Exp Brain Res*. 3: 248-270.

Kirschfeld K. 1967b. [The projection of the optical environment on the screen of the rhabdomere in the compound eye of the Musca] (Original in German). *Exp Brain Res*. 3: 248-270.

Klein T, Arias AM. 1998. Interactions among Delta, Serrate and Fringe modulate Notch activity during Drosophila wing development. *Development*. 125: 2951-2962.

Kniazeva MF, Chiang MF, Cutting GR, Zack DJ, Han M, Zhang K. 1999. Clinical and genetic studies of an autosomal dominant cone-rod dystrophy with features of Stargardt disease. *Ophthalmic Genet*. 20: 71-81.

Knust E. 2007. Photoreceptor morphogenesis and retinal degeneration: lessons from Drosophila. *Curr Opin Neurobiol*. 17: 541-547.

Knust E, Tepass U, Wodarz A. 1993. crumbs and stardust, two genes of Drosophila required for the development of epithelial cell polarity. *Dev Suppl*: 261-268.

Kopan R, Ilagan MX. 2009. The canonical Notch signaling pathway: unfolding the activation mechanism. *Cell*. 137: 216-233.

Kopan R, Nye JS, Weintraub H. 1994. The intracellular domain of mouse Notch: a constitutively activated repressor of myogenesis directed at the basic helix-loop-helix region of MyoD. *Development*. 120: 2385-2396.

Krantz DE, Zipursky SL. 1990. Drosophila chaoptin, a member of the leucine-rich repeat family, is a photoreceptor cell-specific adhesion molecule. *EMBO J*. 9: 1969-1977.

Kumar JP. 2011. My what big eyes you have: how the Drosophila retina grows. *Dev Neurobiol*. 71: 1133-1152.

Kumar JP. 2012. Building an ommatidium one cell at a time. *Dev Dyn*. 241: 136-149.

Kumar JP, Ready DF. 1995. Rhodopsin plays an essential structural role in Drosophila photoreceptor development. *Development*. 121: 4359-4370.

Kuroda K, Tani S, Tamura K, Minoguchi S, Kurooka H, Honjo T. 1999. Delta-induced Notch signaling mediated by RBP-J inhibits MyoD expression and myogenesis. *J Biol Chem*. 274: 7238-7244.

Kurosawa S, Stearns DJ, Jackson KW, Esmon CT. 1988. A 10-kDa cyanogen bromide fragment from the epidermal growth factor homology domain of rabbit thrombomodulin contains the primary thrombin binding site. *J Biol Chem*. 263: 5993-5996.

LeBon L, Lee TV, Sprinzak D, Jafar-Nejad H, Elowitz MB. 2014. Fringe proteins modulate Notch-ligand cis and trans interactions to specify signaling states. *Elife*. 3: e02950.

Lee TV, Sethi MK, Leonardi L, Rana NA, Buettner FF, Haltiwanger RS, Bakker H, Jafar-Nejad H. 2013. Negative regulation of Notch signaling by xylose. *PLoS Genet*. 9: e1003547.

Leonard DS, Bowman VD, Ready DF, Pak WL. 1992. Degeneration of photoreceptors in rhodopsin mutants of Drosophila. *J Neurobiol*. 23: 605-626.

Leonardi J, Fernandez-Valdivia R, Li YD, Simcox AA, Jafar-Nejad H. 2011. Multiple O-glucosylation sites on Notch function as a buffer against temperature-dependent loss of signaling. *Development*. 138: 3569-3578.

Letizia A, Ricardo S, Moussian B, Martin N, Llimargas M. 2013. A functional role of the extracellular domain of Crumbs in cell architecture and apicobasal polarity. *J Cell Sci*. 126: 2157-2163.

Li BX, Satoh AK, Ready DF. 2007. Myosin V, Rab11, and dRip11 direct apical secretion and cellular morphogenesis in developing Drosophila photoreceptors. *J Cell Biol*. 177: 659-669.

Li M, Cheng R, Liang J, Yan H, Zhang H, Yang L, Li C, Jiao Q, Lu Z, He J, et al. 2013. Mutations in POFUT1, Encoding Protein O-fucosyltransferase 1, Cause Generalized Dowling-Degos Disease. *Am J Hum Genet*.

Lieber T, Kidd S, Young MW. 2002. kuzbanian-mediated cleavage of Drosophila Notch. *Genes Dev*. 16: 209-221.

Ling C, Zheng Y, Yin F, Yu J, Huang J, Hong Y, Wu S, Pan D. 2010. The apical transmembrane protein Crumbs functions as a tumor suppressor that regulates Hippo signaling by binding to Expanded. *Proc Natl Acad Sci U S A*. 107: 10532-10537.

Littink KW, van den Born LI, Koenekoop RK, Collin RW, Zonneveld MN, Blokland EA, Khan H, Theelen T, Hoyng CB, Cremers FP, et al. 2010. Mutations in the EYS gene account for approximately 5% of autosomal recessive retinitis pigmentosa and cause a fairly homogeneous phenotype. *Ophthalmology*. 117: 2026-2033, 2033. e2021-2027.

Longley RL, Jr., Ready DF. 1995. Integrins and the development of three-dimensional structure in the Drosophila compound eye. *Dev Biol*. 171: 415-433.

Lu Q, Hasty P, Shur BD. 1997. Targeted mutation in beta1,4-galactosyltransferase leads to pituitary insufficiency and neonatal lethality. *Dev Biol*. 181: 257-267.

Luo Y, Haltiwanger RS. 2005. O-fucosylation of notch occurs in the endoplasmic reticulum. *J Biol Chem*. 280: 11289-11294.

Mahoney MB, Parks AL, Ruddy DA, Tiong SY, Esengil H, Phan AC, Philandrinos P, Winter CG, Chatterjee R, Huppert K, et al. 2006. Presenilin-based genetic screens in Drosophila melanogaster identify novel notch pathway modifiers. *Genetics*. 172: 2309-2324.

Makarova O, Roh MH, Liu CJ, Laurinec S, Margolis B. 2003. Mammalian Crumbs3 is a small transmembrane protein linked to protein associated with Lin-7 (Pals1). *Gene*. 302: 21-29.

Matsui T, Amano M, Yamamoto T, Chihara K, Nakafuku M, Ito M, Nakano T, Okawa K, Iwamatsu A, Kaibuchi K. 1996. Rho-associated kinase, a novel serine/threonine kinase, as a putative target for small GTP binding protein Rho. *EMBO J*. 15: 2208-2216.

Matsuura A, Ito M, Sakaidani Y, Kondo T, Murakami K, Furukawa K, Nadano D, Matsuda T, Okajima T. 2008. O-linked N-acetylglucosamine is present on the extracellular domain of notch receptors. *J Biol Chem*. 283: 35486-35495.

Maw MA, Corbeil D, Koch J, Hellwig A, Wilson-Wheeler JC, Bridges RJ, Kumaramanickavel G, John S, Nancarrow D, Roper K, et al. 2000. A frameshift mutation in prominin (mouse)-like 1 causes human retinal degeneration. *Hum Mol Genet*. 9: 27-34.

Mehalow AK, Kameya S, Smith RS, Hawes NL, Denegre JM, Young JA, Bechtold L, Haider NB, Tepass U, Heckenlively JR, et al. 2003. CRB1 is essential for external limiting membrane integrity and photoreceptor morphogenesis in the mammalian retina. *Hum Mol Genet*. 12: 2179-2189.

Michaelides M, Johnson S, Poulson A, Bradshaw K, Bellmann C, Hunt DM, Moore AT. 2003. An autosomal dominant bull's-eye macular dystrophy (MCDR2) that maps to the short arm of chromosome 4. *Invest Ophthalmol Vis Sci*. 44: 1657-1662.

Miraglia S, Godfrey W, Yin AH, Atkins K, Warnke R, Holden JT, Bray RA, Waller EK, Buck DW. 1997. A novel five-transmembrane hematopoietic stem cell antigen: isolation, characterization, and molecular cloning. *Blood*. 90: 5013-5021.

Moloney DJ, Panin VM, Johnston SH, Chen J, Shao L, Wilson R, Wang Y, Stanley P, Irvine KD, Haltiwanger RS, et al. 2000a. Fringe is a glycosyltransferase that modifies Notch. *Nature*. 406: 369-375.

Moloney DJ, Shair LH, Lu FM, Xia J, Locke R, Matta KL, Haltiwanger RS. 2000b. Mammalian Notch1 is modified with two unusual forms of O-linked glycosylation found on epidermal growth factor-like modules. *J Biol Chem*. 275: 9604-9611.

Moran JL, Levorse JM, Vogt TF. 1999. Limbs move beyond the radical fringe. *Nature*. 399: 742-743.

Moran JL, Shifley ET, Levorse JM, Mani S, Ostmann K, Perez-Balaguer A, Walker DM, Vogt TF, Cole SE. 2009. Manic fringe is not required for embryonic development, and fringe family members do not exhibit redundant functions in the axial skeleton, limb, or hindbrain. *Dev Dyn*. 238: 1803-1812.

Morante J, Desplan C. 2004. Building a projection map for photoreceptor neurons in the Drosophila optic lobes. *Semin Cell Dev Biol*. 15: 137-143.

Mori R, Kondo T, Nishie T, Ohshima T, Asano M. 2004. Impairment of skin wound healing in beta-1,4-galactosyltransferase-deficient mice with reduced leukocyte recruitment. *Am J Pathol*. 164: 1303-1314.

Muller R, Jenny A, Stanley P. 2013. The EGF Repeat-Specific O-GlcNAc-Transferase Eogt Interacts with Notch Signaling and Pyrimidine Metabolism Pathways in Drosophila. *PLoS One*. 8: e62835.

Nichols R, Pak WL. 1985. Characterization of Drosophila melanogaster rhodopsin. *J Biol Chem*. 260: 12670-12674.

Nie J, Mahato S, Mustill W, Tipping C, Bhattacharya SS, Zelhof AC. 2012. Cross species analysis of Prominin reveals a conserved cellular role in invertebrate and vertebrate photoreceptor cells. *Dev Biol*. 371: 312-320.

Nie J, Mahato S, Zelhof AC. 2014. The actomyosin machinery is required for Drosophila retinal lumen formation. *PLoS Genet*. 10: e1004608.

Nilsson DE. 1990. From cornea to retinal image in invertebrate eyes. *Trends Neurosci*. 13: 55-64.

Nishimura H, Kawabata S, Kisiel W, Hase S, Ikenaka T, Takao T, Shimonishi Y, Iwanaga S. 1989. Identification of a disaccharide (Xyl-Glc) and a trisaccharide (Xyl2-Glc) O-glycosidically linked to a serine residue in the first epidermal growth factor-like domain of human factors VII and IX and protein Z and bovine protein Z. *J Biol Chem*. 264: 20320-20325.

Nishimura H, Takao T, Hase S, Shimonishi Y, Iwanaga S. 1992. Human factor IX has a tetrasaccharide O-glycosidically linked to serine 61 through the fucose residue. *J Biol Chem*. 267: 17520-17525.

Nita-Lazar A, Haltiwanger RS. 2006. Methods for analysis of O-linked modifications on epidermal growth factor-like and thrombospondin type 1 repeats. *Methods Enzymol*. 417: 93-111.

Nolo R, Abbott LA, Bellen HJ. 2000. Senseless, a Zn finger transcription factor, is necessary and sufficient for sensory organ development in Drosophila. *Cell*. 102: 349-362.

Oishi M, Oishi A, Gotoh N, Ogino K, Higasa K, Iida K, Makiyama Y, Morooka S, Matsuda F, Yoshimura N. 2014. Comprehensive molecular diagnosis of a large cohort of Japanese retinitis pigmentosa and Usher syndrome patients by next-generation sequencing. *Invest Ophthalmol Vis Sci*. 55: 7369-7375.

Oka C, Nakano T, Wakeham A, de la Pompa JL, Mori C, Sakai T, Okazaki S, Kawaichi M, Shiota K, Mak TW, et al. 1995. Disruption of the mouse RBP-J kappa gene results in early embryonic death. *Development*. 121: 3291-3301.

Okajima T, Irvine KD. 2002. Regulation of notch signaling by o-linked fucose. *Cell*. 111: 893-904.

Okajima T, Reddy B, Matsuda T, Irvine KD. 2008. Contributions of chaperone and glycosyltransferase activities of O-fucosyltransferase 1 to Notch signaling. *BMC Biol*. 6: 1.

Okajima T, Xu A, Irvine KD. 2003. Modulation of notch-ligand binding by protein O-fucosyltransferase 1 and fringe. *J Biol Chem*. 278: 42340-42345.

Okajima T, Xu A, Lei L, Irvine KD. 2005. Chaperone activity of protein O-fucosyltransferase 1 promotes notch receptor folding. *Science*. 307: 1599-1603.

Okamura Y, Saga Y. 2008. Pofut1 is required for the proper localization of the Notch receptor during mouse development. *Mech Dev*. 125: 663-673.

Panin VM, Papayannopoulos V, Wilson R, Irvine KD. 1997. Fringe modulates Notch-ligand interactions. *Nature*. 387: 908-912.

Panin VM, Shao L, Lei L, Moloney DJ, Irvine KD, Haltiwanger RS. 2002. Notch ligands are substrates for protein O-fucosyltransferase-1 and Fringe. *J Biol Chem*. 277: 29945-29952.

Pei Z, Baker NE. 2008. Competition between Delta and the Abruptex domain of Notch. *BMC Dev Biol*. 8: 4.

Pellikka M, Tanentzapf G, Pinto M, Smith C, McGlade CJ, Ready DF, Tepass U. 2002. Crumbs, the Drosophila homologue of human CRB1/RP12, is essential for photoreceptor morphogenesis. *Nature*. 416: 143-149.

Perdigoto CN, Schweisguth F, Bardin AJ. 2011. Distinct levels of Notch activity for commitment and terminal differentiation of stem cells in the adult fly intestine. *Development*. 138: 4585-4595.

Permanyer J, Navarro R, Friedman J, Pomares E, Castro-Navarro J, Marfany G, Swaroop A, Gonzalez-Duarte R. 2010. Autosomal recessive retinitis pigmentosa with early macular affectation caused by premature truncation in PROM1. *Invest Ophthalmol Vis Sci*. 51: 2656-2663.

Pocha SM, Shevchenko A, Knust E. 2011. Crumbs regulates rhodopsin transport by interacting with and stabilizing myosin V. *J Cell Biol*. 195: 827-838.

Poulson DF. 1937. Chromosomal Deficiencies and the Embryonic Development of Drosophila Melanogaster. *Proc Natl Acad Sci U S A*. 23: 133-137.

Pras E, Abu A, Rotenstreich Y, Avni I, Reish O, Morad Y, Reznik-Wolf H, Pras E. 2009. Cone-rod dystrophy and a frameshift mutation in the PROM1 gene. *Mol Vis*. 15: 1709-1716.

Prout M, Damania Z, Soong J, Fristrom D, Fristrom JW. 1997. Autosomal mutations affecting adhesion between wing surfaces in Drosophila melanogaster. *Genetics*. 146: 275-285.

Radtke F, Wilson A, Stark G, Bauer M, van Meerwijk J, MacDonald HR, Aguet M. 1999. Deficient T cell fate specification in mice with an induced inactivation of Notch1. *Immunity*. 10: 547-558.

Rampal R, Luther KB, Haltiwanger RS. 2007. Notch signaling in normal and disease States: possible therapies related to glycosylation. *Curr Mol Med*. 7: 427-445.

Rana NA, Nita-Lazar A, Takeuchi H, Kakuda S, Luther KB, Haltiwanger RS. 2011. O-glucose trisaccharide is present at high but variable stoichiometry at multiple sites on mouse Notch1. *J Biol Chem*. 286: 31623-31637.

Rand MD, Lindblom A, Carlson J, Villoutreix BO, Stenflo J. 1997. Calcium binding to tandem repeats of EGF-like modules. Expression and characterization of the EGF-like modules of human Notch-1 implicated in receptor-ligand interactions. *Protein Sci*. 6: 2059-2071.

Ready DF, Hanson TE, Benzer S. 1976. Development of the Drosophila retina, a neurocrystalline lattice. *Dev Biol*. 53: 217-240.

Rebay I, Fleming RJ, Fehon RG, Cherbas L, Cherbas P, Artavanis-Tsakonas S. 1991. Specific EGF repeats of Notch mediate interactions with Delta and Serrate: implications for Notch as a multifunctional receptor. *Cell*. 67: 687-699.

Reinke R, Krantz DE, Yen D, Zipursky SL. 1988. Chaoptin, a cell surface glycoprotein required for Drosophila photoreceptor cell morphogenesis, contains a repeat motif found in yeast and human. *Cell*. 52: 291-301.

Ren F, Sheng WQ, Du X. 2013. CD133: a cancer stem cells marker, is used in colorectal cancers. *World J Gastroenterol*. 19: 2603-2611.

Richard M, Muschalik N, Grawe F, Ozuyaman S, Knust E. 2009. A role for the extracellular domain of Crumbs in morphogenesis of Drosophila photoreceptor cells. *Eur J Cell Biol*. 88: 765-777.

Richardson EC, Pichaud F. 2010. Crumbs is required to achieve proper organ size control during Drosophila head development. *Development*. 137: 641-650.

Rister J, Pauls D, Schnell B, Ting CY, Lee CH, Sinakevitch I, Morante J, Strausfeld NJ, Ito K, Heisenberg M. 2007. Dissection of the peripheral motion channel in the visual system of Drosophila melanogaster. *Neuron*. 56: 155-170.

Rizki RM, Rizki TM. 1965. Morphogenetic effects of 6-azauracil and 6-azauridine. *Science*. 150: 222-223.

Robinson BS, Huang J, Hong Y, Moberg KH. 2010. Crumbs regulates Salvador/Warts/Hippo signaling in Drosophila via the FERM-domain protein Expanded. *Curr Biol*. 20: 582-590.

Roper K. 2012. Anisotropy of Crumbs and aPKC drives myosin cable assembly during tube formation. *Developmental cell*. 23: 939-953.

Ryoo HD, Domingos PM, Kang MJ, Steller H. 2007. Unfolded protein response in a Drosophila model for retinal degeneration. *EMBO J*. 26: 242-252.

Sakaidani Y, Ichiyanagi N, Saito C, Nomura T, Ito M, Nishio Y, Nadano D, Matsuda T, Furukawa K, Okajima T. 2012. O-linked-N-acetylglucosamine modification of mammalian Notch receptors by an atypical O-GlcNAc transferase Eogt1. *Biochem Biophys Res Commun*. 419: 14-19.

Sakaidani Y, Nomura T, Matsuura A, Ito M, Suzuki E, Murakami K, Nadano D, Matsuda T, Furukawa K, Okajima T. 2011. O-linked-N-acetylglucosamine on extracellular protein domains mediates epithelial cell-matrix interactions. *Nat Commun*. 2: 583.

Sang TK, Ready DF. 2002. Eyes closed, a Drosophila p47 homolog, is essential for photoreceptor morphogenesis. *Development*. 129: 143-154.

Sasamura T, Ishikawa HO, Sasaki N, Higashi S, Kanai M, Nakao S, Ayukawa T, Aigaki T, Noda K, Miyoshi E, et al. 2007. The O-fucosyltransferase O-fut1 is an extracellular component that is essential for the constitutive endocytic trafficking of Notch in Drosophila. *Development*. 134: 1347-1356.

Sasamura T, Sasaki N, Miyashita F, Nakao S, Ishikawa HO, Ito M, Kitagawa M, Harigaya K, Spana E, Bilder D, et al. 2003. neurotic, a novel maternal neurogenic gene, encodes an O-fucosyltransferase that is essential for Notch-Delta interactions. *Development*. 130: 4785-4795.

Satoh AK, O'Tousa JE, Ozaki K, Ready DF. 2005. Rab11 mediates post-Golgi trafficking of rhodopsin to the photosensitive apical membrane of Drosophila photoreceptors. *Development*. 132: 1487-1497.

Savage CR, Jr., Hash JH, Cohen S. 1973. Epidermal growth factor. Location of disulfide bonds. *J Biol Chem*. 248: 7669-7672.

Schuster-Gossler K, Harris B, Johnson KR, Serth J, Gossler A. 2009. Notch signalling in the paraxial mesoderm is most sensitive to reduced Pofut1 levels during early mouse development. *BMC Dev Biol*. 9: 6.

Segall JE, Tyerech S, Boselli L, Masseling S, Helft J, Chan A, Jones J, Condeelis J. 1996. EGF stimulates lamellipod extension in metastatic mammary adenocarcinoma cells by an actin-dependent mechanism. *Clin Exp Metastasis*. 14: 61-72.

Sethi MK, Buettner FF, Ashikov A, Krylov VB, Takeuchi H, Nifantiev NE, Haltiwanger RS, Gerardy-Schahn R, Bakker H. 2012. Molecular cloning of a xylosyltransferase that transfers the second xylose to O-glucosylated epidermal growth factor repeats of notch. *J Biol Chem*. 287: 2739-2748.

Sethi MK, Buettner FF, Krylov VB, Takeuchi H, Nifantiev NE, Haltiwanger RS, Gerardy-Schahn R, Bakker H. 2010. Identification of glycosyltransferase 8 family members as xylosyltransferases acting on O-glucosylated notch epidermal growth factor repeats. *J Biol Chem*. 285: 1582-1586.

Shaheen R, Aglan M, Keppler-Noreuil K, Faqeih E, Ansari S, Horton K, Ashour A, Zaki MS, Al-Zahrani F, Cueto-Gonzalez AM, et al. 2013. Mutations in EOGT confirm the genetic heterogeneity of autosomal-recessive Adams-Oliver syndrome. *Am J Hum Genet*. 92: 598-604.

Shi S, Stanley P. 2003. Protein O-fucosyltransferase 1 is an essential component of Notch signaling pathways. *Proc Natl Acad Sci U S A*. 100: 5234-5239.

Siegal ML, Hartl DL. 1996. Transgene Coplacement and high efficiency site-specific recombination with the Cre/loxP system in Drosophila. *Genetics*. 144: 715-726.

Sisson JC, Field C, Ventura R, Royou A, Sullivan W. 2000. Lava lamp, a novel peripheral golgi protein, is required for Drosophila melanogaster cellularization. *J Cell Biol*. 151: 905-918.

Sparrow DB, Chapman G, Wouters MA, Whittock NV, Ellard S, Fatkin D, Turnpenny PD, Kusumi K, Sillence D, Dunwoodie SL. 2006. Mutation of the LUNATIC FRINGE gene in humans causes spondylocostal dysostosis with a severe vertebral phenotype. *Am J Hum Genet*. 78: 28-37.

Sprinzak D, Lakhanpal A, Lebon L, Santat LA, Fontes ME, Anderson GA, Garcia-Ojalvo J, Elowitz MB. 2010. Cis-interactions between Notch and Delta generate mutually exclusive signalling states. *Nature*. 465: 86-90.

Stahl M, Uemura K, Ge C, Shi S, Tashima Y, Stanley P. 2008. Roles of Pofut1 and O-fucose in mammalian Notch signaling. *J Biol Chem*. 283: 13638-13651.

Stanley P, Guidos CJ. 2009. Regulation of Notch signaling during T- and B-cell development by O-fucose glycans. *Immunol Rev*. 230: 201-215.

Stittrich AB, Lehman A, Bodian DL, Ashworth J, Zong Z, Li H, Lam P, Khromykh A, Iyer RK, Vockley JG, et al. 2014. Mutations in NOTCH1 cause Adams-Oliver syndrome. *Am J Hum Genet*. 95: 275-284.

Stroman P. 1974. Pyrimidine-sensitive drosophila wing mutants: withered (whd), tilt (tt) and dumpy (dp). *Hereditas*. 78: 157-168.

Suzuki K, Hayashi T, Nishioka J, Kosaka Y, Zushi M, Honda G, Yamamoto S. 1989. A domain composed of epidermal growth factor-like structures of human thrombomodulin is essential for thrombin binding and for protein C activation. *J Biol Chem*. 264: 4872-4876.

Takeuchi H, Fernandez-Valdivia RC, Caswell DS, Nita-Lazar A, Rana NA, Garner TP, Weldeghiorghis TK, Macnaughtan MA, Jafar-Nejad H, Haltiwanger RS. 2011. Rumi functions as both a protein O-glucosyltransferase and a protein O-xylosyltransferase. *Proc Natl Acad Sci U S A*. 108: 16600-16605.

Takeuchi H, Kantharia J, Sethi MK, Bakker H, Haltiwanger RS. 2012. Site-specific O-glucosylation of the epidermal growth factor-like (EGF) repeats of notch: efficiency of glycosylation is affected by proper folding and amino acid sequence of individual EGF repeats. *J Biol Chem*. 287: 33934-33944.

Taylor P, Takeuchi H, Sheppard D, Chillakuri C, Lea SM, Haltiwanger RS, Handford PA. 2014. Fringe-mediated extension of O-linked fucose in the ligand-binding region of Notch1

increases binding to mammalian Notch ligands. *Proc Natl Acad Sci U S A*. 111: 7290-7295.

Tepass U. 1996. Crumbs, a component of the apical membrane, is required for zonula adherens formation in primary epithelia of Drosophila. *Dev Biol*. 177: 217-225.

Tepass U, Theres C, Knust E. 1990. crumbs encodes an EGF-like protein expressed on apical membranes of Drosophila epithelial cells and required for organization of epithelia. *Cell*. 61: 787-799.

Traverse S, Seedorf K, Paterson H, Marshall CJ, Cohen P, Ullrich A. 1994. EGF triggers neuronal differentiation of PC12 cells that overexpress the EGF receptor. *Curr Biol*. 4: 694-701.

Van Vactor D, Jr., Krantz DE, Reinke R, Zipursky SL. 1988. Analysis of mutants in chaoptin, a photoreceptor cell-specific glycoprotein in Drosophila, reveals its role in cellular morphogenesis. *Cell*. 52: 281-290.

Venken KJ, He Y, Hoskins RA, Bellen HJ. 2006. P[acman]: a BAC transgenic platform for targeted insertion of large DNA fragments in D. melanogaster. *Science*. 314: 1747-1751.

Venken KJ, Schulze KL, Haelterman NA, Pan H, He Y, Evans-Holm M, Carlson JW, Levis RW, Spradling AC, Hoskins RA, et al. 2011. MiMIC: a highly versatile transposon insertion resource for engineering Drosophila melanogaster genes. *Nat Methods*. 8: 737-743.

Venken KJT, Bellen HJ, Hoskins RA (2009) MIMIC transposable element ("Minos Mediated Integration Casette").

Visan I, Tan JB, Yuan JS, Harper JA, Koch U, Guidos CJ. 2006. Regulation of T lymphopoiesis by Notch1 and Lunatic fringe-mediated competition for intrathymic niches. *Nat Immunol*. 7: 634-643.

Wagner CR, Mahowald AP, Miller KG. 2002. One of the two cytoplasmic actin isoforms in Drosophila is essential. *Proc Natl Acad Sci U S A*. 99: 8037-8042.

Wang W, Chen Y, Deng J, Zhou J, Zhou Y, Wang S, Zhou J. 2014. The prognostic value of CD133 expression in non-small cell lung cancer: a meta-analysis. *Tumour Biol*. 35: 9769-9775.

Wang W, Nagashima M, Schneider M, Morser J, Nesheim M. 2000. Elements of the primary structure of thrombomodulin required for efficient thrombin-activable fibrinolysis inhibitor activation. *J Biol Chem*. 275: 22942-22947.

Wang Y, Shao L, Shi S, Harris RJ, Spellman MW, Stanley P, Haltiwanger RS. 2001. Modification of epidermal growth factor-like repeats with O-fucose. Molecular cloning and expression of a novel GDP-fucose protein O-fucosyltransferase. *J Biol Chem*. 276: 40338-40345.

Wang Y, Spellman MW. 1998. Purification and characterization of a GDP-fucose:polypeptide fucosyltransferase from Chinese hamster ovary cells. *J Biol Chem*. 273: 8112-8118.

Wardill TJ, List O, Li X, Dongre S, McCulloch M, Ting CY, O'Kane CJ, Tang S, Lee CH, Hardie RC, et al. 2012. Multiple spectral inputs improve motion discrimination in the Drosophila visual system. *Science*. 336: 925-931.

Weigmann A, Corbeil D, Hellwig A, Huttner WB. 1997. Prominin, a novel microvilli-specific polytopic membrane protein of the apical surface of epithelial cells, is targeted to plasmalemmal protrusions of non-epithelial cells. *Proc Natl Acad Sci U S A*. 94: 12425-12430.

Whiteman EL, Fan S, Harder JL, Walton KD, Liu CJ, Soofi A, Fogg VC, Hershenson MB, Dressler GR, Deutsch GH, et al. 2014. Crumbs3 is essential for proper epithelial development and viability. *Mol Cell Biol*. 34: 43-56.

Whitworth GE, Zandberg WF, Clark T, Vocadlo DJ. 2010. Mammalian Notch is modified by D-Xyl-alpha1-3-D-Xyl-alpha1-3-D-Glc-beta1-O-Ser: implementation of a method to study O-glucosylation. *Glycobiology*. 20: 287-299.

Wilkin MB, Becker MN, Mulvey D, Phan I, Chao A, Cooper K, Chung HJ, Campbell ID, Baron M, MacIntyre R. 2000. Drosophila dumpy is a gigantic extracellular protein required to maintain tension at epidermal-cuticle attachment sites. *Curr Biol*. 10: 559-567.

Winkler ME, Bringman T, Marks BJ. 1986. The purification of fully active recombinant transforming growth factor alpha produced in Escherichia coli. *J Biol Chem*. 261: 13838-13843.

Wodarz A, Grawe F, Knust E. 1993. CRUMBS is involved in the control of apical protein targeting during Drosophila epithelial development. *Mech Dev*. 44: 175-187.

Wodarz A, Hinz U, Engelbert M, Knust E. 1995. Expression of crumbs confers apical character on plasma membrane domains of ectodermal epithelia of Drosophila. *Cell*. 82: 67-76.

Wu H, Qi XW, Yan GN, Zhang QB, Xu C, Bian XW. 2014. Is CD133 expression a prognostic biomarker of non-small-cell lung cancer? A systematic review and meta-analysis. *PLoS One*. 9: e100168.

Xiao Z, Patrakka J, Nukui M, Chi L, Niu D, Betsholtz C, Pikkarainen T, Vainio S, Tryggvason K. 2011. Deficiency in Crumbs homolog 2 (Crb2) affects gastrulation and results in embryonic lethality in mice. *Dev Dyn*. 240: 2646-2656.

Xu A, Haines N, Dlugosz M, Rana NA, Takeuchi H, Haltiwanger RS, Irvine KD. 2007. In vitro reconstitution of the modulation of Drosophila Notch-ligand binding by Fringe. *J Biol Chem*. 282: 35153-35162.

Xu D, Wang Y, Willecke R, Chen Z, Ding T, Bergmann A. 2006. The effector caspases drICE and dcp-1 have partially overlapping functions in the apoptotic pathway in Drosophila. *Cell death and differentiation*. 13: 1697-1706.

Yamaguchi S, Wolf R, Desplan C, Heisenberg M. 2008. Motion vision is independent of color in Drosophila. *Proc Natl Acad Sci U S A*. 105: 4910-4915.

Yamamoto S, Charng WL, Rana NA, Kakuda S, Jaiswal M, Bayat V, Xiong B, Zhang K, Sandoval H, David G, et al. 2012. A mutation in EGF repeat-8 of Notch discriminates between Serrate/Jagged and Delta family ligands. *Science*. 338: 1229-1232.

Yamamoto T, Bishop RW, Brown MS, Goldstein JL, Russell DW. 1986. Deletion in cysteine-rich region of LDL receptor impedes transport to cell surface in WHHL rabbit. *Science*. 232: 1230-1237.

Yang LT, Nichols JT, Yao C, Manilay JO, Robey EA, Weinmaster G. 2005. Fringe glycosyltransferases differentially modulate Notch1 proteolysis induced by Delta1 and Jagged1. *Mol Biol Cell*. 16: 927-942.

Yang X, Klein R, Tian X, Cheng HT, Kopan R, Shen J. 2004. Notch activation induces apoptosis in neural progenitor cells through a p53-dependent pathway. *Dev Biol*. 269: 81-94.

Yang Z, Chen Y, Lillo C, Chien J, Yu Z, Michaelides M, Klein M, Howes KA, Li Y, Kaminoh Y, et al. 2008. Mutant prominin 1 found in patients with macular degeneration disrupts photoreceptor disk morphogenesis in mice. *J Clin Invest*. 118: 2908-2916.

Yao D, Huang Y, Huang X, Wang W, Yan Q, Wei L, Xin W, Gerson S, Stanley P, Lowe JB, et al. 2011. Protein O-fucosyltransferase 1 (Pofut1) regulates lymphoid and myeloid homeostasis through modulation of Notch receptor ligand interactions. *Blood*. 117: 5652-5662.

Zaczek A, Brandt B, Bielawski KP. 2005. The diverse signaling network of EGFR, HER2, HER3 and HER4 tyrosine kinase receptors and the consequences for therapeutic approaches. *Histol Histopathol*. 20: 1005-1015.

Zelhof AC, Hardy RW, Becker A, Zuker CS. 2006. Transforming the architecture of compound eyes. *Nature*. 443: 696-699.

Zhang N, Gridley T. 1998. Defects in somite formation in lunatic fringe-deficient mice. *Nature*. 394: 374-377.

Zhang N, Norton CR, Gridley T. 2002. Segmentation defects of Notch pathway mutants and absence of a synergistic phenotype in lunatic fringe/radical fringe double mutant mice. *Genesis*. 33: 21-28.

Zhang Q, Zulfiqar F, Xiao X, Riazuddin SA, Ahmad Z, Caruso R, MacDonald I, Sieving P, Riazuddin S, Hejtmancik JF. 2007. Severe retinitis pigmentosa mapped to 4p15 and associated with a novel mutation in the PROM1 gene. *Hum Genet*. 122: 293-299.

Zhou L, Li LW, Yan Q, Petryniak B, Man Y, Su C, Shim J, Chervin S, Lowe JB. 2008. Notch-dependent control of myelopoiesis is regulated by fucosylation. *Blood*. 112: 308-319.

Zipursky SL, Venkatesh TR, Teplow DB, Benzer S. 1984. Neuronal development in the Drosophila retina: monoclonal antibodies as molecular probes. *Cell*. 36: 15-26.

Vita

Amanda Rae Haltom was born in Fort Worth, Texas on April 7, 1989, the daughter of Brenda Joyce Haltom and James Calvin Haltom. After completing her work at Argyle High School, Argyle, Texas in 2007, she entered Texas A&M University in College Station, Texas. She received the degree of Bachelor of Science with a major in genetics from Texas A&M in August, 2010. In the same month, August 2010, she entered The University of Texas Graduate School of Biomedical Sciences at Houston.

Permanent address:

714 Sam Davis Rd

Argyle, Tx 76226